ARMY RESEARCH LABORATORY

Aerodynamic and Flight Dynamic Characteristics of 5.56-mm Ammunition: M855

by Sidra I. Silton and Bradley E. Howell

ARL-TR-5182 **May 2010**

NOTICES

Disclaimers

The findings in this report are not to be construed as an official Department of the Army position unless so designated by other authorized documents.

Citation of manufacturer's or trade names does not constitute an official endorsement or approval of the use thereof.

Destroy this report when it is no longer needed. Do not return it to the originator.

Army Research Laboratory
Aberdeen Proving Ground, MD 21005-5066

ARL-TR-5182 **May 2010**

Aerodynamic and Flight Dynamic Characteristics of 5.56-mm Ammunition: M855

Sidra I. Silton
Weapons and Materials Research Directorate, ARL

Bradley E. Howell
Data Matrix Solutions, Inc.

REPORT DOCUMENTATION PAGE	Form Approved OMB No. 0704-0188

1. REPORT DATE *(DD-MM-YYYY)*	2. REPORT TYPE	3. DATES COVERED (From - To)
May 2010	Final	August 2005–December 2006

4. TITLE AND SUBTITLE
Aerodynamic and Flight Dynamic Characteristics of 5.56-mm Ammunition: M855

5a. CONTRACT NUMBER

5b. GRANT NUMBER

5c. PROGRAM ELEMENT NUMBER

6. AUTHOR(S)
Sidra I. Silton and Bradley E. Howell*

5d. PROJECT NUMBER
622618.H8000

5e. TASK NUMBER

5f. WORK UNIT NUMBER

7. PERFORMING ORGANIZATION NAME(S) AND ADDRESS(ES)
U.S. Army Research Laboratory
ATTN: RDRL-WML-E
Aberdeen Proving Ground, MD 21005-5066

8. PERFORMING ORGANIZATION REPORT NUMBER
ARL-TR-5182

9. SPONSORING/MONITORING AGENCY NAME(S) AND ADDRESS(ES)
Project Manager for Maneuver Ammunition Systems
SFAE AMO MAS, Bldg. 354
Picatinny Arsenal, NJ
07806-5000

10. SPONSOR/MONITOR'S ACRONYM(S)
PM-MAS

11. SPONSOR/MONITOR'S REPORT NUMBER(S)

12. DISTRIBUTION/AVAILABILITY STATEMENT
Approved for public release; distribution is unlimited.

13. SUPPLEMENTARY NOTES
*Data Matrix Solutions, Inc., 107 Carpenter Dr., Ste. 110, Sterling, VA 20164

14. ABSTRACT
An experimental program for the aerodynamic and flight dynamic characterization of current 5.56-mm small-caliber ammunition has been developed and executed to further enable the U.S. Army's understanding of the ammunition. This report is focused on the M855 round, one of the most commonly used ammunitions for the M4 and M16A2 weapons. The aerodynamic characterization of the M855 round was accomplished at muzzle velocity as well as simulated downrange velocities out to 600 m. The resulting aerodynamic data will be used to update the U.S. Army's aerodynamic model of M855 ammunition to create improved modeling ability. A flight dynamic characterization, to include yaw limit cycle and Magnus moment instabilities, was accomplished at the same velocities. The predicted downrange yaw limit cycles were compared with previously obtained at-range yaw limit cycles with some success.

15. SUBJECT TERMS
5.56-mm ammunition, M855, aerodynamic experimental facility

16. SECURITY CLASSIFICATION OF:			17. LIMITATION OF ABSTRACT	18. NUMBER OF PAGES	19a. NAME OF RESPONSIBLE PERSON
a. REPORT	b. ABSTRACT	c. THIS PAGE			Sidra I. Silton
Unclassified	Unclassified	Unclassified	UU	110	19b. TELEPHONE NUMBER (*Include area code*) 410-306-0792

Standard Form 298 (Rev. 8/98)
Prescribed by ANSI Std. Z39.18

Contents

List of Figures

List of Tables

Acknowledgments

The authors would like to thank the following U.S. Army Research Laboratory personnel:

- Ronald Anderson for reading the spark range film images and digitizing the data;
- Bernard Guidos and Ilmars Celmins for their input during technical review;
- James Hall at the machine shop for spin pin insertion;
- Robert Keppinger for measuring and recording projectile physical parameters;
- Donald McClellan for film developing, setup, and vast experience;
- Kenneth Paxton for film developing, setup, and data acquisition;
- Tom Puckett for acting as test director and gunner;
- Joyce Smith for reading the spark range film images and digitizing the data;
- Gregory Watt for reading the spark range film images and digitizing the data; and
- Dr. Paul Weinacht for providing the velocities associated with the downrange locations for each ammunition type and multiple discussions pertaining to the limit cycle/trim angle determinations.

The authors would also like to thank Wayne Hathaway for his technical assistance in the initial analysis of the spark range data using the Aeroballistics Research Facility Data Analysis System reductions.

INTENTIONALLY LEFT BLANK.

1. Introduction

The aerodynamic and flight dynamic characterization of ammunition is an essential element in any study for which the basic understanding of the projectile flight is desired. Over the past several years, there had been a renewed interested in small-caliber ammunition, specifically the 5.56-mm ammunition. Although this caliber of ammunition has been used by the U.S. Army for many years, there is a limited amount of either aerodynamic or flight dynamic data available.

In order to better understand the current generation of 5.56-mm ammunition, the Project Manager for Maneuver Ammunition Systems under the Program Executive Office for Ammunitions made the decision to fund the aerodynamic and flight dynamic characterization of many of the 5.56-mm ammunitions currently in use by the Soldier. This characterization, out to simulated ranges of 600 m, was undertaken by the Aerodynamics Branch at the U.S. Army Research Laboratory (ARL). As the testing was quite comprehensive (seven ammunition types), a series of reports will be presented to cover the findings.

The current report presents the findings from the study completed on the M855 ammunition in the Aerodynamic Experimental Facility (AEF) at ARL. While the M855 ammunition had been previously tested and reported on by McCoy (*1*), a very limited number of rounds (seven total) were available for aerodynamic data. Slightly more data was obtained for the real-range yaw limit cycle tests (between 10 and 15 rounds at each range). Therefore, the current test was completed to supplement this original data, providing a more complete understanding of the ammunition. Of particular interest is the ability to predict the yaw limit cycle using simulated ranges, as real-range yaw limit cycle tests are costly.

2. Experimental Setup

The spark range test was designed to determine the aerodynamics and flight dynamics of the 5.56-mm projectiles investigated over their first 600 m of flight. Prior to the test, the projectile's physical properties, not including asymmetries, were measured. During the spark range test, the projectiles and flow field images were studied, and the spin rates of the projectiles were tracked. The subsequent analysis characterized the observed flight dynamics of each configuration and defined the aerodynamic model of each projectile at Mach numbers corresponding to the approximate velocities at the muzzle and 200, 400, and 600 m downrange. The velocities corresponding to these ranges were chosen based on the known flight behavior of small-caliber projectiles (figure 1), with each range of interest indicated by the small circle. The projectile

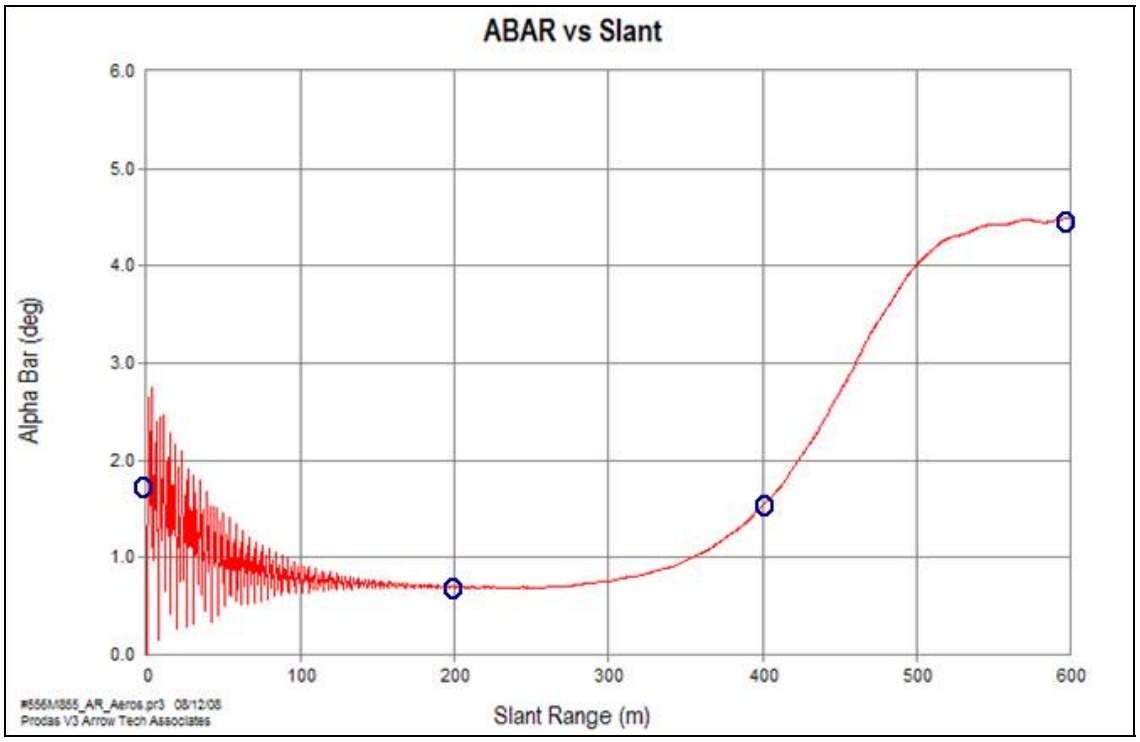

Figure 1. Yaw behavior of small-caliber ammunition over its first 600 m of flight.

exits the muzzle with some angular rate that causes yaw, hence the muzzle conditions. Due to the dynamic stability of the round, this yaw is known to damp out over the first 100–150 m of flight. It is desired to understand the projectile's aerodynamic behavior once the projectile yaw has damped out (200-m velocity). Between 300 and 400 m, a dynamic instability begins to occur, causing the yaw to grow. The cause of this dynamic instability isn't well understood, and a better aerodynamic characterization will always be helpful. By 600 m, a yaw limit cycle is believed to exist, and an aerodynamic characterization will help to better quantify the level.

2.1 Ammunition Types

Seven common 5.56-mm ammunition types were tested over the course of the study (figure 2): M193, M855, MK262, IMI, Sierra 69 gr, ATK 86 gr, and M995. The focus of this report is the M855 ammunition, specifically, the R011 reference lot (figure 3). The key dimensional and physical characteristics of the M855 ammunition are listed in table 1 and were obtained by measuring five projectiles and averaging the results. The reference diameter, *d*, corresponding to the maximum diameter of the projectile, is 5.69 mm. Figure 4 displays the key dimensions, in calibers, for the M855. The reader should note that the dimensions in figure 4 are not the same as those reported by McCoy (*1*), which were obtained by measuring the projectile on an optical comparator. The projectile physicals, however, are nearly identical. Most, but not all, of the

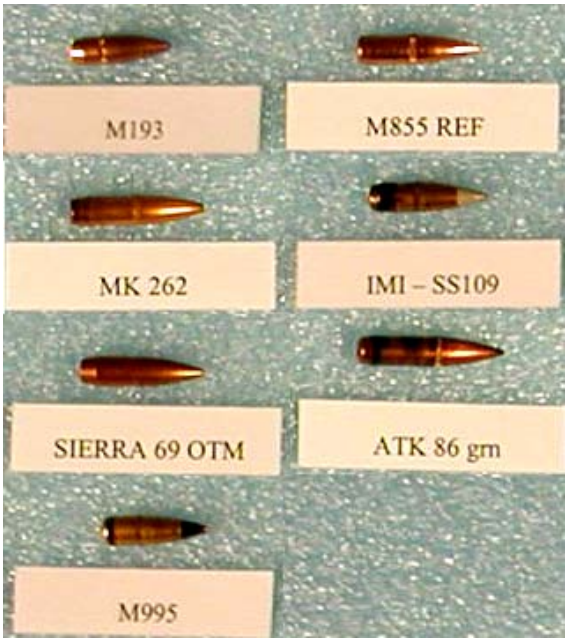

Figure 2. The 5.56-mm ammunition types tested in the current study.

Figure 3. Close-up picture of M855 ammunition discussed in this report.

Table 1. M855 projectile physical parameters.

Length (mm)	23.057
Mass, *m* (g)	4.04
Center of Gravity, X_{CG} (mm from nose)	14.279
Axial Moment of Inertia, I_x (g-cm^2)	0.1416
Transverse Moment of Inertia, I_y (g-cm^2)	1.138

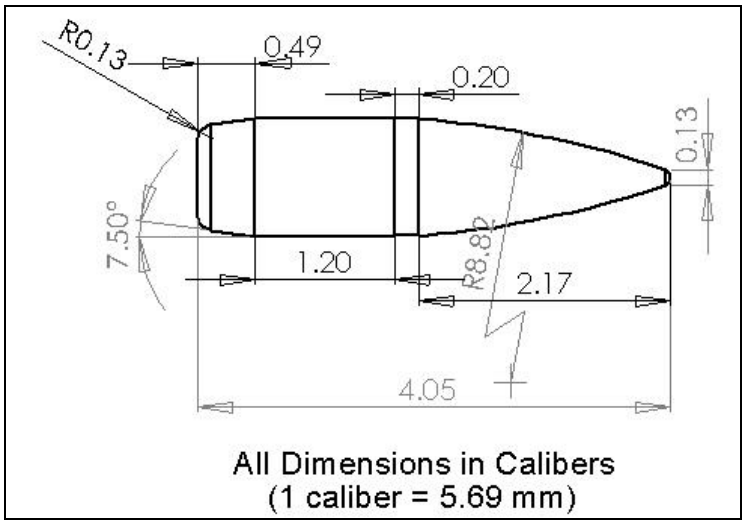

Figure 4. Dimensions of the M855 ammunition.

projectiles were fitted with a spin pin to allow for a spin analysis. The spin pins were 0.031-in-diameter piano wire or solid steel pins inserted into the base of the projectile ~0.065 in off the centerline. The wire was inserted into the base of the projectile such that 0.050–0.060 in were exposed behind the projectile. The length of the exposed spin pin was recorded for each relevant shot.

For each Mach number, a minimum of five data rounds across a spectrum of yaw levels was obtained. For the M855 ammunition, 38 rounds across five Mach numbers were used in the final analysis. Table 2 shows the Mach number used for the corresponding downrange location and the number of rounds included in the final analysis. Five Mach numbers were investigated for the M855 rather than the intended four because the Mach number originally chosen for the equivalent 600-m-downrange location (Mach 1.5) was found to correspond to the velocity at 450 m downrange when a trajectory analysis with the revised drag data was accomplished. The decision was made that additional data at the lower Mach number was necessary for a complete characterization of the flight dynamics as this is the critical Mach number regime for yaw growth. As such, a follow-on test was conducted to obtain data rounds for analysis at Mach 1.2, the newly determined 600-m-downrange velocity. Additional rounds were used for charge establishment at the Mach numbers associated with the downrange location or designated as a warmer round for setup and range instrumentation calibration.

Table 2. Shots fired at each Mach number for M855 ammunition.

Equivalent Location	Mach No.	No. of Shots
Muzzle	2.6	5
200 m	2.2	8
400 m	1.7	8
450 m	1.5	11
600 m	1.2	6

2.2 Indoor Spark Range Facility

The firings were conducted in the ARL AEF (*2*). This facility is a 100-m-long spark shadowgraph facility designed to obtain aerodynamic coefficients from free-flight trajectory data. A schematic of the facility is shown in figure 5.

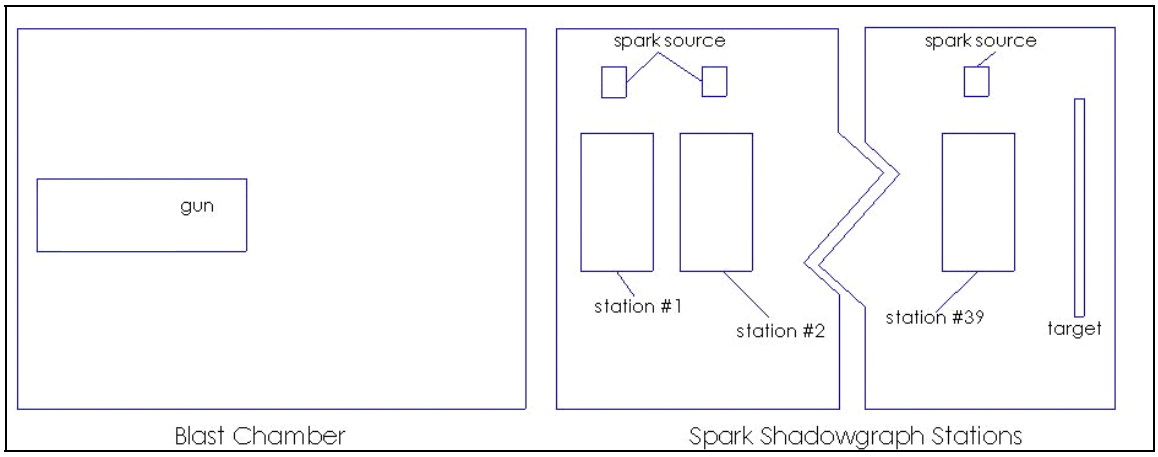

Figure 5. Schematic of ARL's AEF.

There are 39 dual-plane, direct-image spark shadowgraph stations arranged in five groups, with the first station ~1.8 m from the muzzle of the gun (i.e., end of flash suppressor) for most of the current test. For the Mach 1.2 shots, the gun muzzle was 1.9 m from the first station. A close view of a shadowgraph station is shown in figure 6. As the projectile passes each station, an infrared sensor triggers the spark source that causes the projectile image to be captured on 29.9- × 35.6-cm (11- × 14-in) film. The spark sources are connected to a computer so that the time when the spark source is triggered can be recorded. Each station is surveyed into a fiducial system that is simultaneously imaged onto the film with the projectile.

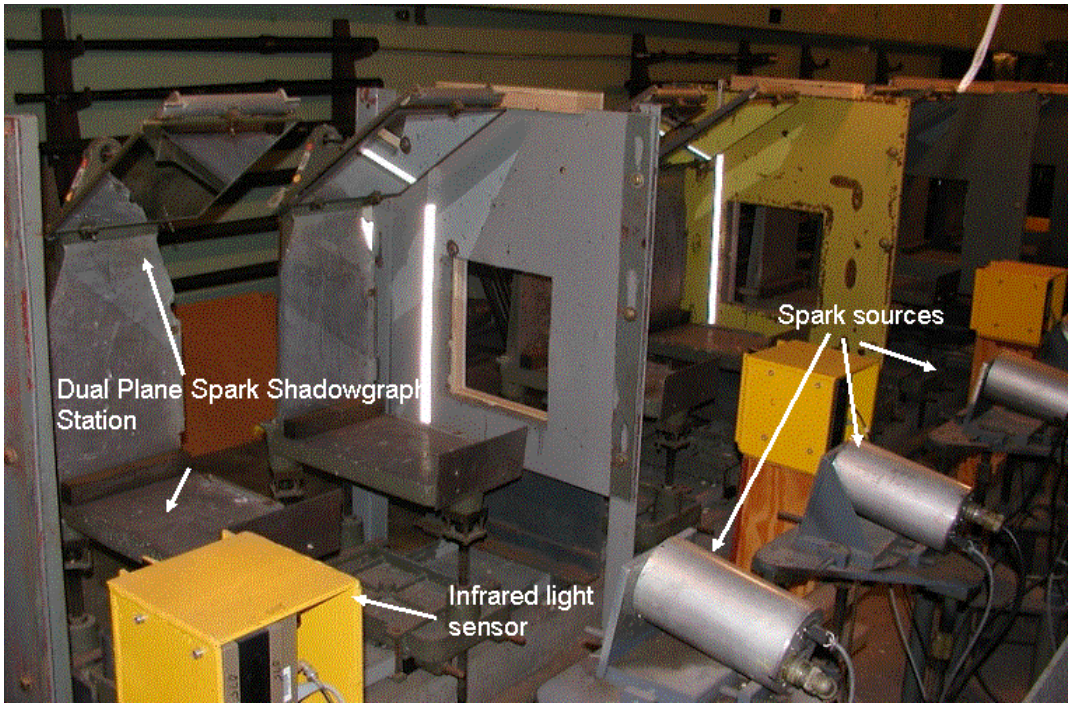

Figure 6. Close view of a spark shadowgraph station in ARL's AEF.

The film is developed after each shot and then read on a precision light table to produce the measured spatial coordinates (range, deflection, altitude) and angular orientation (pitch, yaw, roll) relative to an earth-fixed range coordinate system, all as a function of the spark time.

The expected accuracy of the measured positions and angles is as follows:

- position: 0.0003–0.0005 m,
- pitch/yaw: 0.05°–0.10°, and
- roll: 1.0°–5.0°.

The measurement accuracy depends on the flow conditions and model contours. The accuracy of the roll orientation also depends on the distance between the model centerline and the radial position to the roll pin. For these 5.56-mm ammunition types, the accuracy is slightly less than the values just indicated. Even though the AEF was constructed in 1943, it remains the most accurate spark range in the world.

2.3 Launch Considerations

2.3.1 Gun Barrel

The M16A2 weapon (figure 7) was secured into either a hard or recoil mount. Due to the requirements of other testing that used these ammunition types, the mount was modified as the testing progressed. For the Mach 1.2 shots, an M4 weapon was secured in the recoil mount.

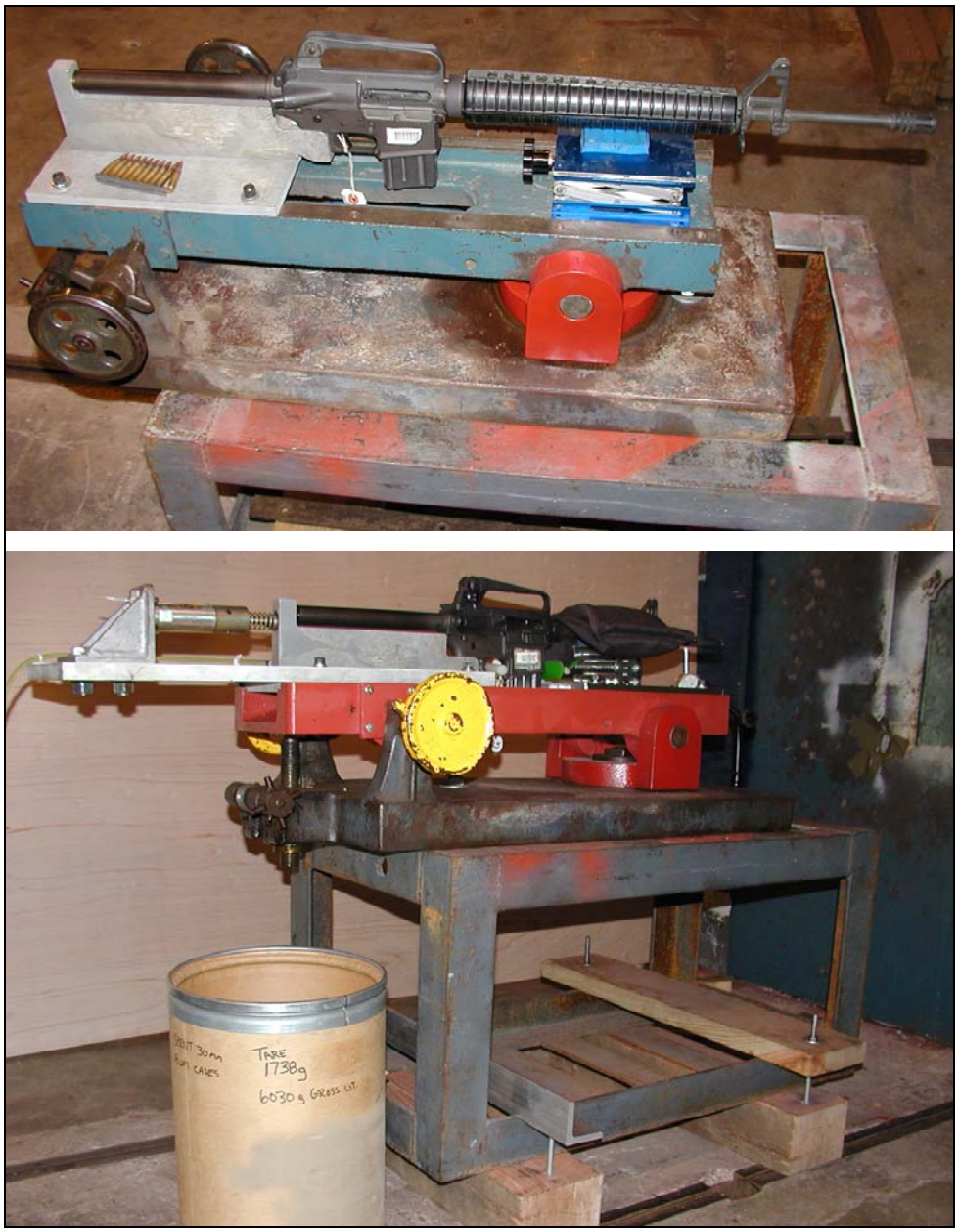

Figure 7. M16A2 weapon mounted in original hard mount and recoil mount.

Neither mount appeared to affect the aerodynamics or flight dynamics of the projectile. Both weapon barrels had an interior bore diameter of 5.56 mm and a gun twist of 1 revolution in 7 inches (1-in-7 twist). The difference between the weapons is that the M16A2 barrel is 20 in long, while the M4 barrel is only 16 in long. The shorter barrel made it easier to consistently obtain the lower velocity. The flash suppressor was used at all times on both weapons. The mounts allowed for adjustments in gun aim point to ensure projectile travel through the entire range and for easy barrel swap. Both mounts provided support under the barrel. Additionally, a

20-lb shot bag was placed on top of the barrel to simulate a soldier holding the weapon (not shown in hard mount). Initially, the weapon was fired remotely using a lanyard on the trigger. This was modified to a hydraulic-controlled system to eliminate the possible jerking of the weapon due to the lanyard (again, this does not affect the aerodynamics of the projectile in flight but possibly produces more consistent launch dynamics).

2.3.2 Charge Establishment

A charge establishment study was conducted prior to firing the actual test in order to determine a nominal charge weight for each desired velocity. The primed cases were standard M855 cartridge cases, and the standard WC844 powder was used for the higher velocities. For the lower velocities, it was necessary to use a faster burning powder (IMR 4198) to help ensure that consistent velocities were obtained. Additionally, at the lowest velocities, when the cartridges cases were only partially full, either tissue paper or 0.125-in-thick pink foam discs, 0.3125 inch in diameter, were used as ullage to provide for a more consistent powder burn. The approximate charge weights required to obtain the desired midrange velocities are shown in table 3.

Table 3. Nominal charge weights for M855.

Velocity	Propellant	Charge Weight (gr)
Mach 2.6	WC844	26.1
Mach 2.2	WC844	23.9
Mach 1.7	IMR 4198	13.2
Mach 1.5	IMR 4198	10.6
Mach 1.2	IMR 4198	9.5

2.3.3 Launch Yaw Control

In order to obtain nonlinear aerodynamic coefficients, it is necessary to measure the flight dynamics across a characteristic spread of the anticipated flight yaw. To ensure a spread in yaw levels, a standard technique used in spark range testing is to produce variability in yaw with a yaw inducer.

The range of first maximum yaw values varied between Mach numbers. For the M855, only the Mach 1.2 shots achieved the required spread of first maximum yaw without yaw induction. For the remainder of the downrange Mach numbers investigated, a yaw inducer was used to increase the launch yaw spread. During a previous study of 5.56-mm ammunition types, multiple half-moon-type inducers were tried with minimal success. It was found that one or more pieces of cardboard, angled at 45° and spaced 1 in apart (when more than one sheet was used), provided the most consistent yaw induction (figure 8). Table 4 lists those shots that used a yaw modifier.

Figure 8. Angled cardboard setup for yaw induction.

Table 4. List of shots that used a yaw modifier.

Shot No.	Mach No.	Pieces of Cardboard
26831	2.2	2
26832		3
26833		3
26834		3
27350	1.7	4
27351		4
27352		4
27353		4
28104	1.5	1
28105		1
28106		1
28107		1

2.4 Data Analysis

Extraction of the aerodynamic coefficients and dynamic derivatives is the primary goal in analyzing the trajectories measured in the AEF spark range. The process is summarized in figure 9 and is accomplished with the Aeroballistics Research Facility Data Analysis System (ARFDAS) code (*3*). ARFDAS incorporates a standard linear theory analysis (*4*, *5*) and a 6-degrees-of-freedom (6-DOF) numerical integration technique (*6*). The 6-DOF routine incorporates the maximum likelihood method (MLM) to match the theoretical trajectory to the experimentally measured trajectory. The MLM is an iterative procedure that adjusts the aerodynamic coefficients to maximize a likelihood function. Using this likelihood function eliminates the inherent assumption in least squares theory that the magnitude of the measurement noise must be consistent between dynamic parameters (regardless of units). In general, the aerodynamic coefficients can be nonlinear functions of the angle of attack (AOA), Mach number, and aerodynamic roll angle.

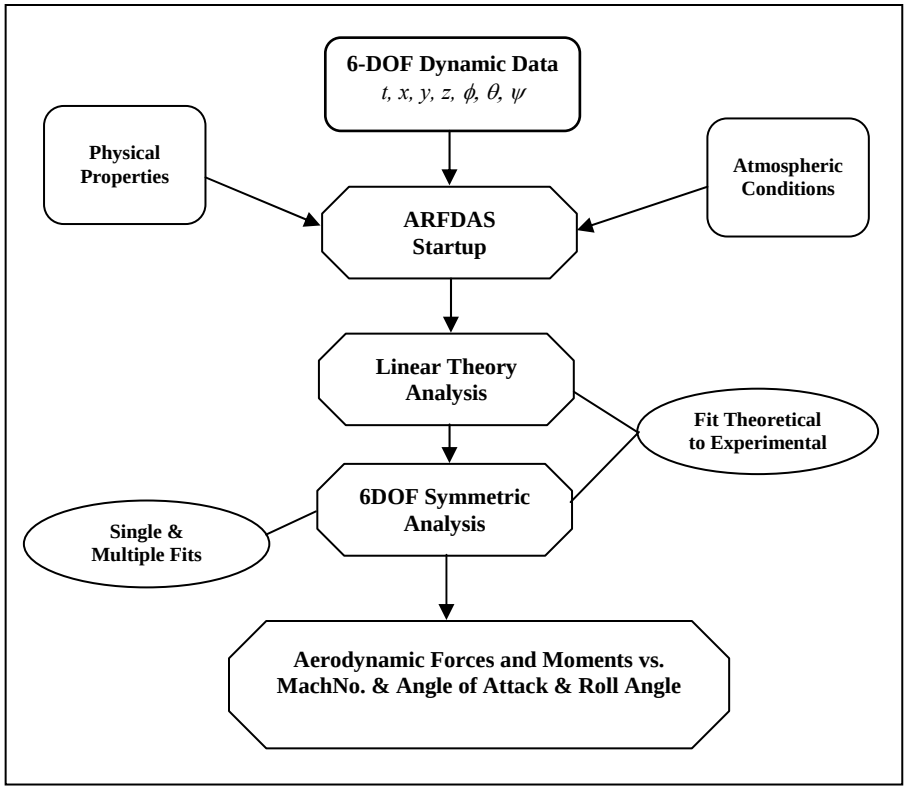

Figure 9. ARFDAS parameter identification process.

ARFDAS represents a complete ballistics range data reduction system capable of analyzing symmetric and asymmetric bodies. Within ARFDAS, each data round was first analyzed individually; then, rounds were combined in appropriate Mach number groups for simultaneous analysis via the multiple fit capability. Multiple fits are also used to extract the nonlinear aerodynamic coefficients as a function of yaw and Mach number dependence.

As part of the data reduction, ARFDAS provides an estimate of the fast- and slow-mode damping estimates. Additionally, an estimate of the Magnus bounds from which any Magnus moment instability can be determined is also given. Both of these estimates are for the projectile spin rate in the given shot. Note the projectile is not spin-matched at muzzle exit for the downrange velocities as it is fired from an M16, not a high-twist barrel. Therefore, the nondimensional spin rate is below that which the projectile would experience in flight.

3. Results and Discussion

3.1 Flow Analysis

Analyses of the spark shadowgraphs show minimal differences between the flow fields of the different velocities. Figures 10–13 show shadowgraphs for shots at Mach 1.47, 1.69, 2.21, and 2.61, respectively. At all speeds, a shock wave stands just off the nose tip of the projectile, with the distance between the shock and the nose tip decreasing with increasing Mach number such that the shock looks almost attached at Mach 2.6. Additionally, the shock angle becomes smaller at higher Mach numbers, as expected. The turbulent wake flow evident behind the base remains consistent between Mach numbers. No shadowgraph is shown for shots at Mach 1.2 as it is very similar to that at Mach 1.47, only the shock angle further decreases.

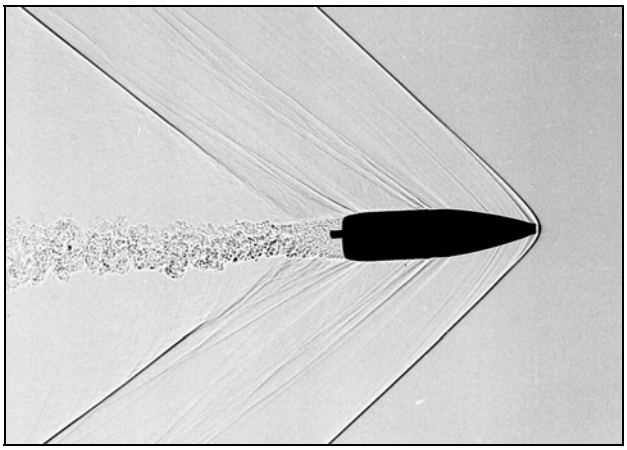

Figure 10. Spark shadowgraph picture, shot 28096, station 40H, Mach 1.47.

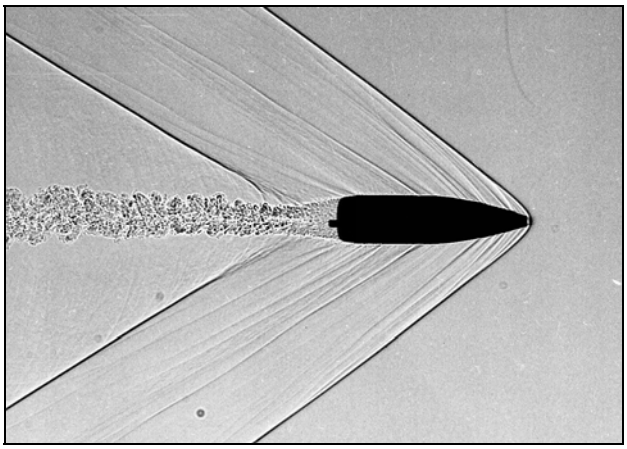

Figure 11. Spark shadowgraph picture, shot 27353, station 15H, Mach 1.69.

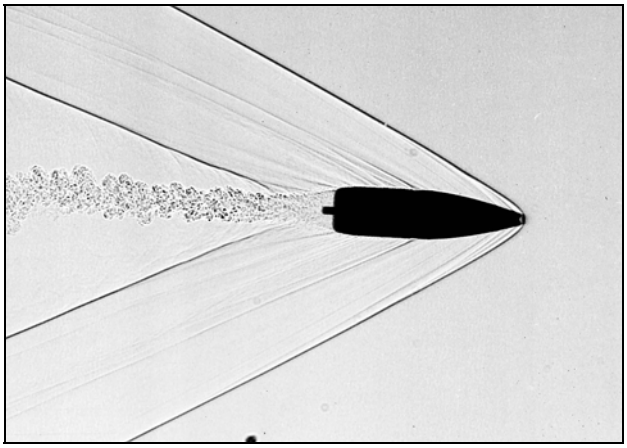

Figure 12. Spark shadowgraph picture, shot 26833, station 15H, Mach 2.21.

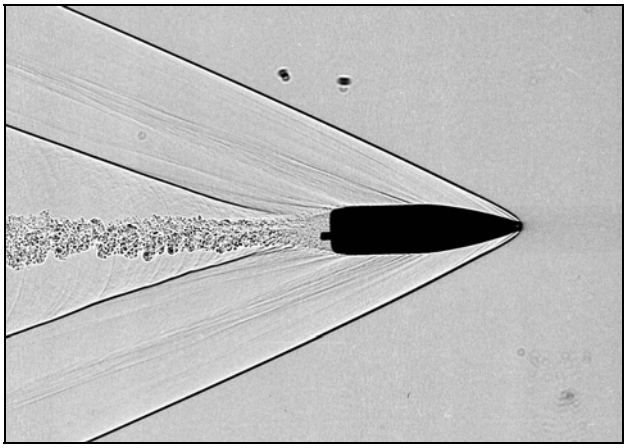

Figure 13. Spark shadowgraph picture, shot 26598, station 45H, Mach 2.61.

3.2 Trajectory Analysis

The aerodynamic coefficients listed in table 5 were the set of fitted parameters in the 6-DOF analysis. Additional parameters of interest from the 6-DOF analysis are listed in table 6. The commonly used second-order aerodynamic expansions relating total, zero yaw, and yaw-induced coefficients for the nonlinear analysis are presented in reference *4*. Figure 14 defines the total positive aerodynamic coefficients relative to the projectile. Note the pitch-damping coefficient is not shown.

Table 5. Aerodynamic coefficients used in 6-DOF analysis.

Variable	Description
C_X	Axial force coefficient
C_{X_0}	Zero-yaw axial force coefficient
C_{X_2}	Yaw axial force coefficient
C_{m_α}	Overturning moment coefficient derivative
$C_{m_{\alpha_0}}$	Zero-yaw overturning moment coefficient derivative
$C_{m_{\alpha_3}}$	Cubic overturning moment coefficient derivative
C_{N_α}	Normal force coefficient derivative
$C_{m_q} + C_{m_{\dot{\alpha}}}$	Pitch-damping moment coefficient
C_{l_p}	Roll-damping coefficient
C_{n_p}	Magnus moment coefficient
$C_{n_{p\alpha}}$	Magnus moment coefficient derivative
$C_{n_{p\alpha_0}}$	Zero-yaw Magnus moment coefficient derivative
$C_{n_{p\alpha_3}}$	Cubic Magnus moment coefficient derivative

Table 6. Other 6-DOF analysis parameters of interest.

Variable	Description	Units
$\overline{\alpha}$ (alpha bar)	Total yaw	Degrees
α_{max}	Maximum yaw	Degrees
$\overline{\delta}$	Mean yaw	Degrees
$\overline{\delta}^2$	Mean squared yaw	Degrees squared
ϕ (phi)	Roll angle	Degrees
θ (theta)	Pitch angle	Degrees
ψ (psi)	Yaw angle	Degrees
X_{CP}	Normal force center of pressure	Calibers
PE_x	Probable error in x	Meters
PE_{yz}	Probable error in y-z	Meters
$PE_{\psi\theta}$	Probable error in ψ - θ	Degrees
PE_ϕ	Probable error in ϕ	Degrees

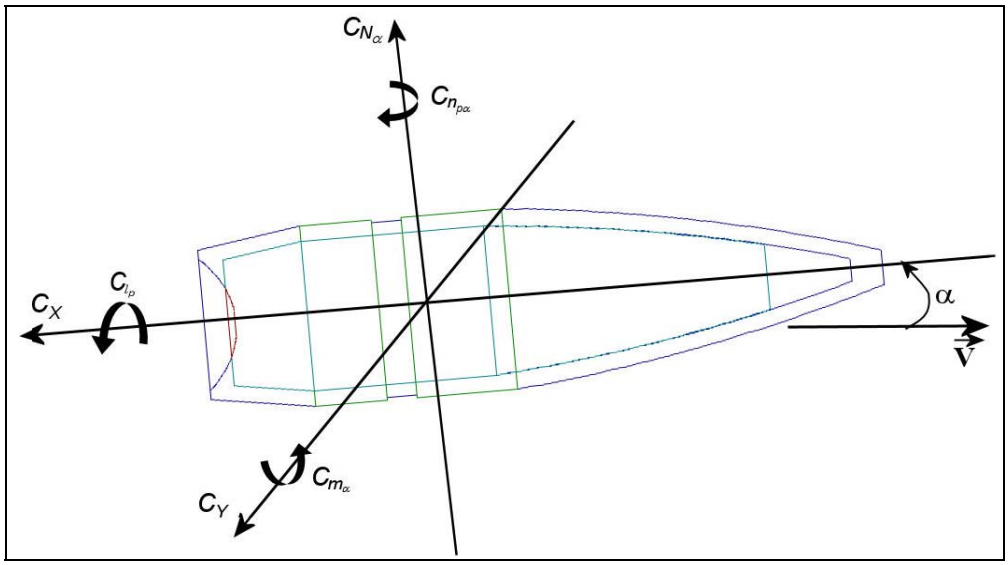

Figure 14. Total aerodynamic coefficient definition relative to projectile.

From the film reading, the actual projectile motion is known (i.e., the raw data). During the ARFDAS reduction, the projectile motion based on the aerodynamic model, as determined by the 6-DOF fit for each round, is simulated. Figures 15–23 are a complete set of motion plots for shot 28097, an M855 projectile at Mach 1.47 (simulated 500-m range). In each figure, the circles represent the raw data and the solid line represents the 6-DOF fit. A complete set of motion plots is presented in appendix A for a representative round at each Mach number.

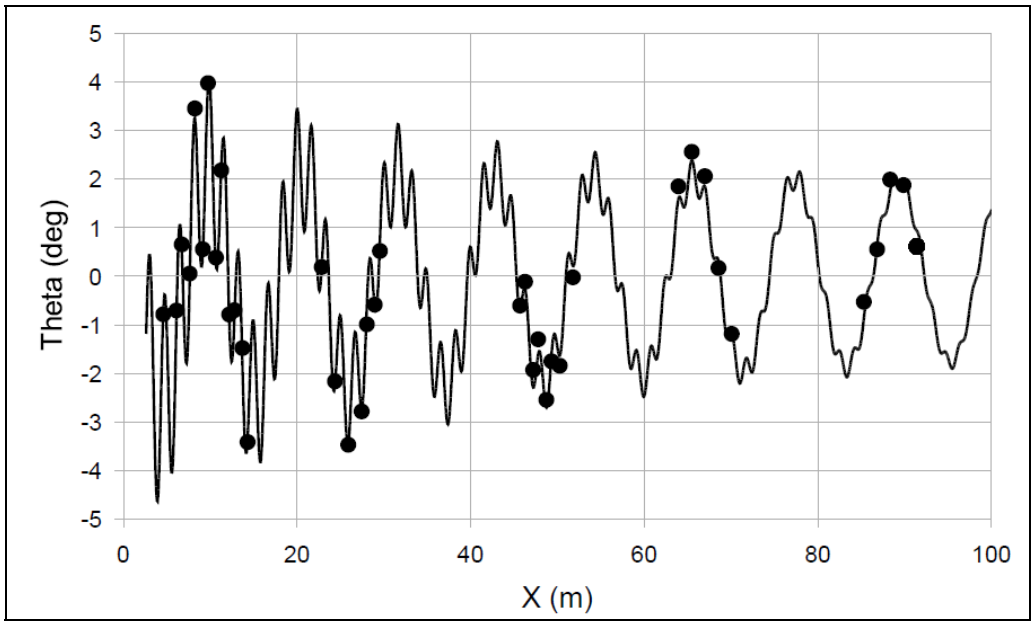

Figure 15. Pitch angle vs. range for round 28097 (M855 at Mach 1.47).

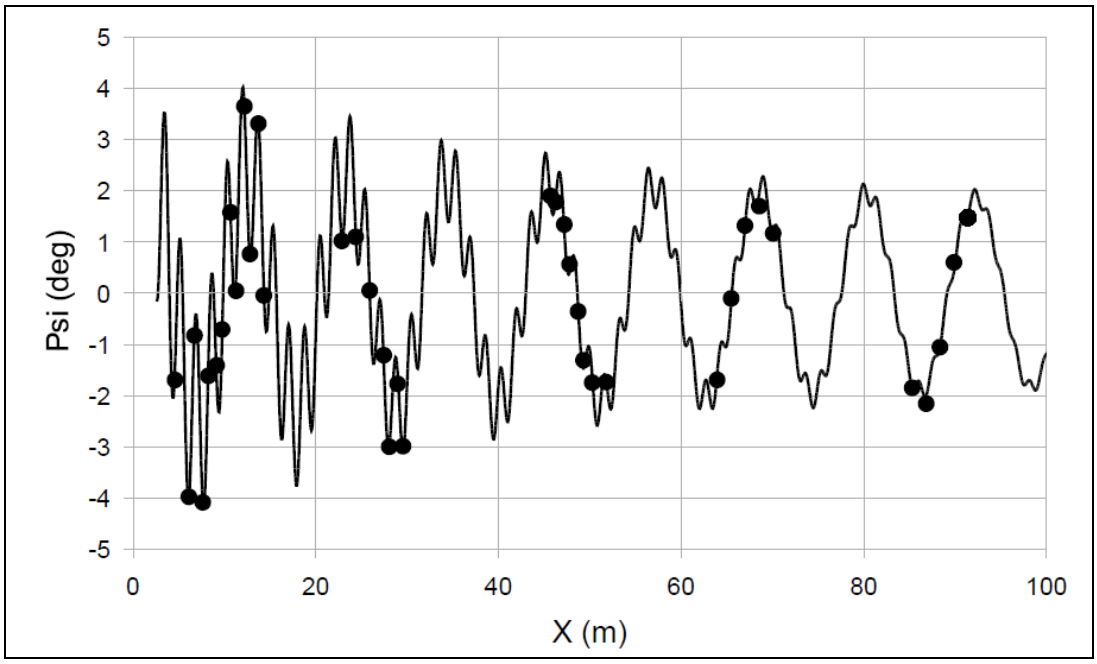

Figure 16. Yaw angle vs. range for round 28097 (M855 at Mach 1.47).

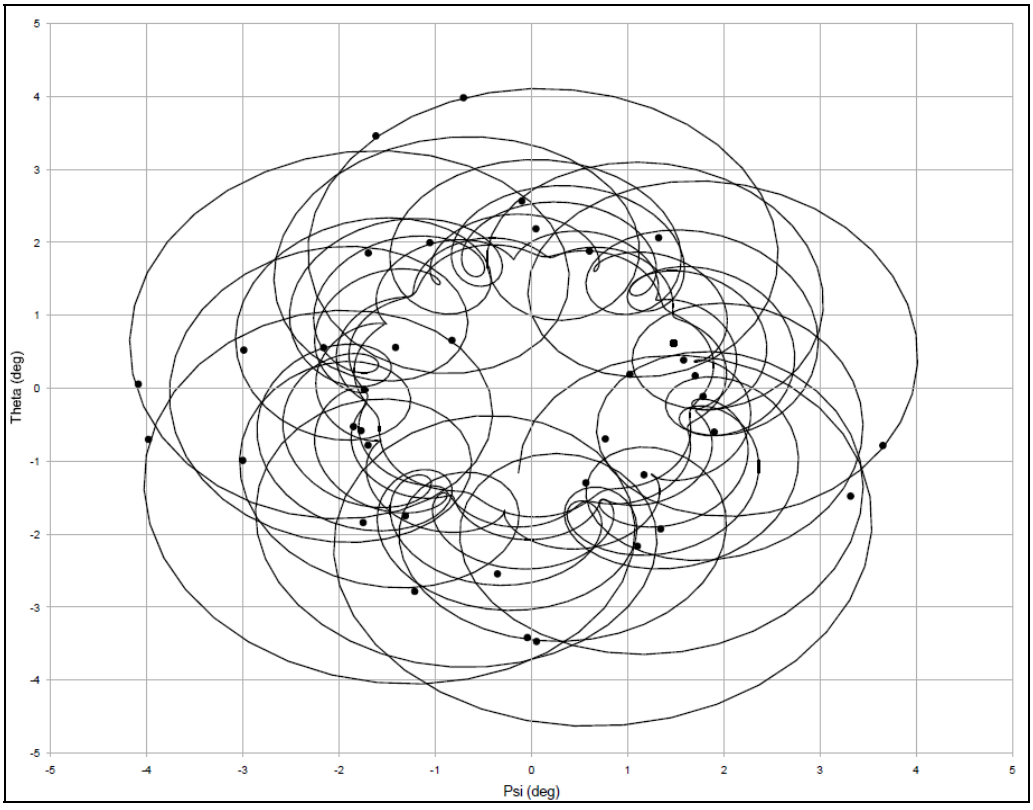

Figure 17. Pitch angle vs. yaw angle for round 28097 (M855 at Mach 1.47).

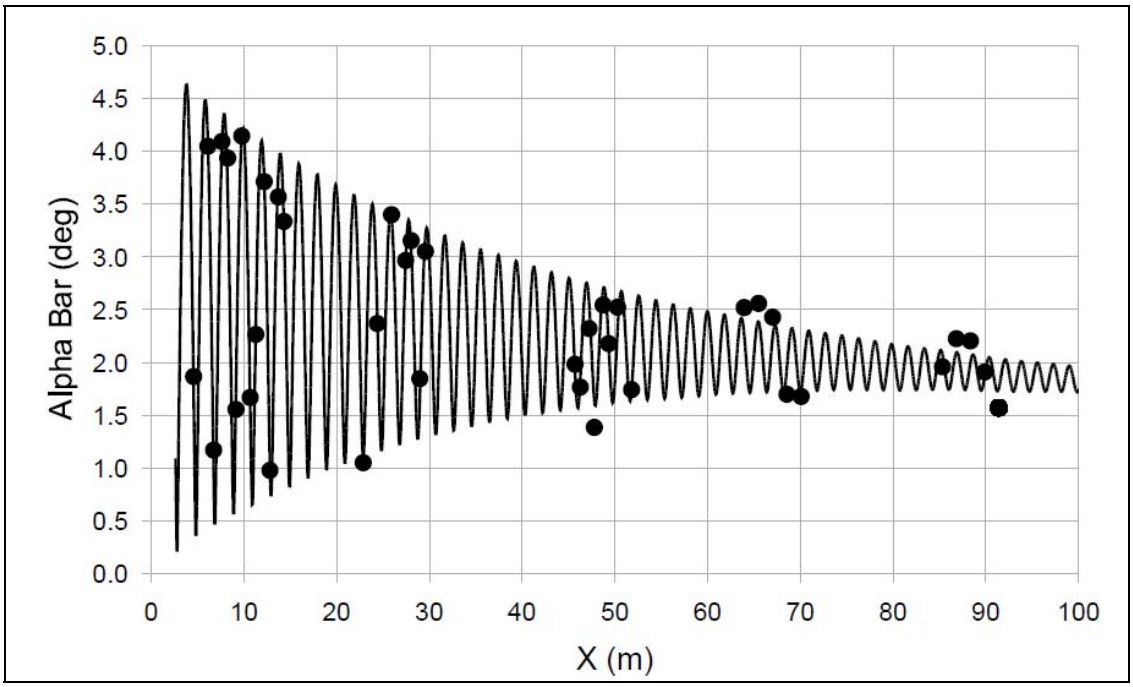

Figure 18. Total yaw vs. range for round 28097 (M855 at Mach 1.47).

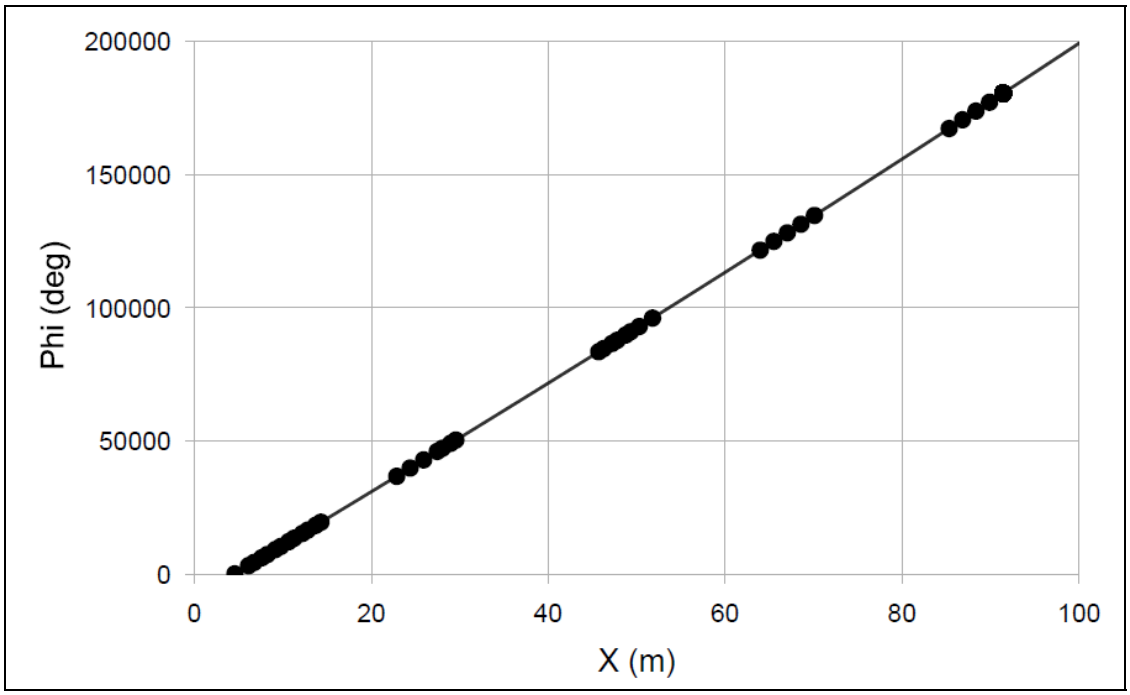

Figure 19. Roll angle vs. range for round 28097 (M855 at Mach 1.47).

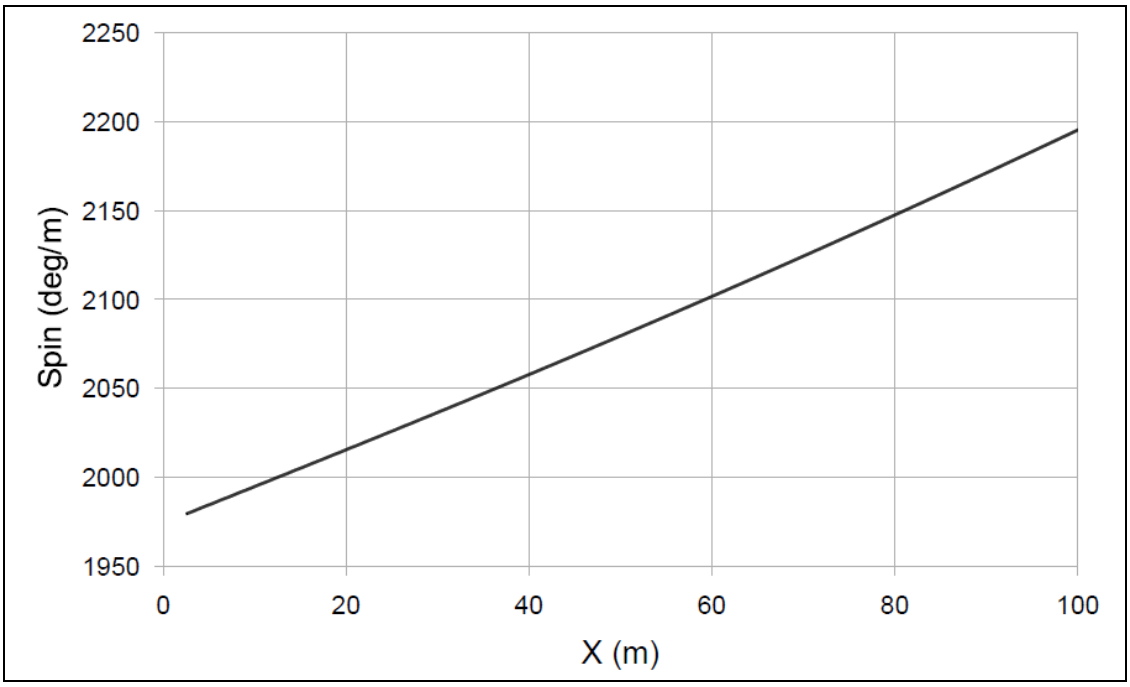

Figure 20. Spin vs. range for round 28097 (M855 at Mach 1.47).

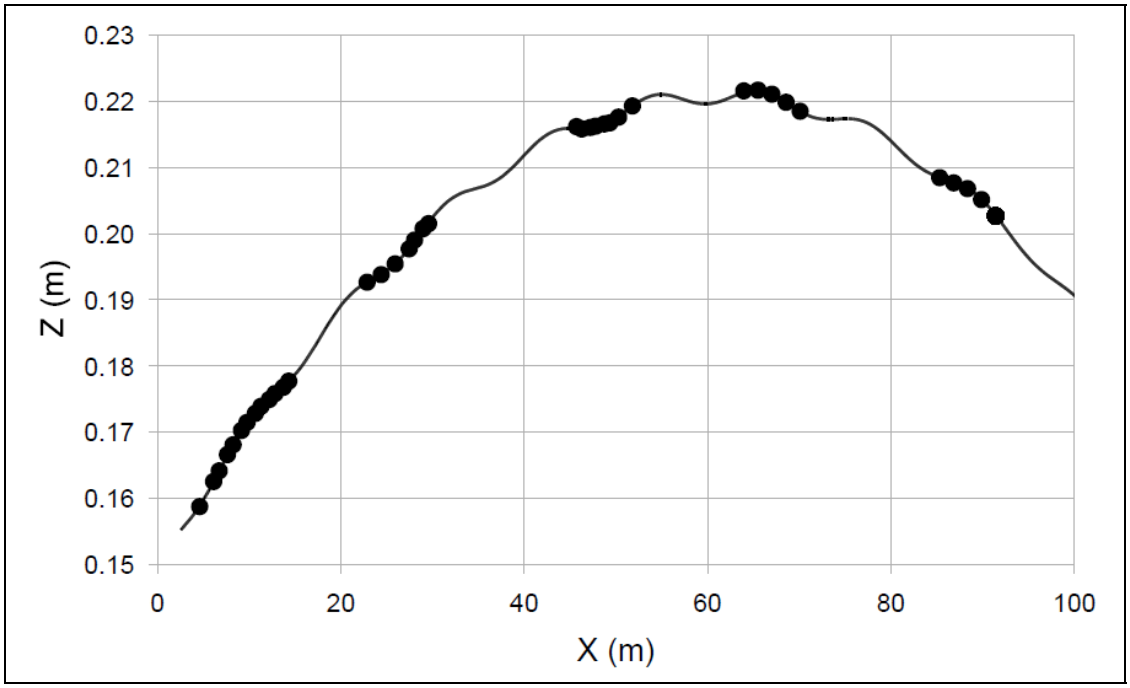

Figure 21. Vertical position vs. range for round 28097 (M855 at Mach 1.47).

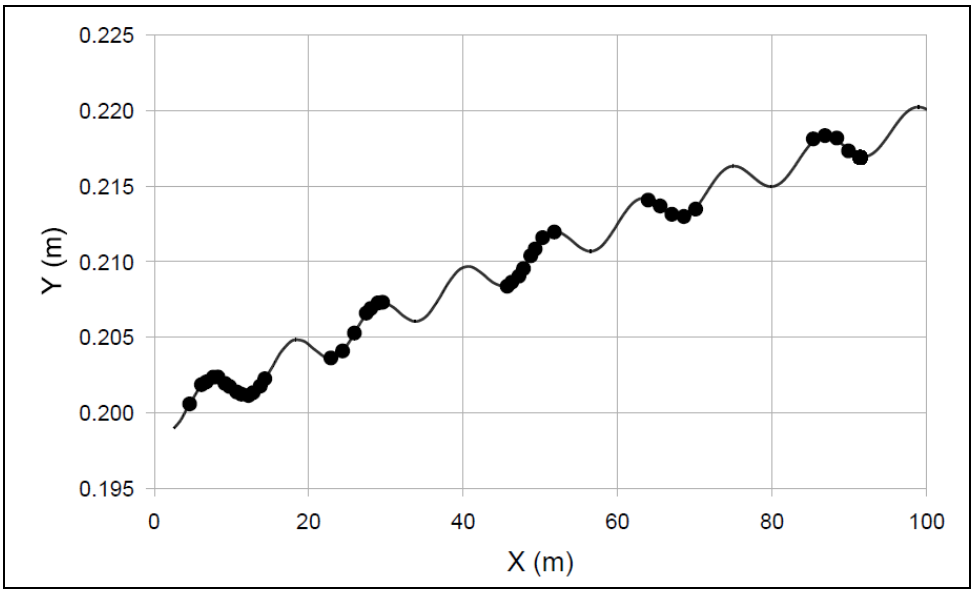

Figure 22. Lateral position vs. range for round 28097 (M855 at Mach 1.47).

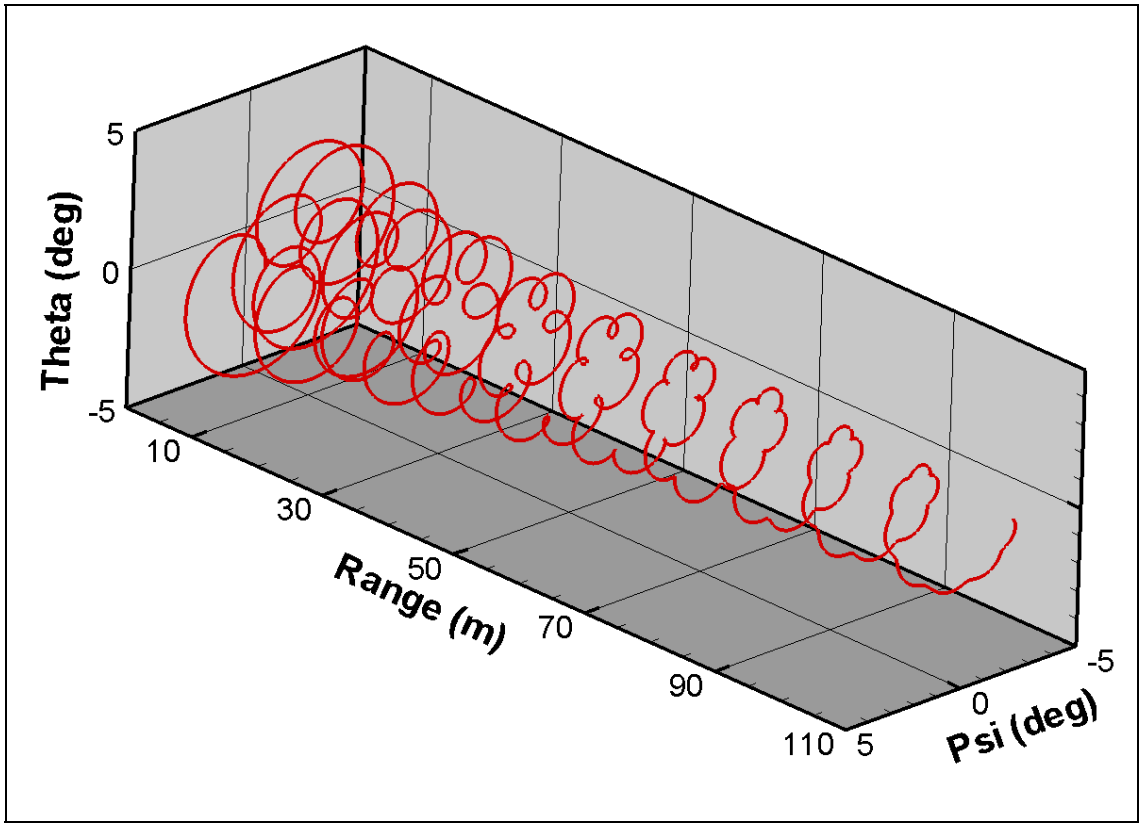

Figure 23. Three-dimensional projectile motion through the range for round 28097 (M855 at Mach 1.47).

The probable errors for the final ARFDAS multiple shot group fits at each Mach number are shown in table 7. The multiple fits were separated into high and low yaw groupings because the nonlinear characteristics of the projectiles were dependant on yaw. Some groups have a very limited yaw variation, thus making it difficult to determine the nonlinear coefficients. The group at Mach 2.46 was created using shots at Mach 2.6 and 2.25 to result in an average of Mach 2.46. The aerodynamic coefficients resulting from these fits (both individual and group) are able to reproduce the flight of the projectile observed in the range.

Table 7. Probable error for final group fit analyses.

Mach No.	$\bar{\delta}^2$ (degree^2)	PE_x (m)	PE_{yz} (m)	$PE_{\psi\theta}$ (degree)	PE_{ϕ} (degree)
2.62	2.97	0.0003	0.0004	0.3166	5.1636
2.46	6.10	0.0003	0.0002	0.2661	7.1820
2.24	6.27	0.0003	0.0002	0.2517	5.0596
2.21	6.68	0.0004	0.0002	0.2752	6.3327
1.68	28.08	0.0005	0.0003	0.2496	11.2821
1.70	6.00	0.0005	0.0002	0.2304	6.2651
1.47	10.61	0.0004	0.0001	0.2116	6.0615
1.49	6.73	0.0004	0.0001	0.2405	4.4380
1.18	13.04	0.0005	0.0001	0.2146	5.1990

3.3 Spin Rates

Spin rates were obtained as a function of range position from fits to the roll pin data, when available. When unavailable, due to lack of roll pin (as was the case for seven projectiles), the initial spin rate and roll-damping coefficient is prescribed using the results from the group fits at a similar Mach number. At each of the downrange velocities investigated, the projectile is in an underspun condition, i.e., it is spinning at a slower rate than it would be had it been launched at full spin and velocity and allowed to arrive at the downrange velocity with drag and roll damping. The underspun condition occurs because although the downrange velocity is approximately matched, the projectile is being launched from a standard M16A2 (or M4) barrel with a twist rate of 1-in-7. In order to match the spin that occurs at the downrange velocities, higher twist barrels would have to be used (e.g., 1-in-6, 1-in-5, etc.). Previous computational and experimental works (*7*, *8*) have shown that small changes in spin rate, such as these, have minimal effect on the aerodynamic behavior of 5.56-mm projectiles. To date, the effect on the flight dynamic behavior has not been characterized.

3.4 Aerodynamic Coefficients

The results of the multiple shot group fits are presented, analyzed, and compared here. The aerodynamic coefficients obtained from the multiple shot group fits are listed in table 8. The results of all individual shots and multiple shot groups can be found in appendix B.

Table 8. Multiple shot group fit aerodynamic coefficients.

Mach No.	$\overline{\delta}^2$	C_{X_0}	C_{X_2}	C_{N_α}	$C_{m_{\alpha_0}}$	$C_{m_{\alpha_3}}$	$C_{n_{p\alpha_0}}$	$C_{n_{p\alpha_3}}$	$C_{m_q} + C_{m_{\dot{\alpha}}}$	C_{l_p}
2.62	2.97	0.29	3[a]	2.93	2.45	–3[a]	0.32	0[a]	–15.74	–0.026
2.46	6.1	0.33	3.82	2.89	2.53	–4[a]	0.19	0[a]	–11.82	–0.026
2.23	6.13	0.32	2.31	2.92	2.54	–4.98	0.02	25.52	–11.43	–0.025
1.68	28.08	0.38	2.30	2.97	2.71	–1.98	0.07	8.08	–11.97	–0.028
1.47	13.29	0.40	4.37	2.87	2.76	–1.63	–0.20	22.13	–10.21	–0.030
1.18	13.04	0.45	3.36	2.72	2.81	11.77	–0.82	75.53	–8.54	–0.026

[a]Indicates that value was prescribed in 6-DOF fit.

The multiple fits for the aerodynamic coefficients were separated into high and low yaw groupings for each Mach number as some of the nonlinear coefficients (specifically, Magnus moment coefficient) varied depending on yaw levels. The nonlinear variation in $C_{n_{p\alpha}}$ was easy to recognize from the initial individual fits. By plotting $C_{n_{p\alpha}}$ against $\sin^2(\alpha)$ (figure 24), a change in the behavior of $C_{n_{p\alpha}}$ is noticeable at about $\alpha = 4.5°$ at Mach 1.5 and 1.7. For these Mach numbers, the high and low yaw groupings must be solved separately in order to obtain the best fit. Since the high yaw shots provided a better fit for the nonlinear coefficients, only those groupings are displayed in the table. This bimodal behavior was not apparent at any other Mach number. Therefore, only one grouping was created for the multiple fit in ARFDAS. There were enough good shots to create two groupings at Mach 2.2, even though the mean yaw was similar. The differences in aerodynamic coefficients between the two groups are the approximate error associated with that coefficient, and, therefore, only one set of coefficients is presented.

Figure 25 shows the axial force coefficient as a function of Mach number for both the current test data and previous data from the earlier study conducted by Robert McCoy (*1*). Total axial force, defined as

$$C_X = C_{X_0} + C_{X_2}\overline{\delta}^2 , \tag{1}$$

in which $\overline{\delta}^2$ is the value determined by ARFDAS for the group fit (converted to radians squared), appears to decrease slightly as the Mach number increases. The current test data coincides with McCoy's values, and both data sets behave as expected. The small discrepancies between McCoy's values and the current data set can easily be accounted for by using C_X rather than McCoy's C_D, though they are approximately equal for the small angles found here. The axial forces decrease slightly as the Mach numbers increase out of the high drag transonic regime. The trend of zero-yaw axial force as a function of Mach number (figure 26) is quite similar to that of C_X, indicating that similar yaw levels are achieved for all the shots. The small difference in value is accounted for by the yaw drag.

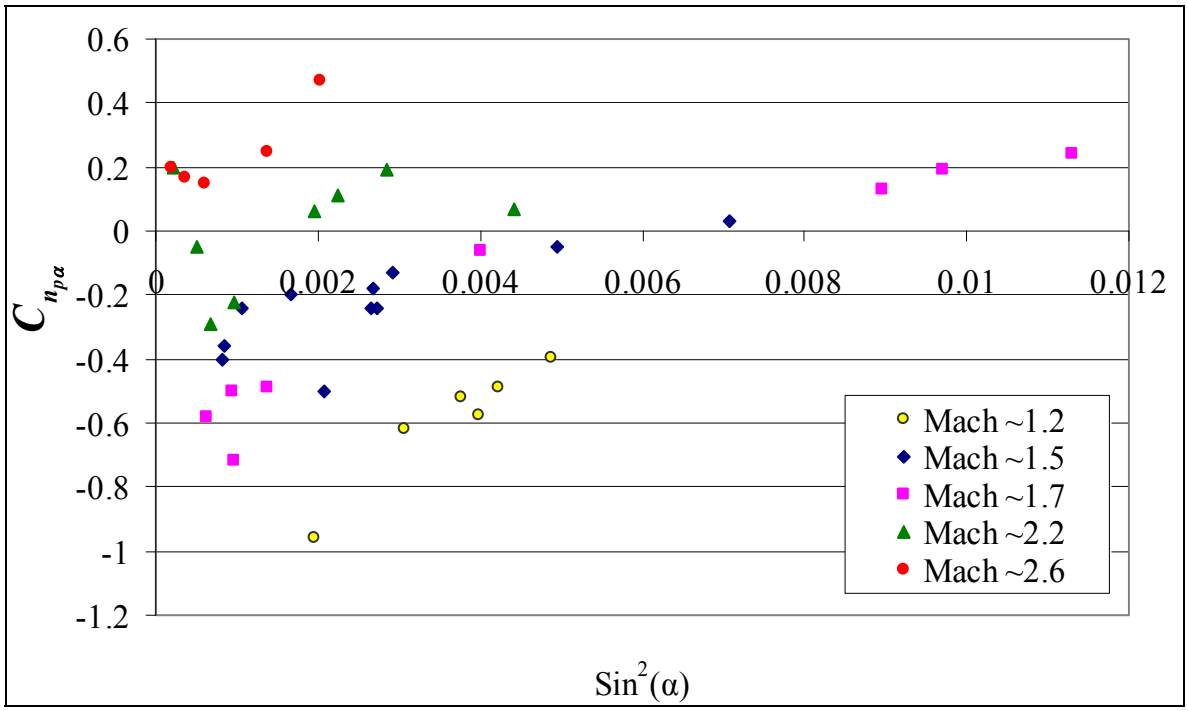

Figure 24. Preliminary Magnus moment coefficient plot to determine groupings for nonlinear characteristics.

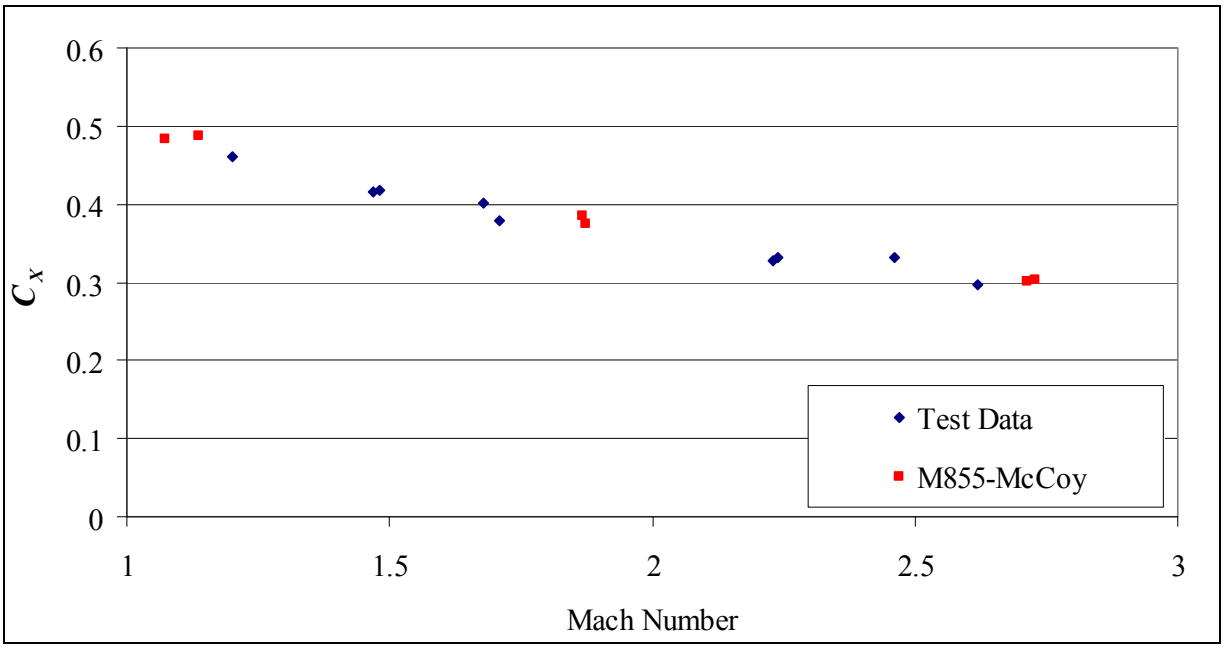

Figure 25. Total axial force coefficient vs. Mach number, group fits.

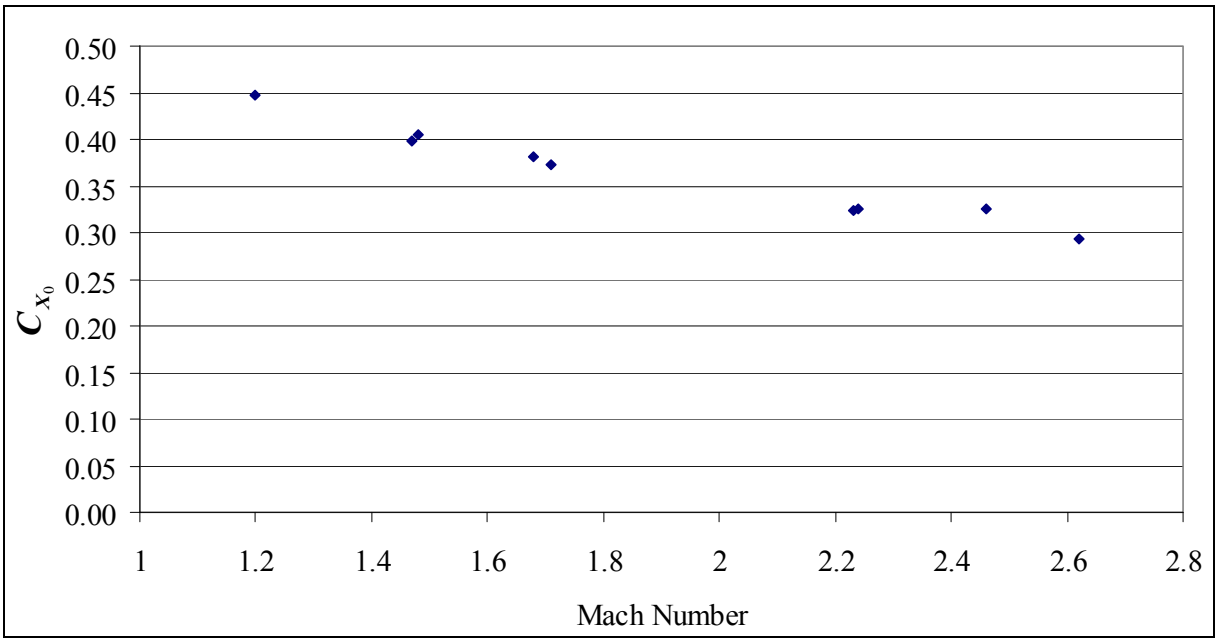

Figure 26. Zero-yaw axial force coefficient vs. Mach number, group fits.

The roll-damping coefficient, presented in figure 27, varies little with Mach number. With the exception of two low yaw groups at Mach 1.5 and 1.7, the coefficient only ranged from –0.025 to –0.03. The difference in C_{l_p} at Mach 1.5 is quite small and can easily be attributed to experimental error. It is unclear at this time what could be the cause of the larger C_{l_p} for the lower yaw grouping at Mach 1.7. At this time, no further explanation beyond experimental error is feasible.

Figure 28 shows the total pitching moment for the current test data and McCoy's data. Agreement between the two data sets is quite good, with the difference well within experimental error. As the Mach number increases, the pitching moment gradually decreases. Figures 29 and 30 illustrate the correlation of the linear pitching moment coefficient and cubic pitching moment coefficient vs. Mach number. While the linear pitching moment coefficient followed a similar trend as the overall pitching coefficient, the cubic pitching moment coefficient did not. It appears that the nonlinear pitching moment is relatively constant above Mach 1.5, with differences possibly due to variation in yaw levels. As the Mach number further decreases to Mach 1.2, there appears to be a drastic change in sign and magnitude for the nonlinear pitching moment. This indicates that the nonlinear behavior becomes a greater influence on the pitching moment as Mach 1 is approached, which is not unreasonable.

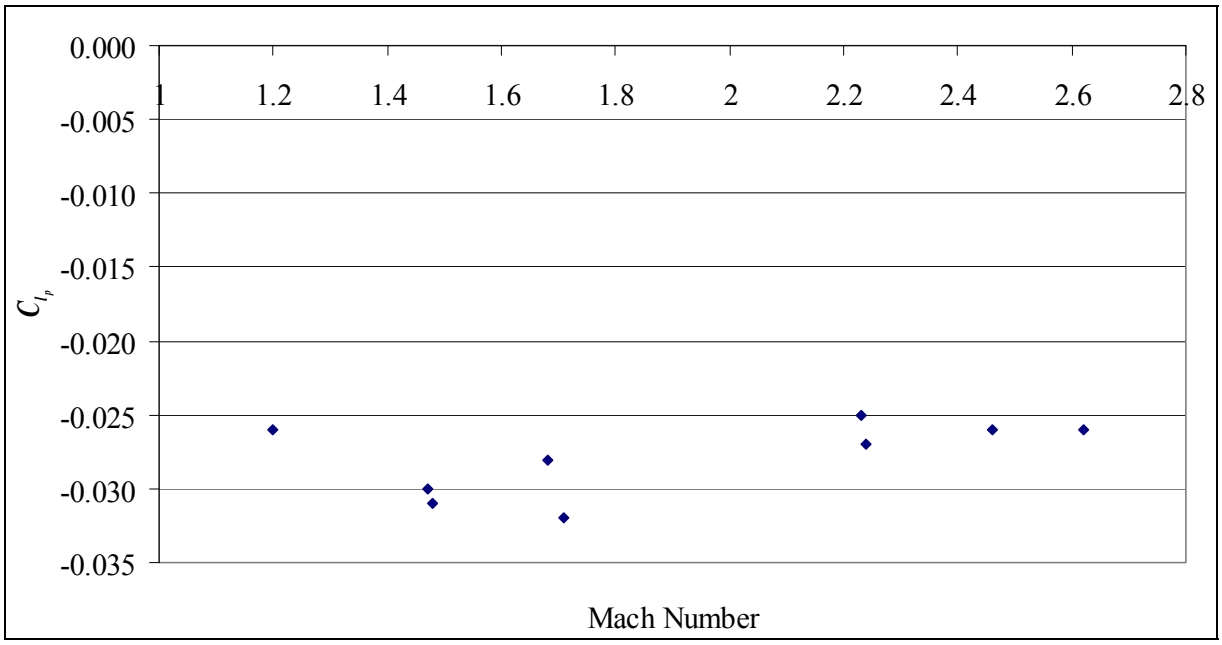

Figure 27. Roll-damping coefficient vs. Mach number, group fits.

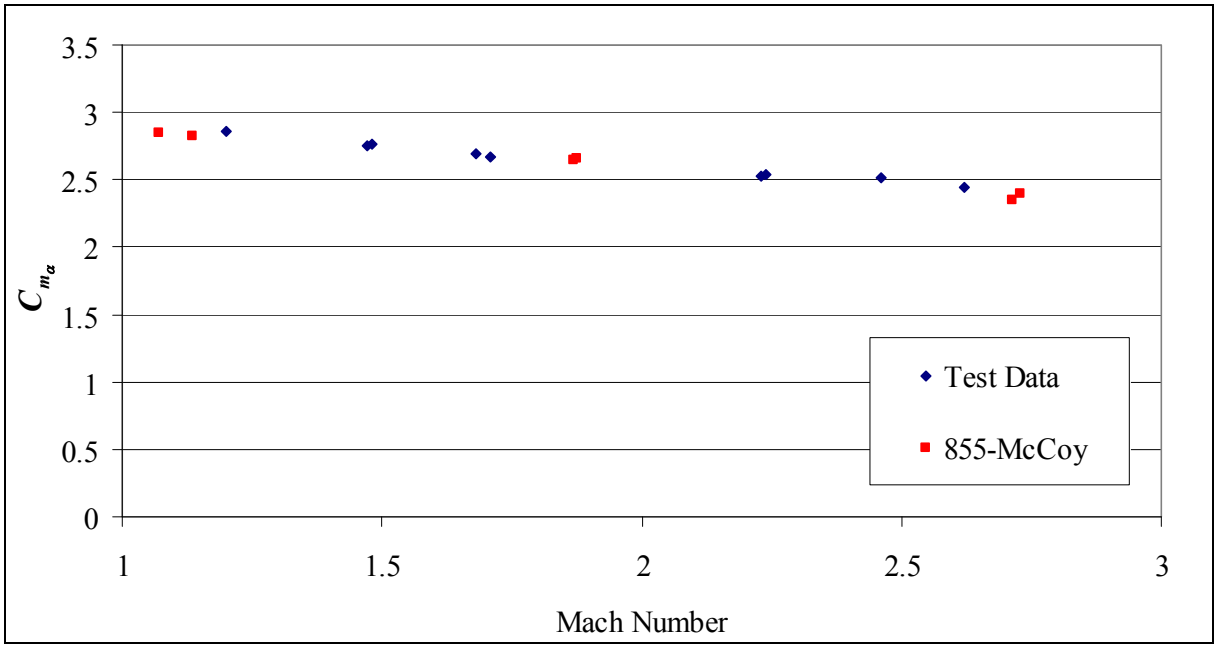

Figure 28. Total pitching moment coefficient vs. Mach number, group fits.

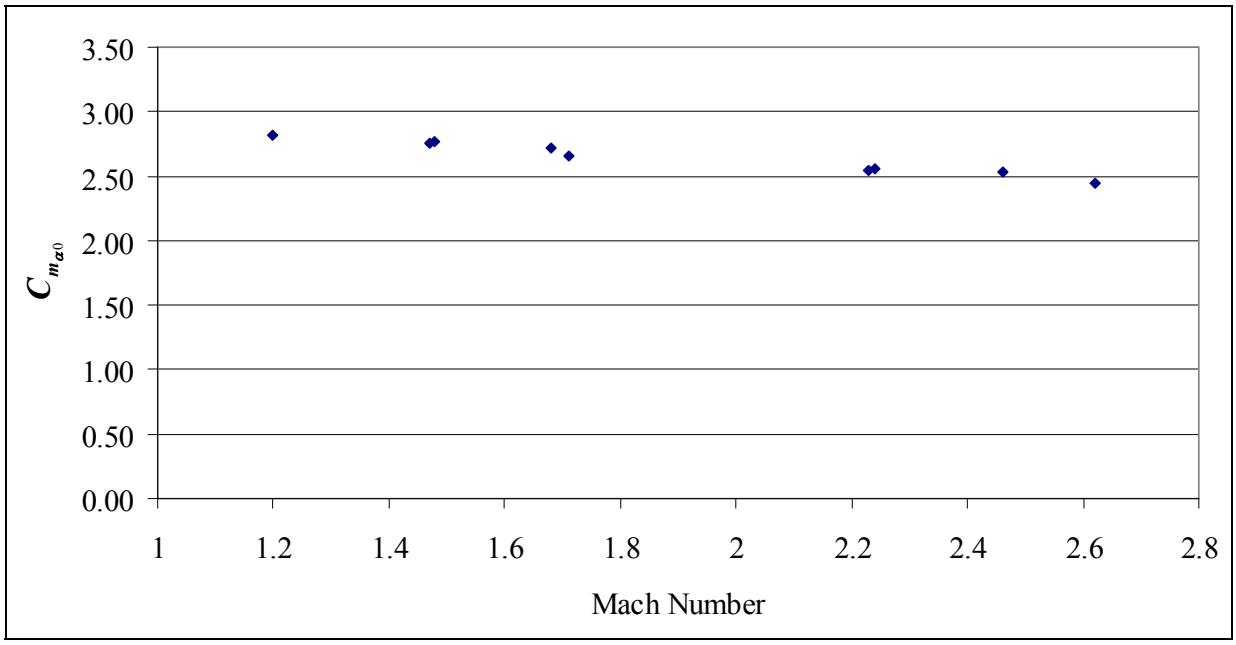

Figure 29. Linear pitching moment coefficient vs. Mach number, group fits.

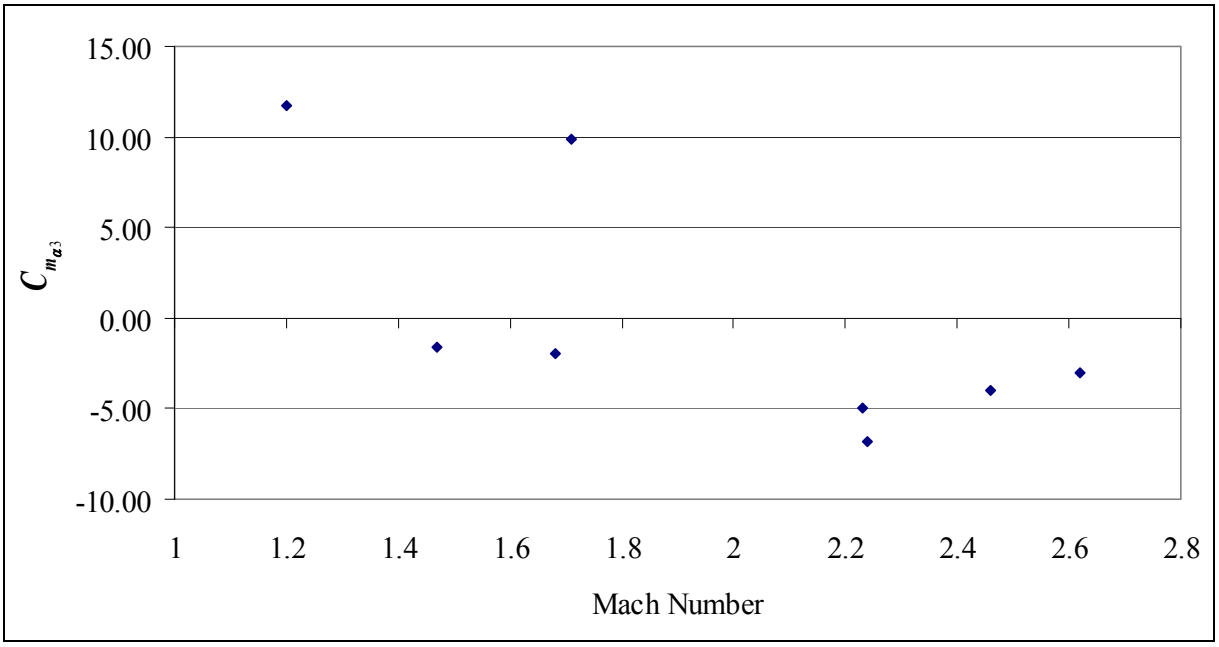

Figure 30. Cubic pitching moment coefficient vs. Mach number, group fits.

Figure 31 shows that the normal force coefficient does not vary significantly due to Mach number. However, groups at similar Mach numbers but different yaw levels did have varying results, though still within 10% (approximately the experimental error) of each other. A cubic normal force coefficient was investigated as a refinement of the normal force coefficient but was excluded from the final aerodynamic model for all shots because it did not improve the results. Therefore, C_{N_α} is equal to $C_{N_{\alpha_0}}$.

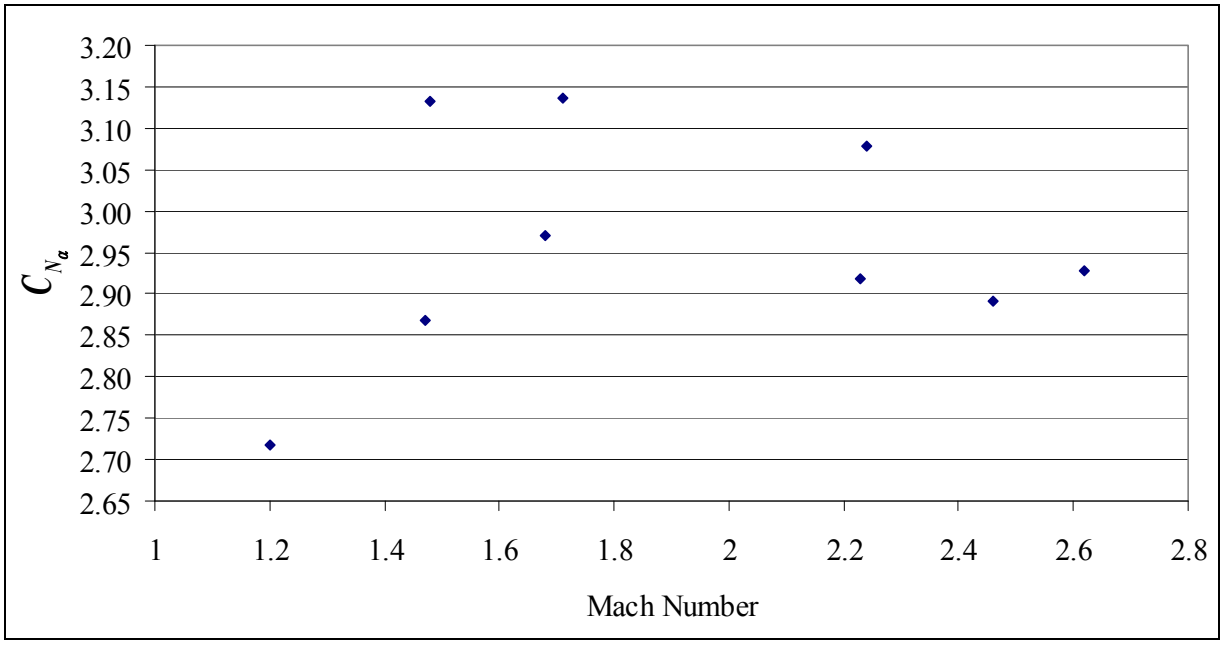

Figure 31. Normal force coefficient derivative vs. Mach number, group fits.

After C_{N_α} and C_{m_α} are determined, the normal force center of pressure, X_{CP}, is determined by the following:

$$c.g. - X_{CP} = \frac{C_{m_\alpha}}{C_{N_\alpha}}. \tag{2}$$

The results of equation 2 are plotted in figure 32. As the Mach number increases, the center of pressure very gradually shifts away from the center of gravity (c.g.).

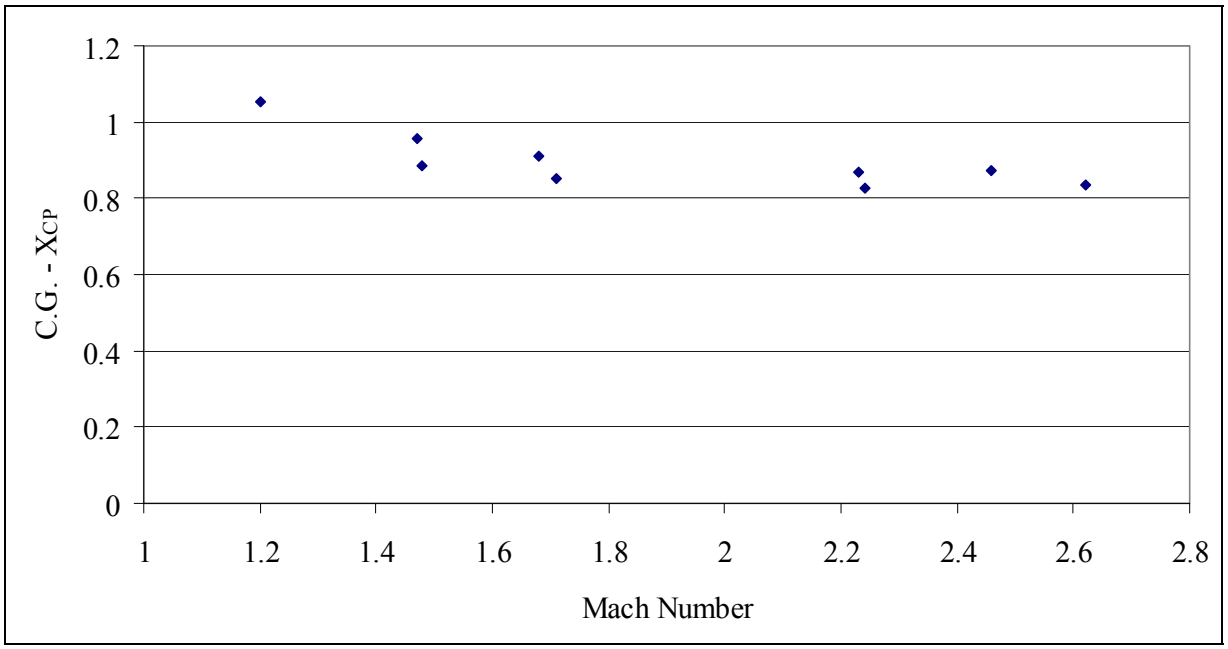

Figure 32. Normal force center of pressure vs. Mach number, group fits.

As equation 3 states, $C_{n_{p\alpha}}$ can be separated into a linear and a nonlinear term. The best projectile design will have the linear term, $C_{n_{p\alpha_0}}$, as near 0 as possible. Figure 33 shows the total Magnus moment coefficient vs. Mach number for the current test data and data collected by McCoy (*1*). There are some differences between the data sets. The differences can easily be accounted for through the different reduction techniques (McCoy is based on linear theory only). The linear and cubic Magnus moment coefficients can be seen in figures 34 and 35, respectively. Not all of the linear coefficients are negative, but the values are close to 0 for each group. While the cubic term at the highest Mach number was prescribed as 0, ARFDAS did, on occasion, provide a better fit for a shot when the cubic term was allowed. Only at the lowest Mach numbers (and low yaw groupings at Mach 1.5 and 1.7) did the nonlinear component become significant.

$$C_{n_{p\alpha}} = C_{n_{p\alpha_0}} + C_{n_{p\alpha_3}} \bar{\delta}^2 \ . \tag{3}$$

Figure 36 shows the pitch-damping coefficient as a function of Mach number for McCoy's data and the test data. Error bars indicate standard deviation predicted by ARFDAS and do not represent the bounds for the projectile. The positive pitch-damping coefficient for one of McCoy's data points is attributed to it being in the transonic regime. The point's proximity to 0 most likely represents the fact that there is simply no damping and the shot has reached its yaw limit cycle.

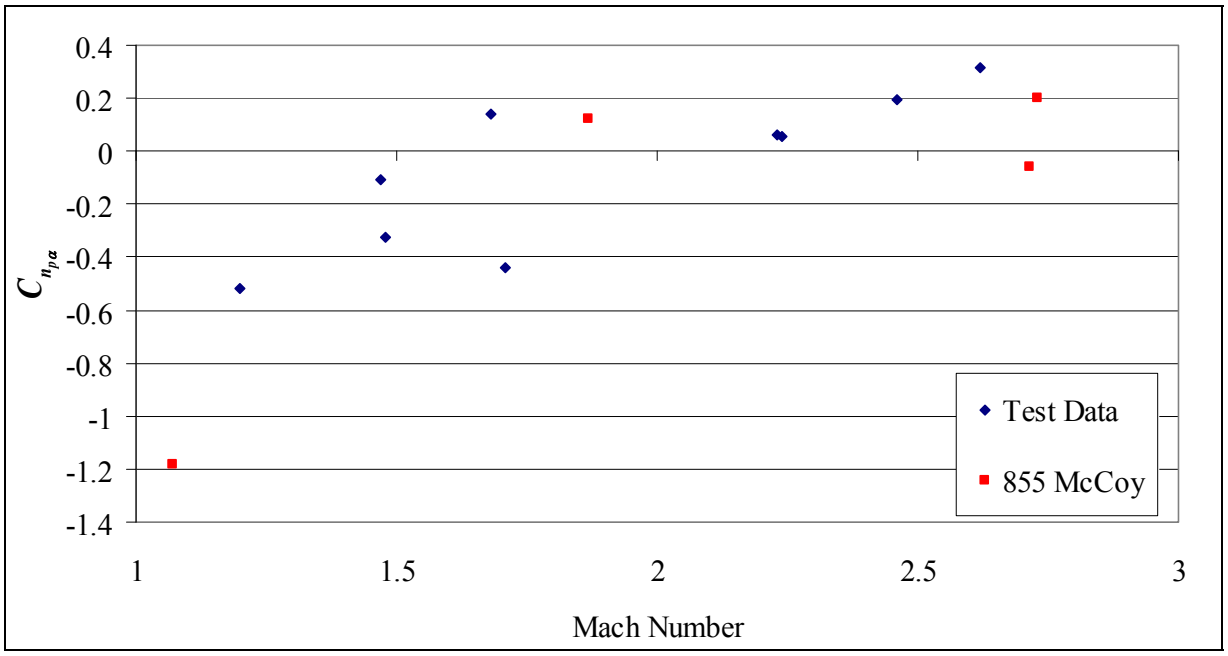

Figure 33. Magnus moment coefficient derivative vs. Mach number, group fits.

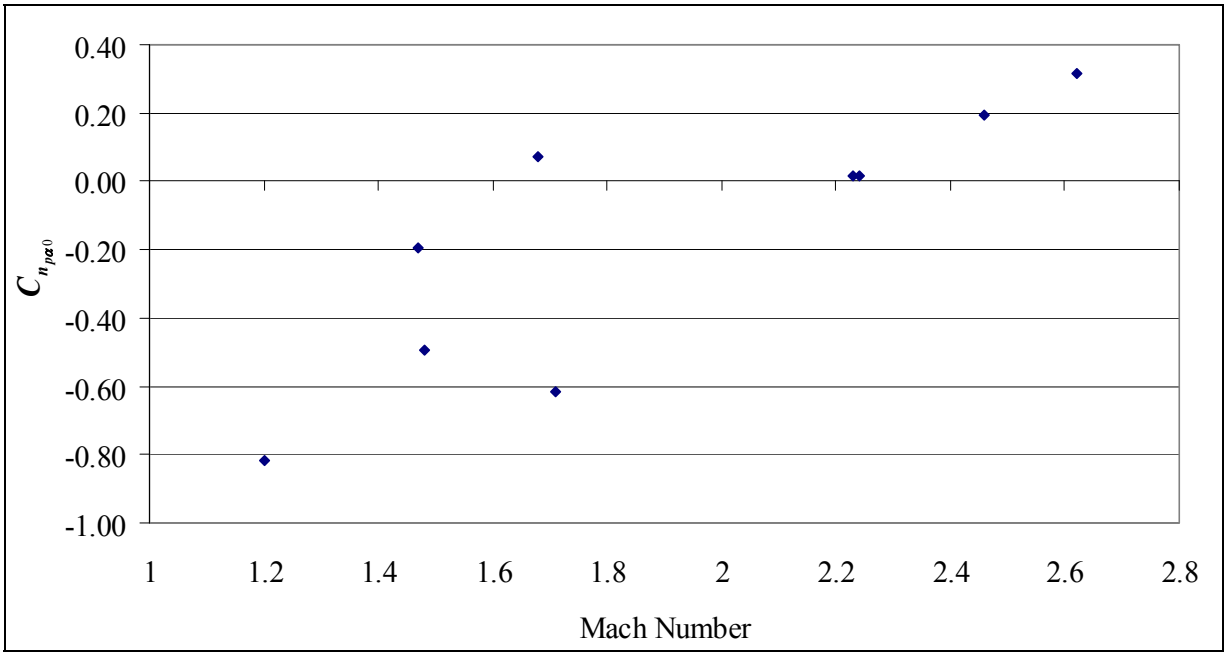

Figure 34. Zero-yaw Magnus moment coefficient derivative vs. Mach number, group fits.

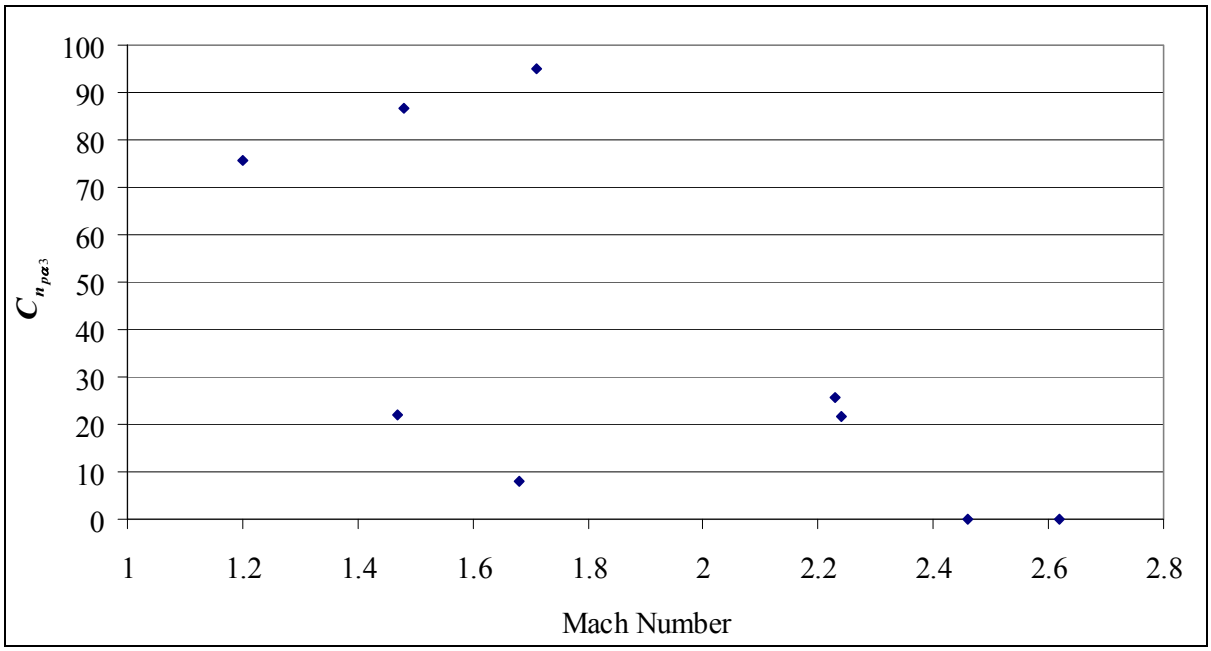

Figure 35. Cubic Magnus moment coefficient derivative vs. Mach number, group fits.

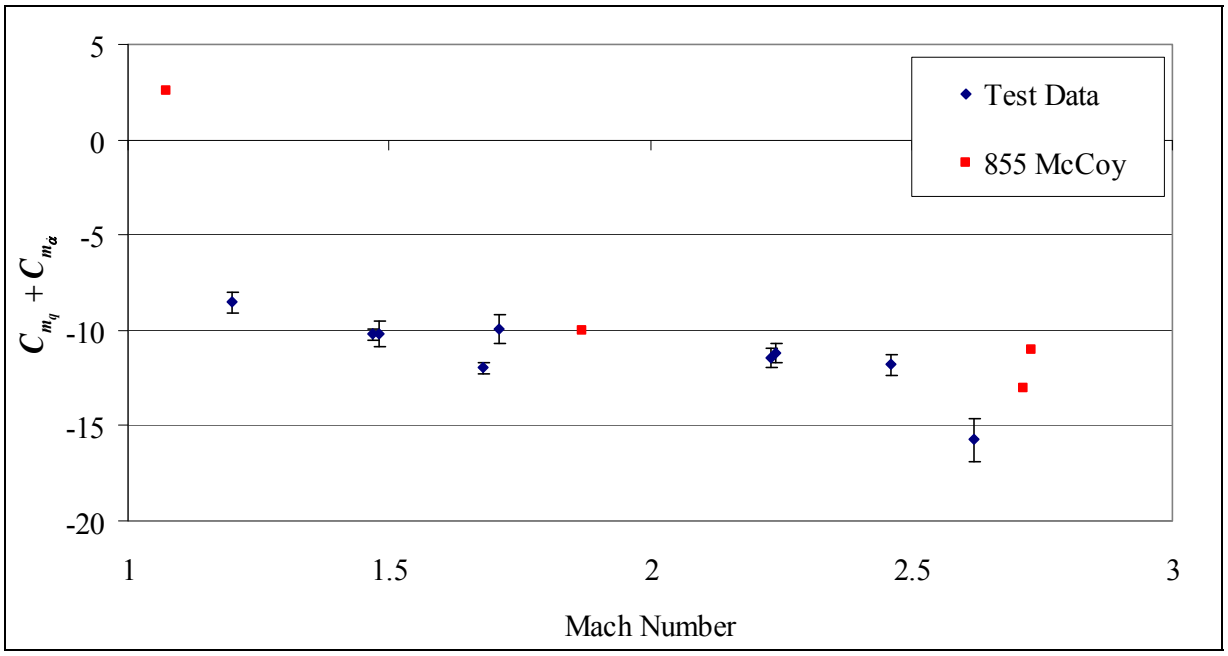

Figure 36. Pitch-damping moment coefficient vs. Mach number, group fits.

3.5 Dynamic Stability

From the motion analysis, it is possible to determine the modal arm damping exponents (figure 37). The value of λ_F determines whether the nutation, or fast, arm damps. The value of λ_S determines if the precession, or slow, arm damps. The values of λ_F and λ_S determined at each Mach number and angle only apply to the spin rates of the experiment. There are four possible combinations of λ_F and λ_S: $\lambda_F > 0$ and $\lambda_S < 0$, $\lambda_F < 0$ and $\lambda_S > 0$, $\lambda_F > 0$ and $\lambda_S > 0$, and $\lambda_F < 0$ and $\lambda_S < 0$. Only two of these four combinations were found during the course of the analysis: $\lambda_F < 0$ and $\lambda_S > 0$ (figure 38) and $\lambda_F < 0$ and $\lambda_S < 0$ (figure 39).

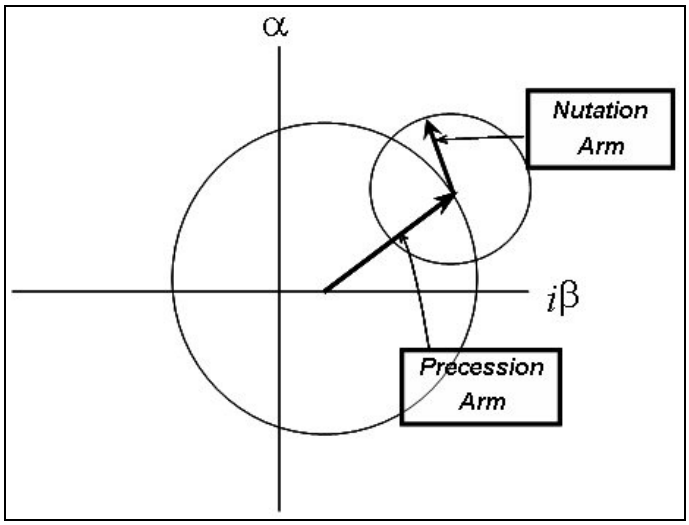

Figure 37. Modal arm damping exponent definitions.

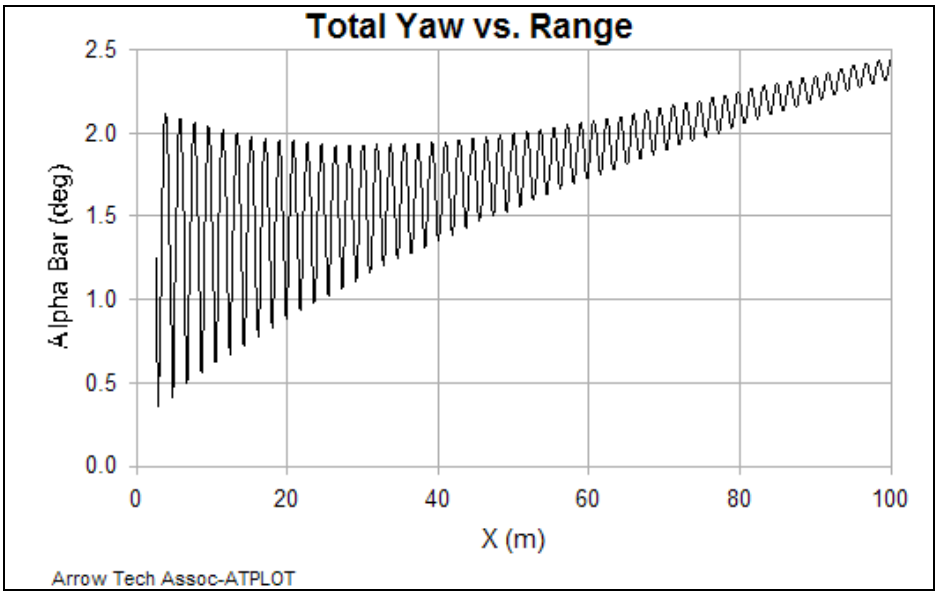

Figure 38. Shot 27344 (Mach 1.69) showing $\lambda_F < 0$ and $\lambda_S > 0$.

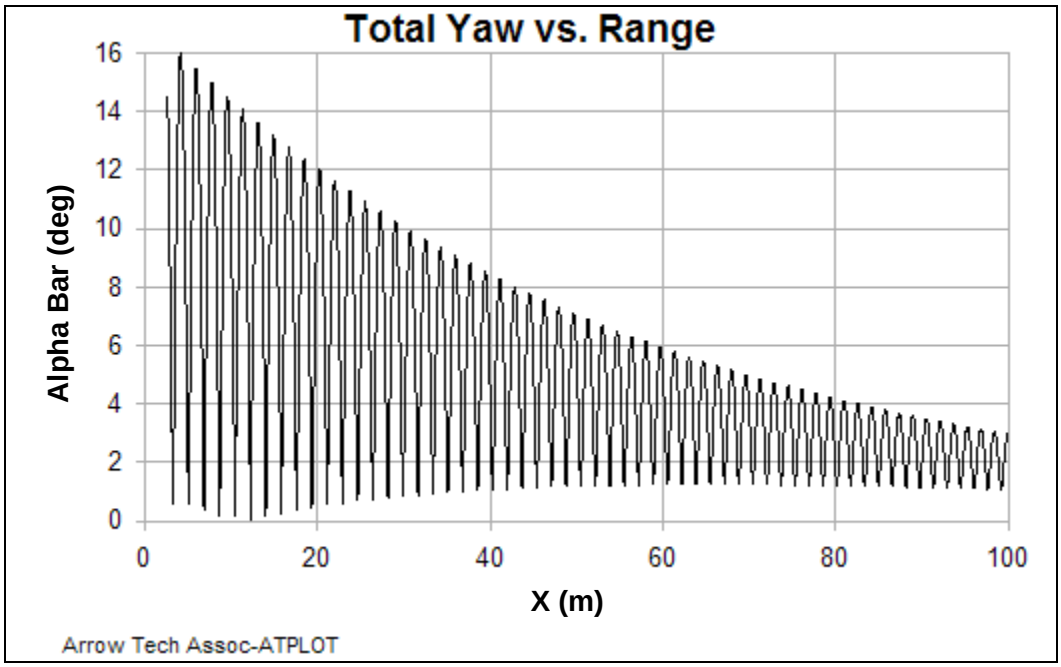

Figure 39. Shot 27352 (Mach 1.70) showing $\lambda_F < 0$and $\lambda_S < 0$.

The damping coefficients are affected by the aerodynamic properties of the projectile. In fact, as outlined by McCoy (*9*) and converted to ARFDAS notation, these are

$$\lambda_{F,S} = -\frac{1}{2}\left[H \pm \frac{P(2T - H)}{\sqrt{P^2 - 4M}} \right], \tag{4}$$

in which

$$P = \frac{I_x}{I_y}\left(\frac{pd}{V} \right), \tag{5}$$

$$M = \frac{C^*_{m_\alpha}}{k_y^2}, \tag{6}$$

$$H = C^*_{L_\alpha} - C^*_D - \frac{\left(C^*_{m_q} + C^*_{m_{\dot\alpha}} \right)}{2k_y^2}, \tag{7}$$

and

$$T = C^*_{L_\alpha} - \frac{C^*_{n_{p\alpha}}}{2k_x^2}, \tag{8}$$

in which

$$k_x^{\,2} = \frac{I_x}{md^2},\ k_y^{\,2} = \frac{I_y}{md^2},\ V = \text{velocity magnitude (m/s), and } p = \text{spin rate (rad/s).} \tag{9}$$

The lift coefficient derivative, C_{L_α}, and C_D are related to C_{N_α} and C_X by

$$C_{L_\alpha} = C_{N_\alpha} \cos\alpha - C_X \sin\alpha \tag{10}$$

and

$$C_D = C_X \cos\alpha - C_{N_\alpha} \sin\alpha \,. \tag{11}$$

The * indicates that the coefficient is multiplied by

$$^* = \frac{\rho S d}{2m} \,, \tag{12}$$

where ρ is the freestream density and S is the cross-sectional area ($\pi d^2/4$). It is important to note that ARFDAS nondimensionalizes the aerodynamic coefficients by $pd/2V$, while McCoy nondimensionalizes them by pd/V.

Plotting the damping exponents vs. AOA allows one to better determine the dynamic stability of the round for a given Mach number. Figures 40–44 display the damping exponents at each of the Mach numbers. Nutation is damped at all five Mach numbers. At Mach 1.2, for the angles of attack observed in this test, precession is undamped (figure 40). The damping exponents for the slow mode do approach 0 at 4°, indicating a yaw limit cycle likely exists. Figures 41 and 42 show that precession is only damped for yaw angles greater than roughly 2.5° at Mach 1.5 and 1.7. With that information, it can be stated that a yaw limit cycle of ~2.5° exists at a simulated range of 400 m due to a slow-mode instability, with an eventual yaw limit-cycle of slightly more than 4° at a simulated range of 600 m. At Machs 2.2 and 2.6 (figures 43 and 44, respectively), the precession and the nutation damping exponents are both negative, indicating that any initial yaw should damp out and remained damped over the first 200 m of flight.

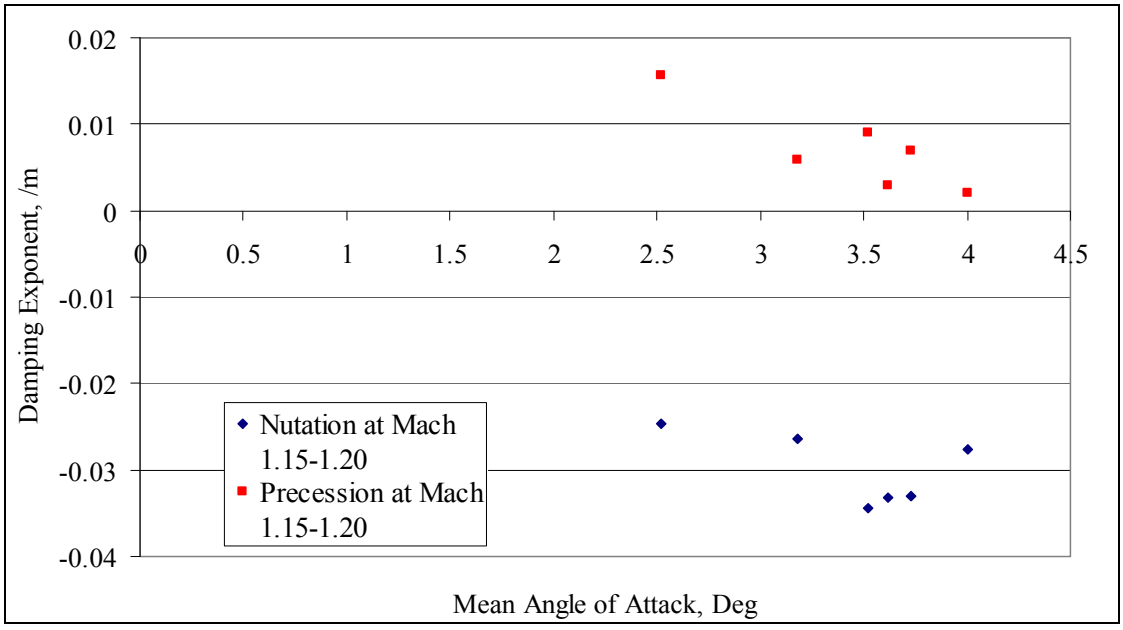

Figure 40. Modal arm damping exponents, Mach 1.15–1.20.

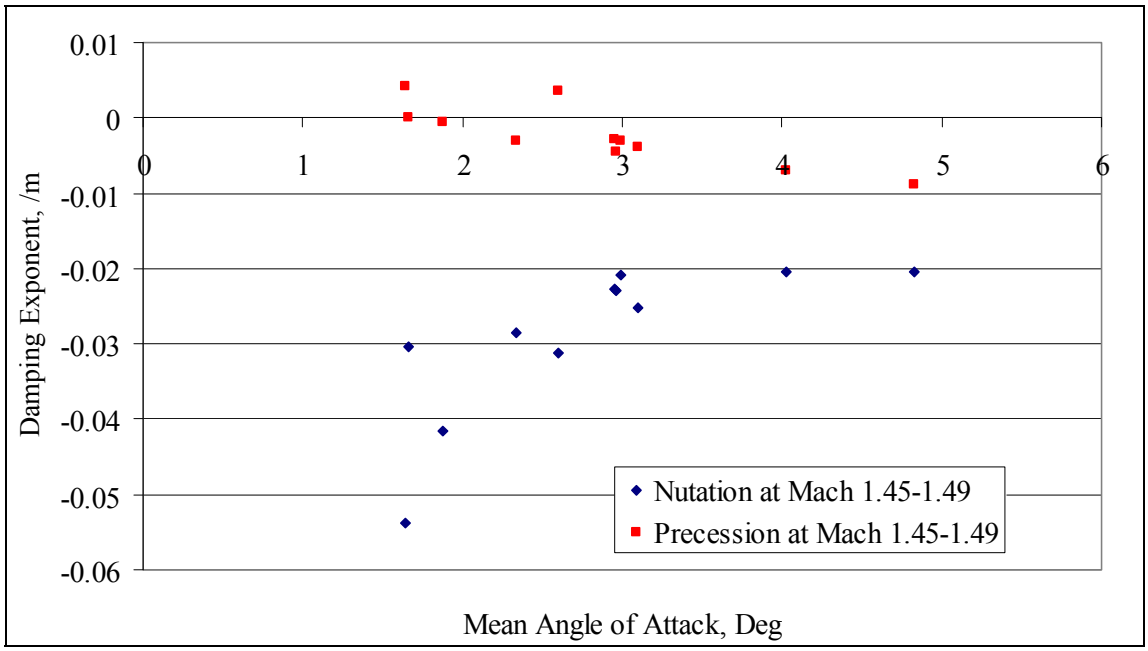

Figure 41. Modal arm damping exponents, Mach 1.45–1.49.

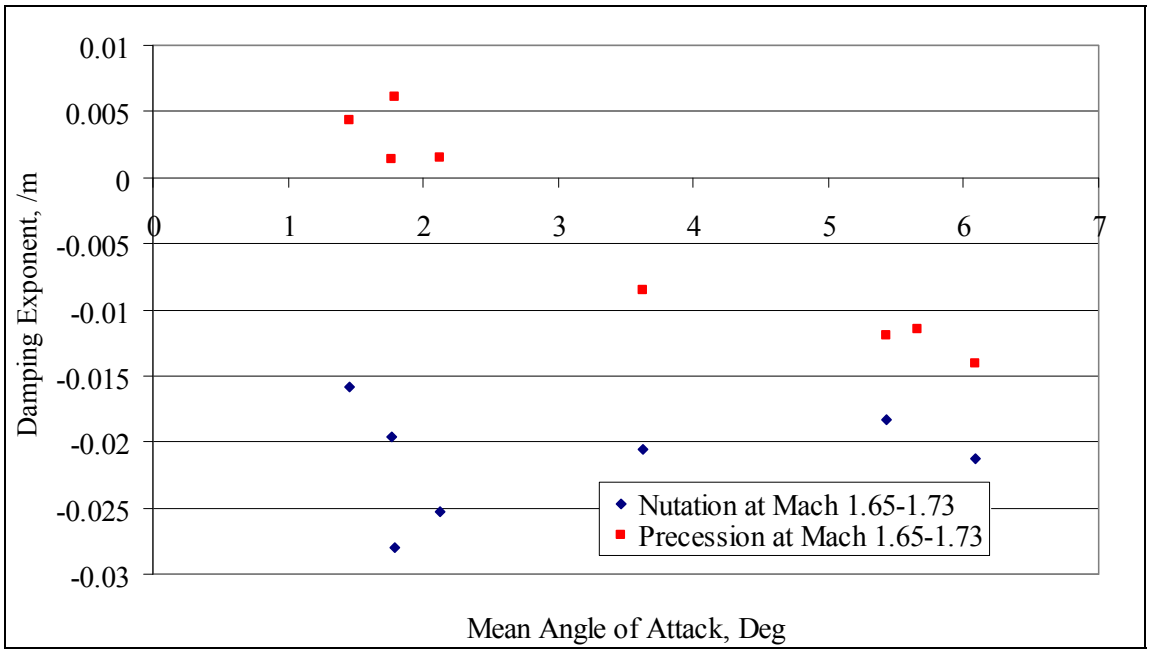

Figure 42. Modal arm damping exponents, Mach 1.65–1.73.

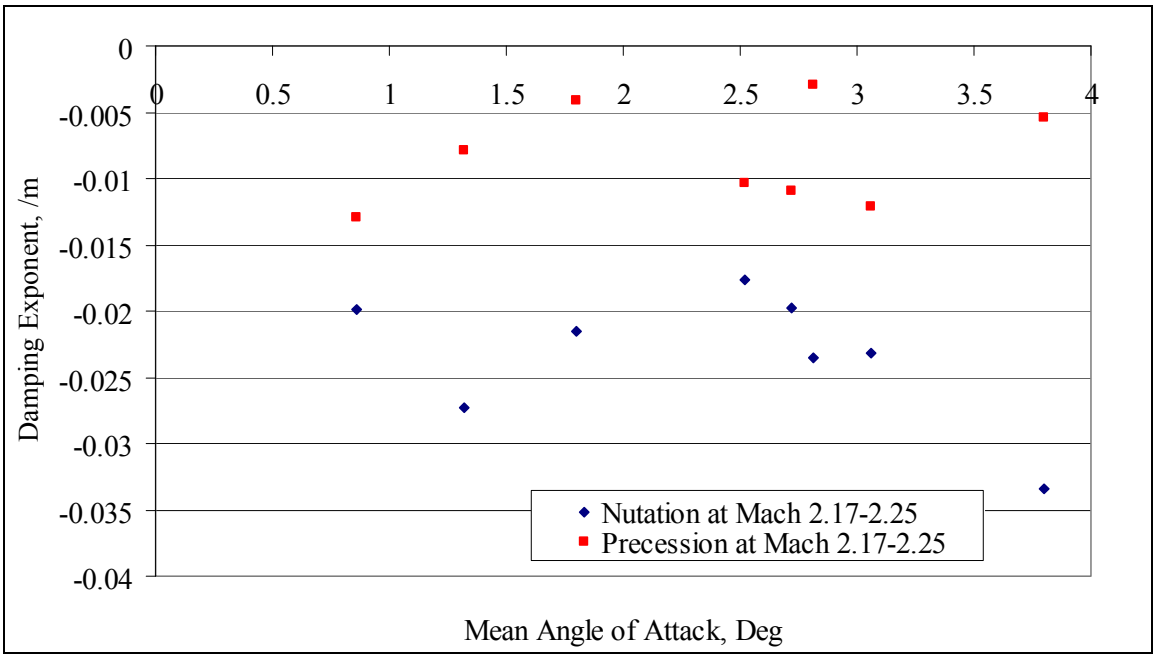

Figure 43. Modal arm damping exponents, Mach 2.17–2.25.

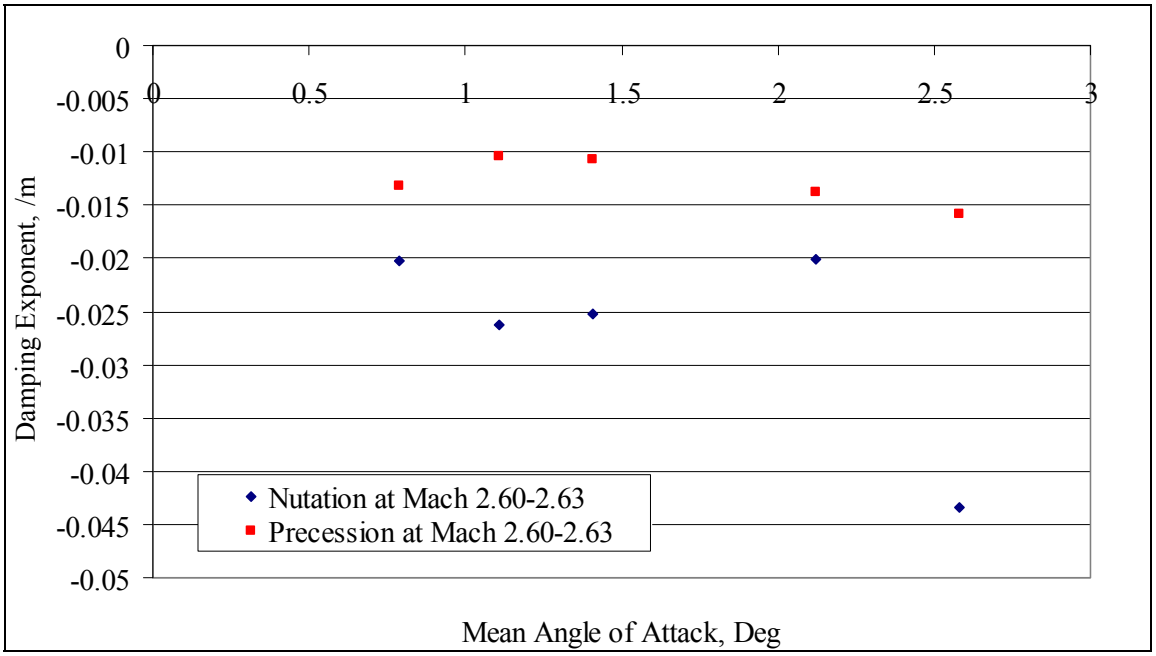

Figure 44. Modal arm damping exponents, Mach 2.60–2.63.

However, these damping exponents are determined using the spin rate due to the twist of the barrel rather than the spin rate that would be experienced by the projectile were it allowed to spin down from muzzle velocity and spin to the desired velocity. Using the C_X and C_{l_p} values determined by the 6-DOF fits, a trajectory simulation was accomplished using the Projectile Rocket Ordnance Design and Analysis System (PRODAS) (*10*) to determine the approximate spin rates at the downrange distances corresponding to the velocities tested and listed in table 9. The values of λ_F and λ_S can then be recalculated from equation 4 for each shot once P in equation 5 is updated using the corresponding spin values in table 9. As mentioned previously, the aerodynamic coefficients have been found to be minimally affected by these changes in spin (*7*, *8*). Since dynamic stability was not of concern at the 200-m distance (λ_F and λ_S were already negative, even for the lower spin rate), the reanalysis was confined to the 400-, 500-, and 600-m velocities. For the Mach numbers and angles of attack present in the range test, increasing the nondimensional spin decreases the values of the damping exponents, indicating that the rounds are more stable. At Mach 1.2, the limit cycle appears to be reduced to below 4°, as the one shot having this mean angle appears to just become stable or at least neutrally stable with $\lambda_S \approx 0$ (figure 45). The stability of the rounds at Machs 1.5 and 1.7 also appears to be increased. At Mach 1.5 (figure 46), most of the rounds show dynamic stability (λ_F and $\lambda_S < 0$). However, two of the rounds show neutral stability, indicating that a yaw limit cycle likely exists; it is just at yaw levels below those present in this study. This is confirmed at Mach 1.7 (figure 47), where slightly smaller yaw levels were observed, as the shots with the lowest yaw levels still have $\lambda_S > 0$, although with a smaller magnitude.

Table 9. Velocity matched spin rate as determined from PRODAS.

Downrange Distance (m)	**Mach No.**	**Spin (rad/s)**
200	2.24	30,171
400	1.7	27,319
500	1.5	26,138
600	1.2	24,448

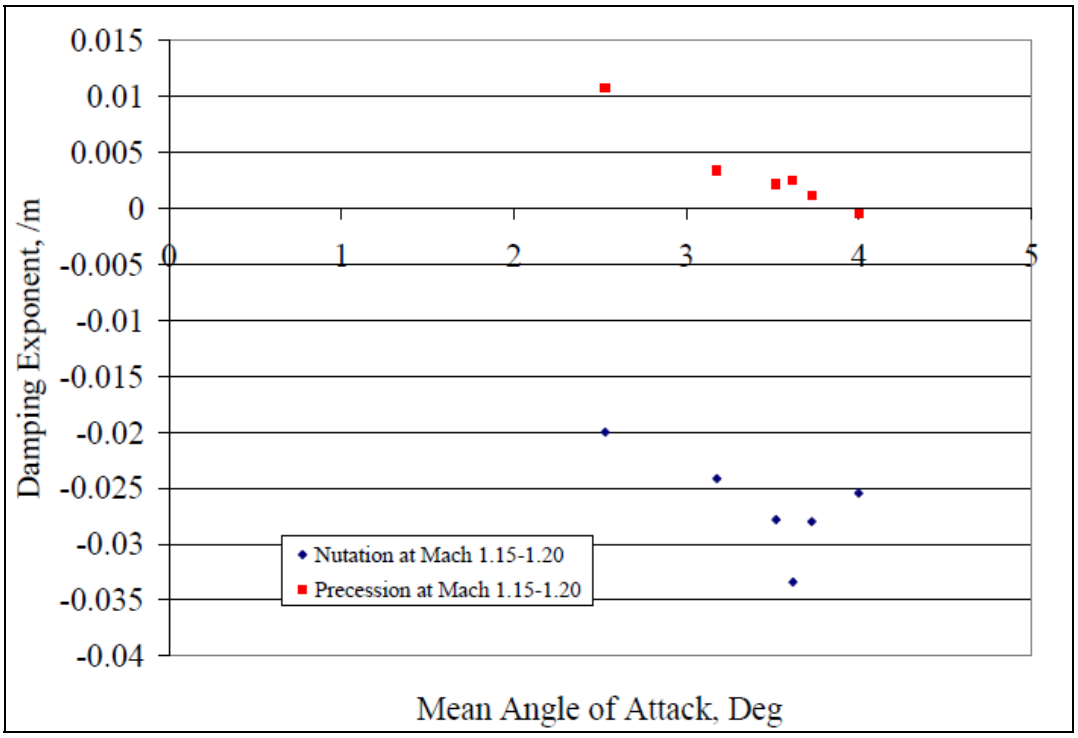

Figure 45. Modal arm damping exponents with matched spin, Mach 1.2.

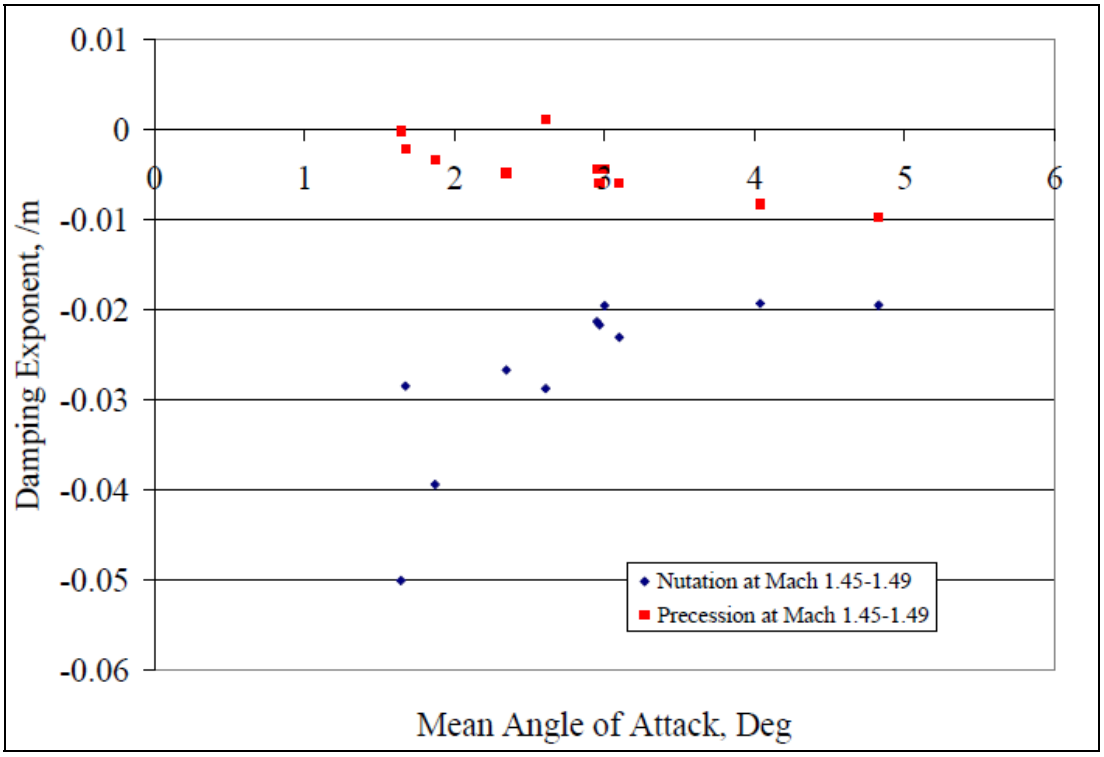

Figure 46. Modal arm damping exponents with matched spin, Mach 1.5.

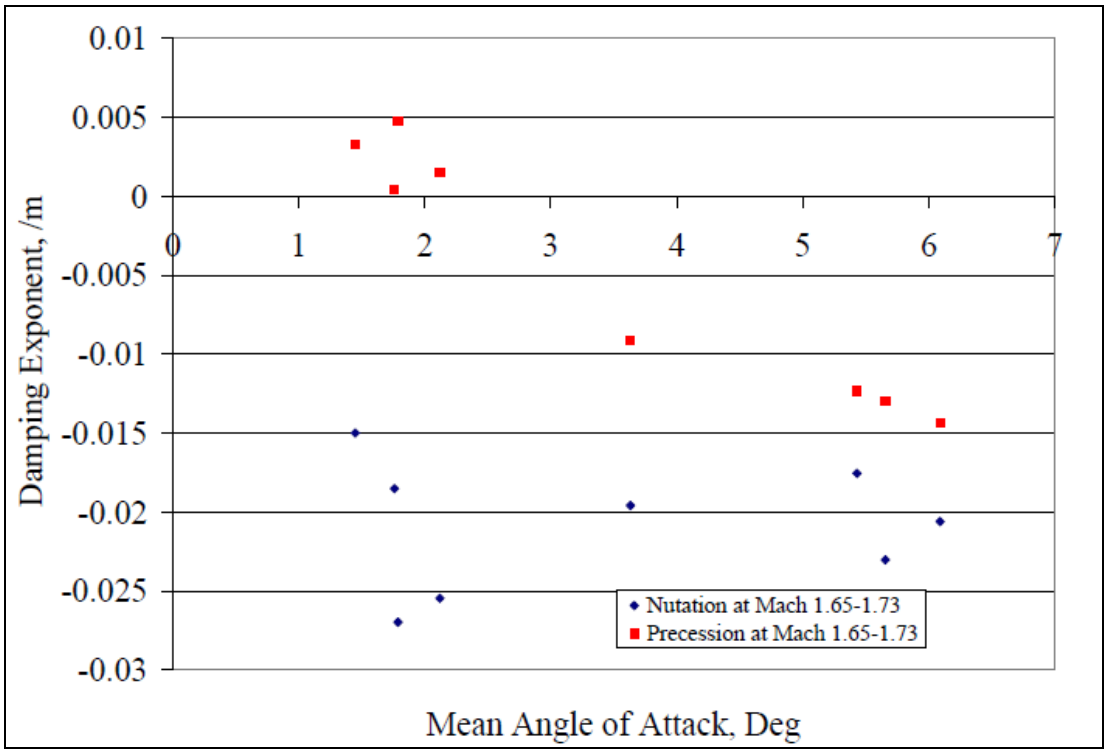

Figure 47. Modal arm damping exponents with matched spin, Mach 1.7.

An additional method to describe dynamic stability is to plot C_{n_p} as a function of AOA, with the expansion

$$C_{n_p} = C_{n_{p\alpha 0}} \bar{\delta} + C_{n_{p\alpha 3}} \bar{\delta}^3 \ , \tag{13}$$

(with $\bar{\delta}$ in radians) and then overlaying the nutation boundary and the precession boundary. The nutation boundary and the precession boundary can be found by setting equation 4 equal to 0 and solving each portion for $C_{n_{p\alpha}}$. In this case, the values used were solved for using ARFDAS (*2*) for each individual shot, with the average value used to represent each group. This provides the slope of the line to be plotted. Typically, the nutation boundary represents the maximum value of C_{n_p} that can exist at a particular Mach number and AOA in order to retain a damped nutation arm. Similarly, the precession boundary represents the minimum value of C_{n_p} that can exist at a particular Mach number and AOA in order to retain a damped precession arm. The region of dynamic stability (i.e., angles of attack for which both arms are damped) lies below the nutation boundary and above the precession boundary. In that case, the AOA where C_{n_p} and the precession boundary intersect is considered the limit cycle for that Mach number. This is predicated on the requirement that the nutation boundary has a larger slope than the precession boundary.

Figures 48–51 include the stability bounds determined directly from the range data (underspun condition). Figure 48 displays the Magnus moment and stability bounds for a group of shots with an average Mach number of 1.18. The slow arm is undamped for yaw levels less than 4.5°. Figures 49 and 50 represent the Magnus moment and stability bounds of two groups with average Mach numbers of 1.47 and 1.48, respectively. At Mach 1.47, the Magnus moment coefficient is within its bounds for the entire yaw range shown. It is important to note that the average yaw for the shots in that group was 3.6°, making the accuracy of the plot at yaw values <2° uncertain. At Mach 1.48, however, precession was undamped at yaw levels smaller than 2°. The average yaw for the shots in the Mach 1.48 group was only 2.5°, thus providing a better indicator of stability at smaller yaw levels. Similarly, figure 51 shows that at Mach 1.7, precession was undamped at yaw angles less than 3°. This indicates that at Mach 1.18, small yaw levels will grow to around 4.5°, and at Machs 1.48 and 1.7, small yaw levels will grow until they reach ~2° and ~3°, respectively. It is possible, however, that at Machs 1.48 and 1.7, the slow arm damping exponent is 0, rather than positive, at low yaw angles since the Magnus moment is only slightly outside of its bounds and other groups at similar speeds are shown to be within the stability bounds. For all other Mach numbers, the Magnus coefficient was within the stability bounds. C_{n_p} plots at different Mach numbers can be found in appendix C. The findings of the Magnus bounds are consistent with the limit cycles predicted using the damping frequencies.

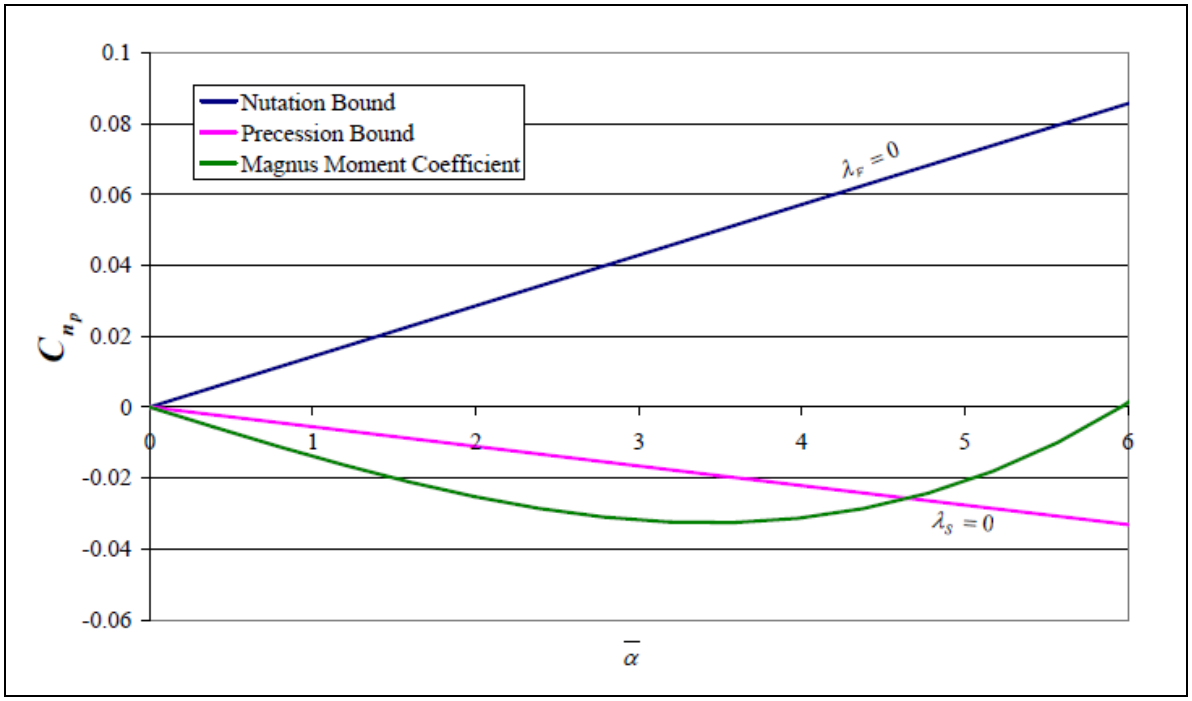

Figure 48. Magnus moment coefficient with stability bounds at Mach 1.18.

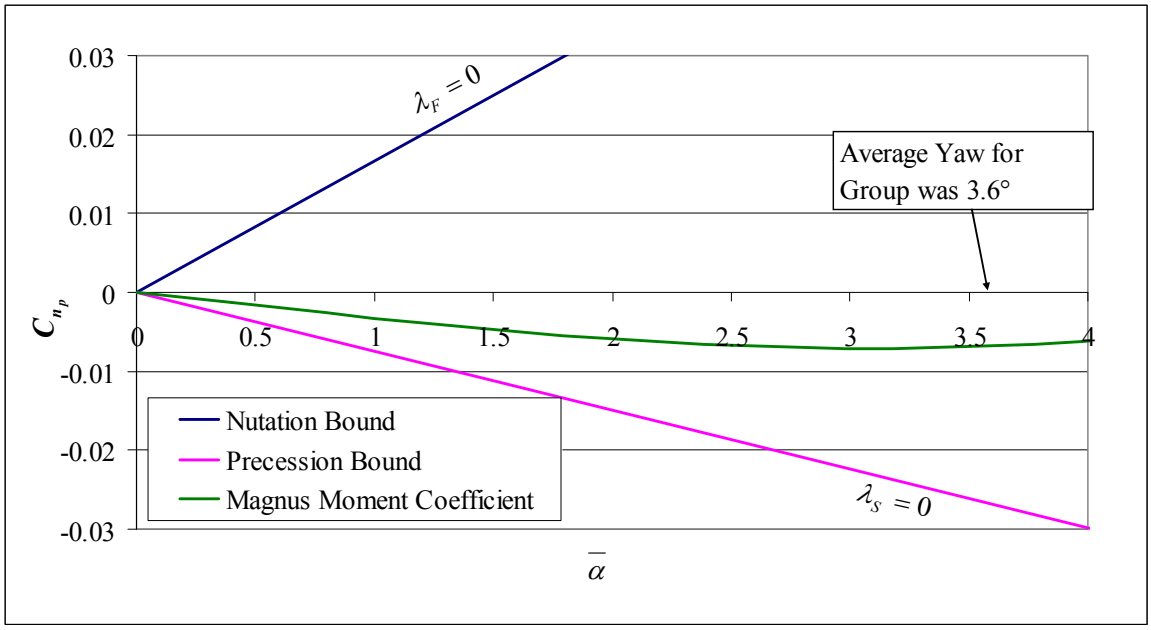

Figure 49. Magnus moment coefficient with stability bounds at Mach 1.47.

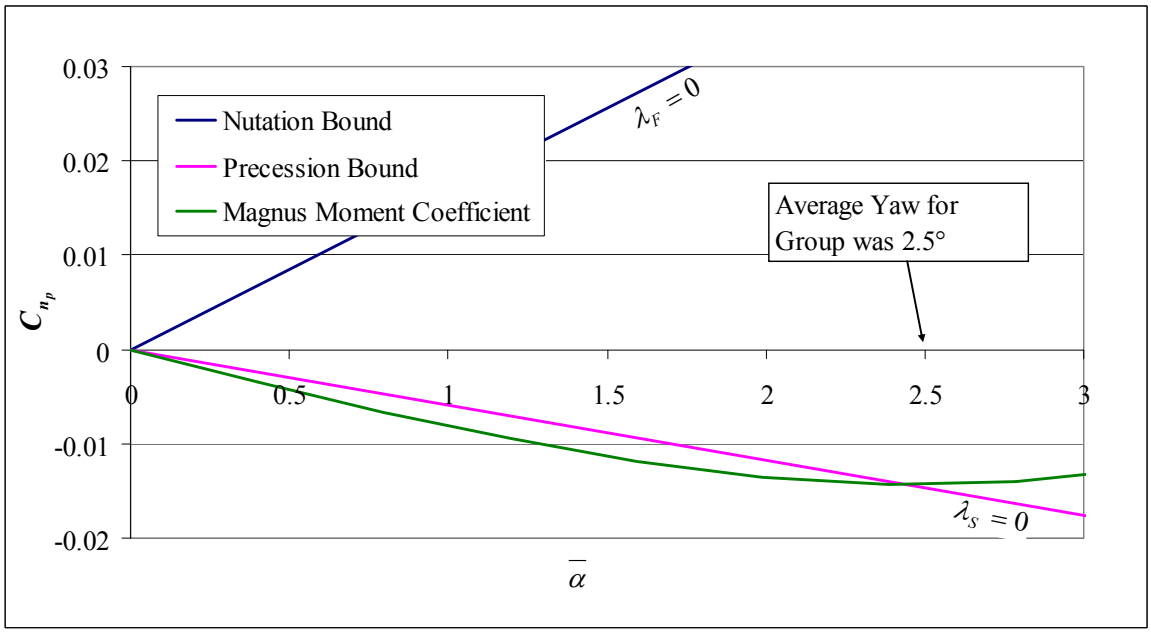

Figure 50. Magnus moment coefficient with stability bounds at Mach 1.48.

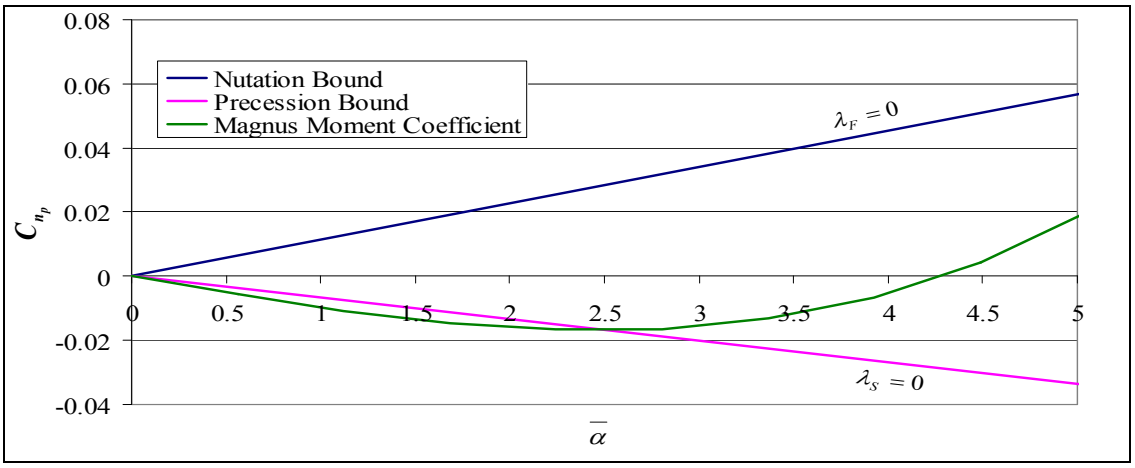

Figure 51. Magnus moment coefficient with stability bounds at Mach 1.70.

As was the case with the damping frequencies, the Magnus bounds are also solved for assuming muzzle spin rates rather than the actual downrange spin rates. Using the downrange spin rates predicted by the trajectory calculations, a second set of "at range" Magnus bounds was calculated using equation 4 set to 0 and an updated *P* value. These "at range" Magnus bounds lay outside the original Magnus bounds, indicating a larger stability region. Figures 52–54 show the same Magnus moment coefficient plots vs. mean AOA, as were shown in figures 48–51 (the Mach 1.47 plot is not included as that case was already shown to be stable). The extended stability region that occurs with matched spin is immediately apparent; the yaw limit cycle is decreased by ~0.5° for these three Mach numbers. While this may not seem significant, the yaw limit cycle experienced by the round may affect its terminal performance.

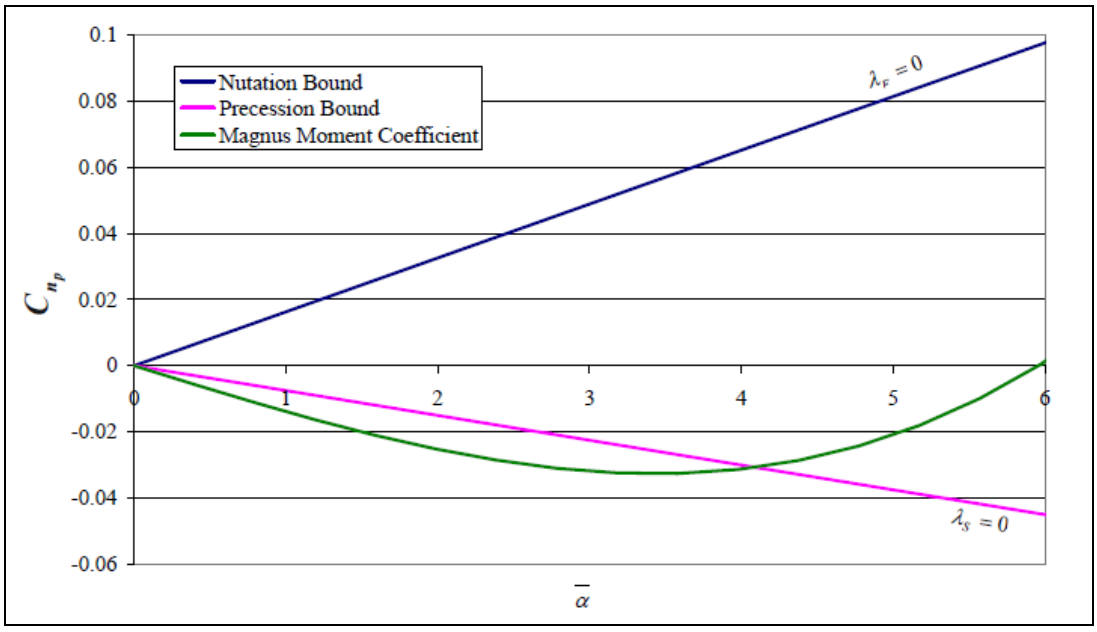

Figure 52. Magnus moment coefficient with matched spin stability bounds at Mach 1.18.

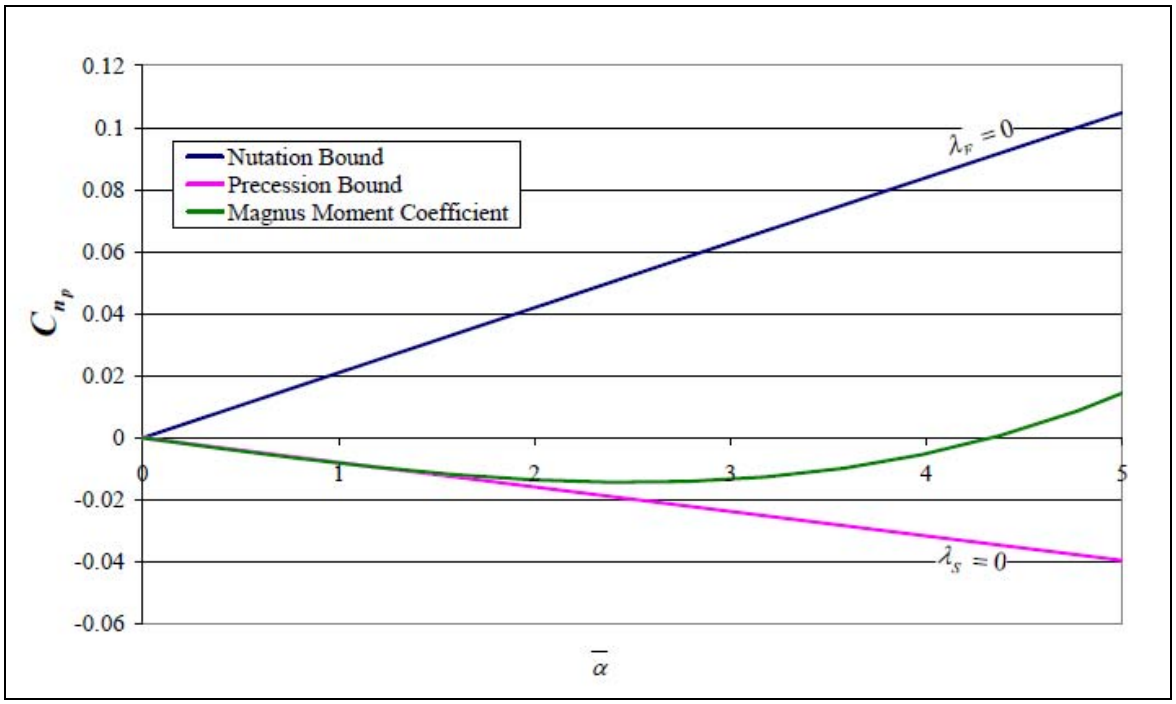

Figure 53. Magnus moment coefficient with matched spin stability bounds at Mach 1.48.

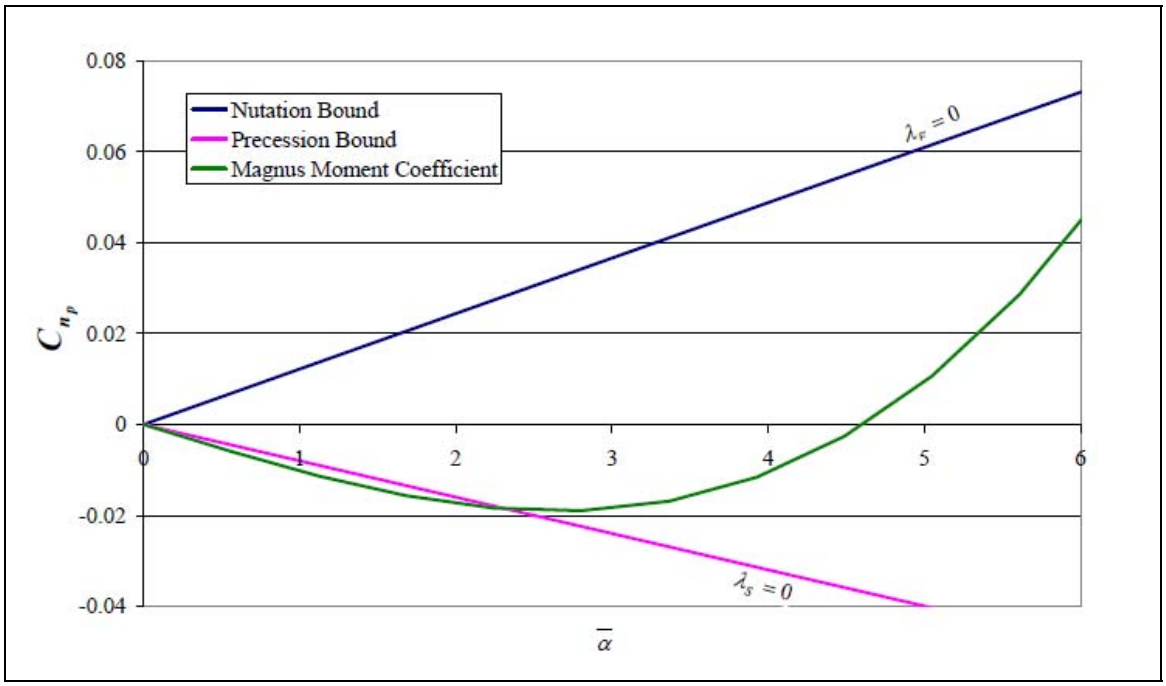

Figure 54. Magnus moment coefficient with matched spin stability bounds at Mach 1.7.

A final method to estimate the simulated range limit cycle at each Mach number is to interrogate the total yaw fit obtained from the ARFDAS solution to extract the average total yaw for each shot during the last 2–3 m of flight. Figure 55 shows the yaw limit cycle as determined by this method. Also included in the plot is data from work previously done by McCoy (*1*). While the recent data at muzzle spin indicates that a significant limit cycle may appear as early as 600 m/s, McCoy's data indicates that the yaw limit cycle does not occur until 400 m/s. This discrepancy is likely due to the rounds in the current test being in an underspun condition (spin is lower than expected for the velocity), causing the round to be less stable than it would be under actual conditions. However, as the round continues to slow down, the magnitude of the limit cycle predicted by the simulated range experiments nearly matches that found by McCoy at range. This indicates that while the simulated range experiments may not accurately predict at what velocity the limit cycle begins to appear, they do accurately predict the limit cycle once it is known to exist.

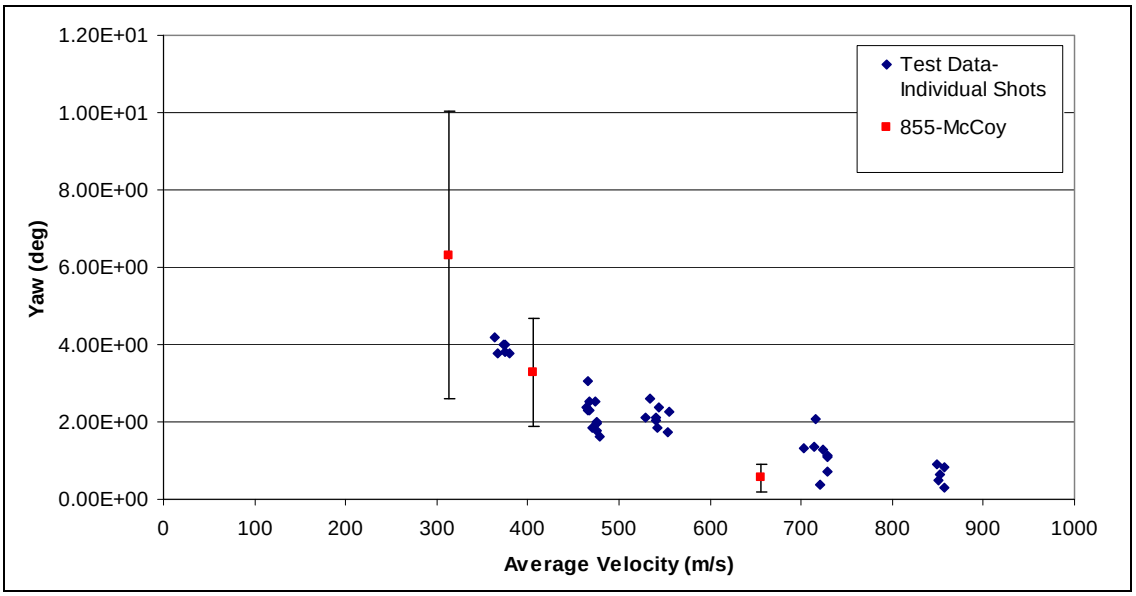

Figure 55. Yaw limit cycle: yaw vs. velocity.

The main purpose of conducting any aerodynamic testing is to create a complete aerodynamic database for future use in simulating trajectories that have nonstandard initial conditions or to determine the effect of weather (i.e., winds, temperature, etc.). To this end, it important to ensure that the aerodynamic coefficients predicted by the simulated range experiments also produce that known downrange behavior. As this is one of the few rounds for which "at range" limit cycle data is available, this prediction capability is investigated.

Using the experimentally obtained aerodynamic coefficients, the existing M855 aerodynamic database in PRODAS was updated. The trajectory simulation available within PRODAS was used to verify that the yaw limit cycles observed in the range could be reproduced at each of the

downrange Mach numbers to ensure that all of the aerodynamic coefficients were accurately determined. The next step was to allow the model to simulate the real range test to see how the results agreed with what McCoy (*1*) observed. The results of this simulation were not expected, and no significant limit cycle was observed (figure 56). PRODAS accurately predicted the damping of the initial yaw. However, there appears to be very little yaw growth (still less than 1°) at 600 m. Very little yaw growth is occurring because the slow-mode (un)damping remains quite small, even at 600 m, as found in the current range test. Without a significant event occurring, it would take a very long distance for a limit cycle such as that seen by McCoy to develop. In the current testing, it is likely that the significant event causing the yaw growth was the initial launch rates. It is unclear at this time why the real-range experiments were showing a limit cycle, while none are predicted. One possibility would be the existence of a small mass asymmetry. However, the Aerodynamics Branch at ARL does not possess the correct instrumentation to verify whether or not a mass asymmetry exists. Additional analyses and studies would need to be completed in order to further address this issue.

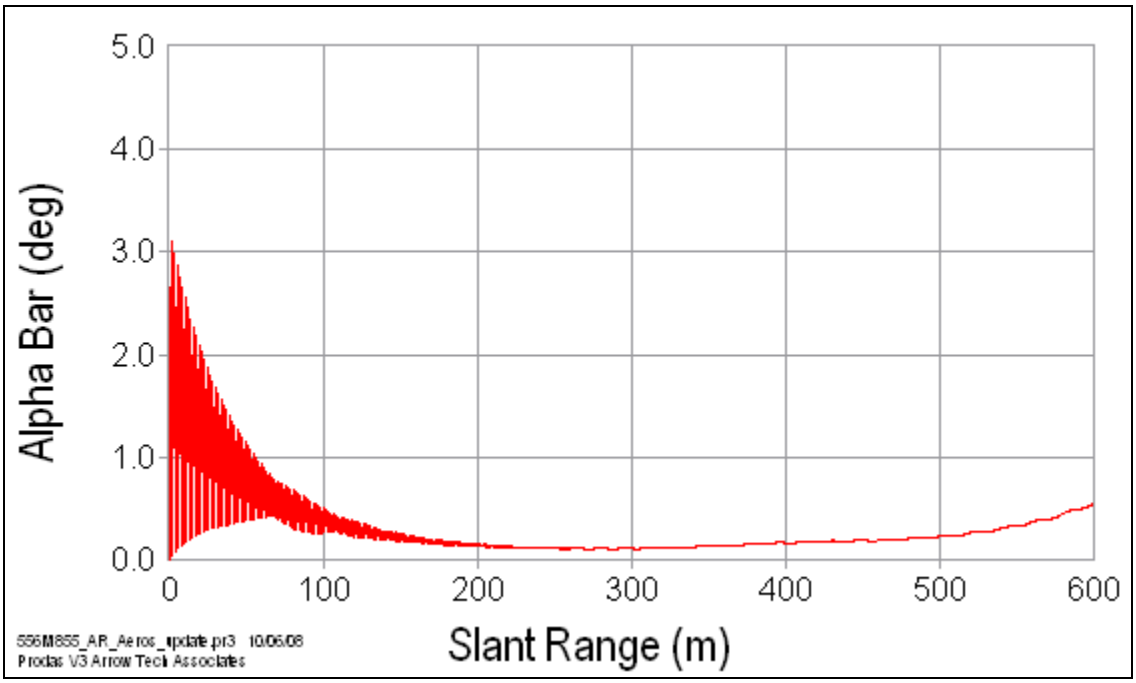

Figure 56. The 6-DOF simulation to 600 m of the M855 projectile using experimentally determined aerodynamic coefficients.

4. Summary and Conclusions

An experimental test was completed for the aerodynamic and flight dynamic characterization of the M855 reference round from the muzzle to a simulated range of ~600 m. Data was collected at five different launch Mach numbers over the simulated 600 m of flight. There were 38 shots for which data was collected, including 5 shots near Mach 2.6, 8 near Mach 2.2, 8 near Mach 1.7, 11 near Mach 1.5, and 6 near Mach 1.2. With the exception of three shots at Mach 1.5 and four shots at Mach 1.2, all of the shots had spin pins for the characterization of spin, specifically, roll damping. At each of the downrange velocities investigated, the projectile is in an underspun condition.

Pitching and yawing motion were well determined at all Mach numbers. This allowed linear and nonlinear aerodynamic coefficients to be obtained with sufficient accuracy. The resulting aerodynamic coefficients and dynamic derivatives can be used to improve the predictive capabilities of flight models with confidence. Coefficients for axial force, pitching moment, Magnus moment, and pitch damping were all found to have values similar to those obtained from previous tests, validating both sets of results. For future tests, a larger range of initial yaw values at the higher Mach numbers would be useful in determining if there is a cubic Magnus moment coefficient.

The round was determined to be dynamically stable at all Mach numbers tested through analysis of the Magnus moment coefficient, stability bounds, and modal arm damping exponents. Analysis of the data for determination of yaw limit cycle at simulated ranges produced mixed results. While the current test found that a yaw limit cycle did exist, it was predicted to occur significantly earlier than for the real-range test. Current results indicate that yaw limit cycle of ~2° begins to occur at a simulated range of 400 m, eventually reaching 4° at 600 m, while the real-range testing indicated that a similar yaw limit cycle didn't occur until 600 m. Completing the stability analysis using matched spin showed that the yaw limit cycle could be reduced by as much as 0.5°. Additionally, this second analysis showed that the yaw limit cycle may not begin until further downrange than predicted by the simulated ranges in the underspun condition. This indicates that if the limit cycle of a particular round is of concern, the extra step should be taken to complete the second stability analysis using matched spin.

With a complete set of aerodynamic coefficients, an updated aerodynamic model was created. This model will allow a better understanding of the flight dynamics of the projectile and better matching capabilities as improvements to the round are made.

5. References

1. McCoy, R. L. *Aerodynamic and Flight Dynamic Characteristics of the New Family of 5.56MM NATO Ammunition*; BRL Report No. 3467; U.S. Army Ballistics Research Laboratory: Aberdeen Proving Ground, MD, October 1985.
2. Braun, W. F. *The Free Flight Aerodynamic Range*; BRL Report No. 1048; U.S. Army Ballistics Research Laboratory: Aberdeen Proving Ground, MD, July 1958.
3. Arrow Tech Associates. *ARFDAS: Ballistic Range Data Analysis System; User and Technical Manual*. South Burlington, VT, May 1997.
4. Murphy, C. H. *Free-Flight Motion of Symmetric Missiles*; BRL Report 1216; U.S. Army Ballistics Research Laboratory: Aberdeen Proving Ground, MD, July 1963.
5. Murphy, C. H. *Data Reduction for Free-Flight Spark Ranges*; BRL Report 900; U.S. Army Ballistics Research Laboratory: Aberdeen Proving Ground, MD, February 1954.
6. Hathaway, W. H.; Whyte, R. H. *Aeroballistic Research Facility Free-Flight Data Analysis Using the Maximum Likelihood Method*; AFATL-TR-79-98; Arrow Tech Associates: South Burlington, VT, December 1979.
7. Weinacht, P. Validation and Prediction of the Effect of Rifling Grooves on Small-Caliber Ammunition Performance. *AIAA Atmospheric Flight Mechanics Conference and Exhibit*, AIAA-2006-6010, Keystone, CO, August 2006.
8. Silton, S.; Webb, D. Experimental Determination of the Effect of Rifling Grooves on the Aerodynamics of Small Caliber Projectiles. *AIAA Atmospheric Flight Mechanics Conference and Exhibit*, AIAA-2006-6009, Keystone, CO, August 2006.
9. McCoy, R. L. *Modern Exterior Ballistics: The Launch and Flight Dynamics of Symmetric Projectiles*. Schiffer Publishing: Atglen, PA, 1999; pp 233, 306, 308.
10. ArrowTech Associates. *PRODAS User's Manual*, Burlington, VT, 2007.

Appendix A. Motion Plots

A complete set of motion plots is presented for a chosen shot to represent each Mach number. On each plot, the line indicates the six degrees of freedom fit and the solid circles are the experimental data. In figures A-1–A-9, the motion plots for a shot at Mach 1.18 are presented. Figures A-10–A-18 show the motion plots at Mach 1.69, and figures A-19–A-27 are the motions plots for a shot fired at Mach 2.21. Finally, figures A-28–A-36 show the motion plots Mach 2.63. The complete set of sample motion plots at Mach 1.5 is shown in the main body of the text.

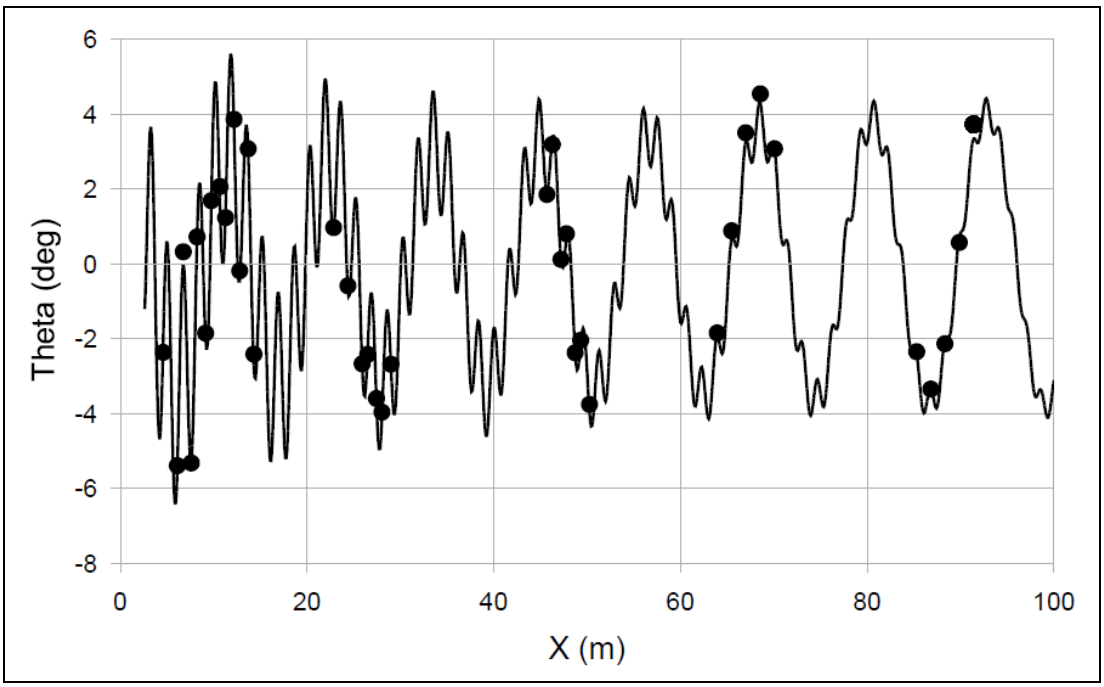

Figure A-1. Pitch angle vs. range for round 29271 (M855 at Mach 1.18).

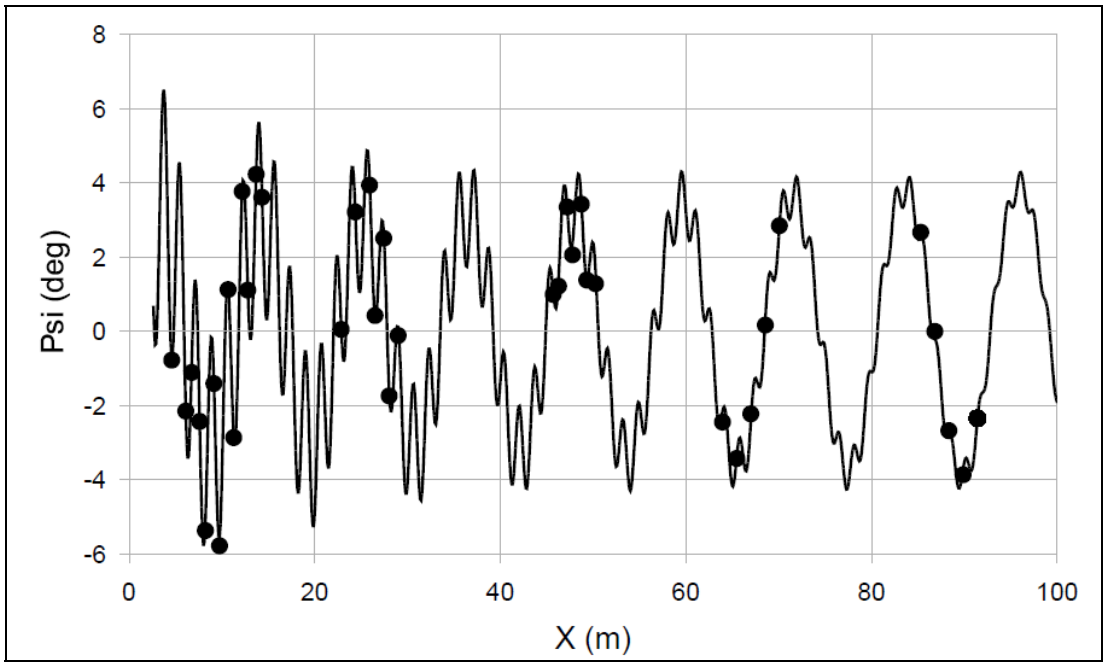

Figure A-2. Yaw angle vs. range for round 29271 (M855 at Mach 1.18).

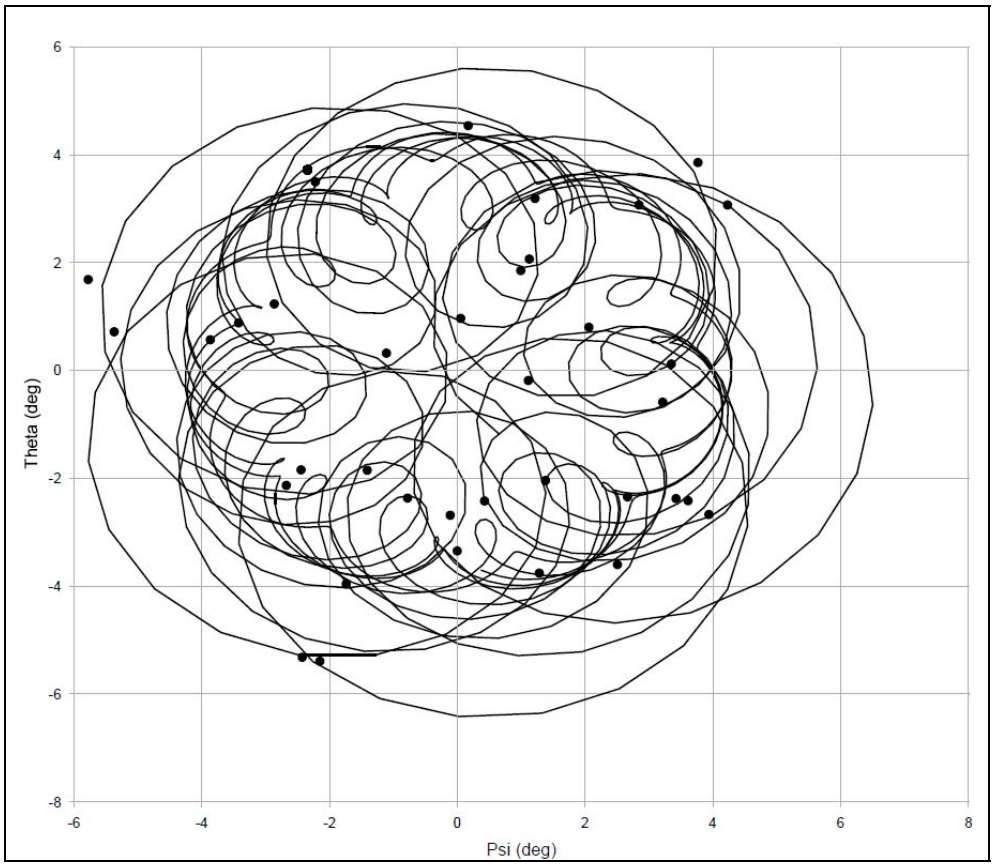

Figure A-3. Pitch angle vs. yaw angle for round 29271 (M855 at Mach 1.18).

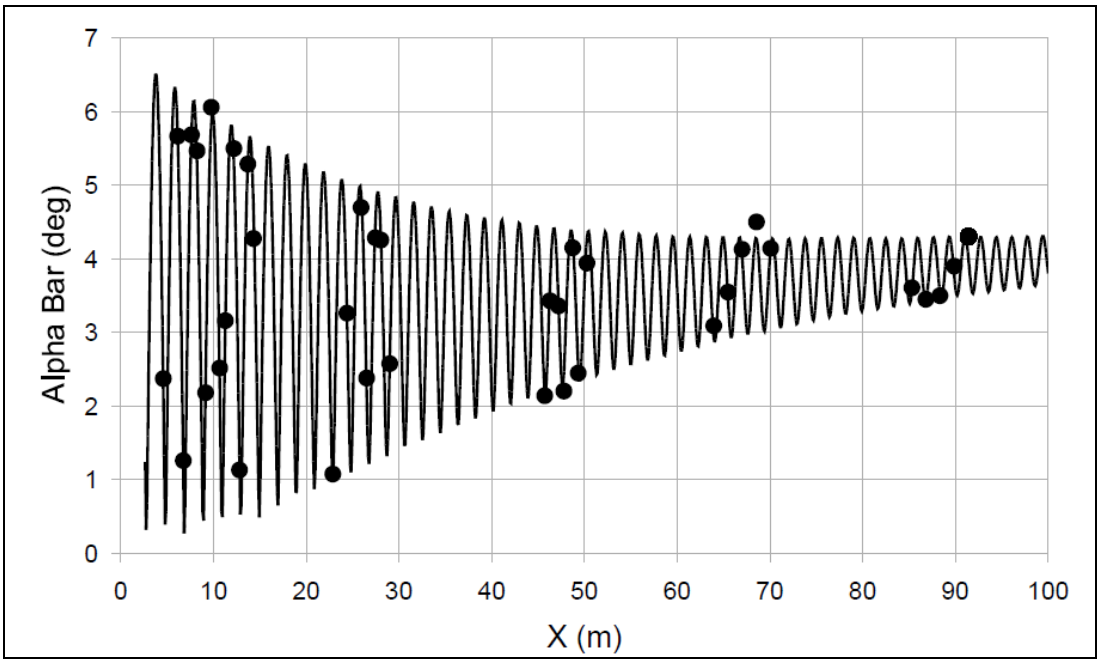

Figure A-4. Total yaw vs. range for round 29271 (M855 at Mach 1.18).

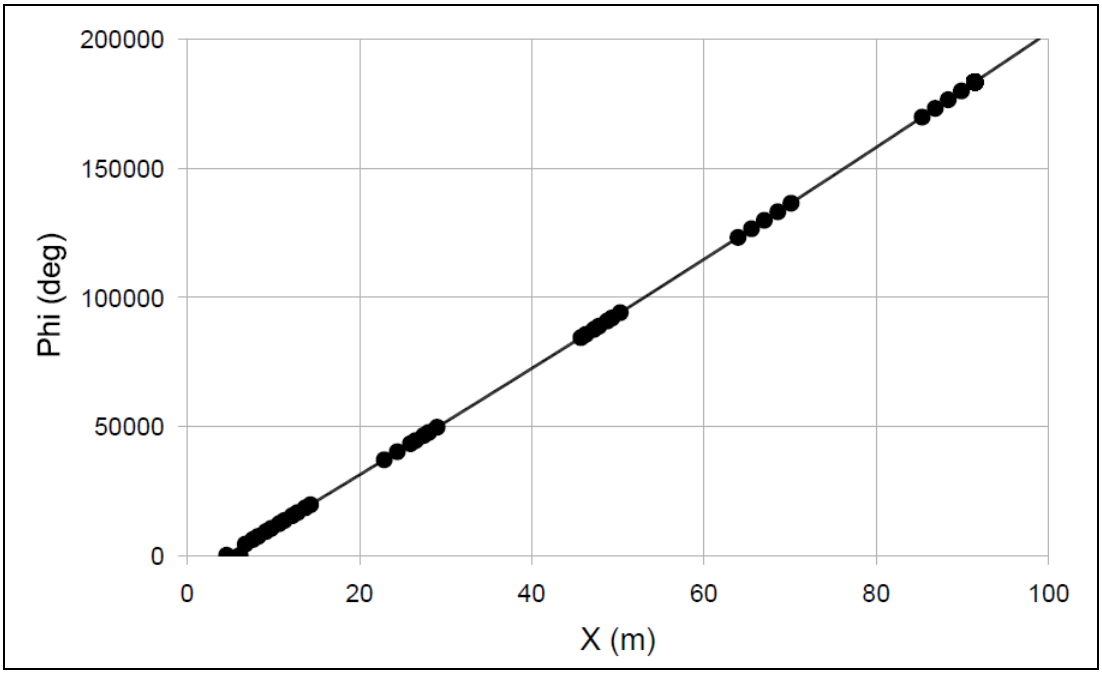

Figure A-5. Roll angle vs. range for round 29271 (M855 at Mach 1.18).

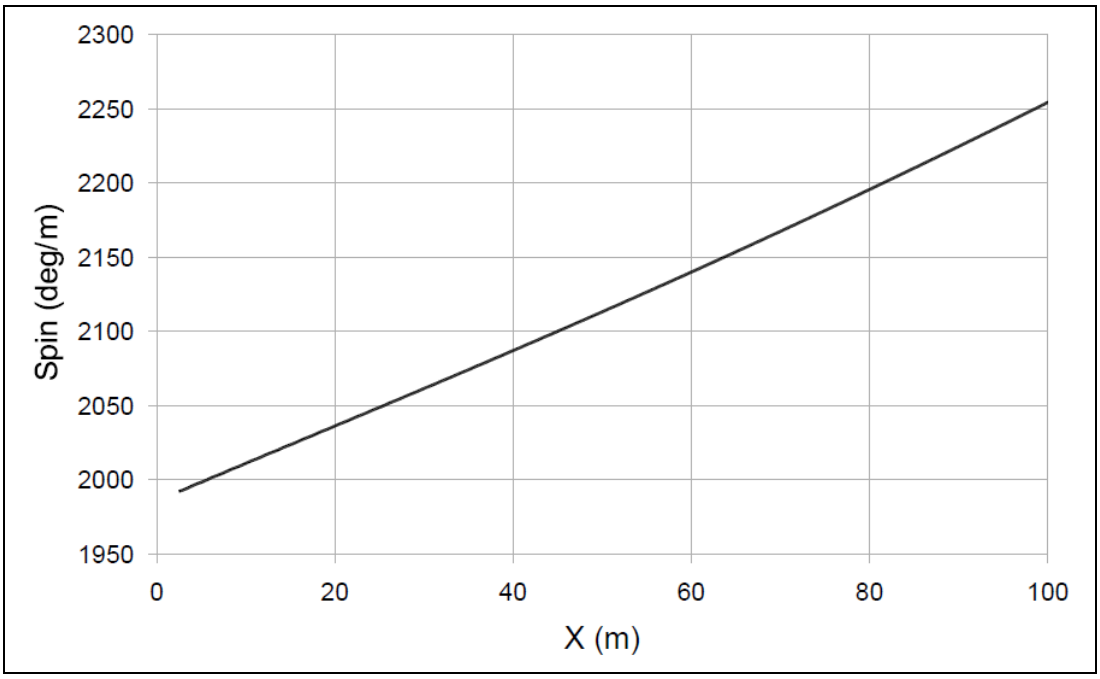

Figure A-6. Spin vs. range for round 29271 (M855 at Mach 1.18).

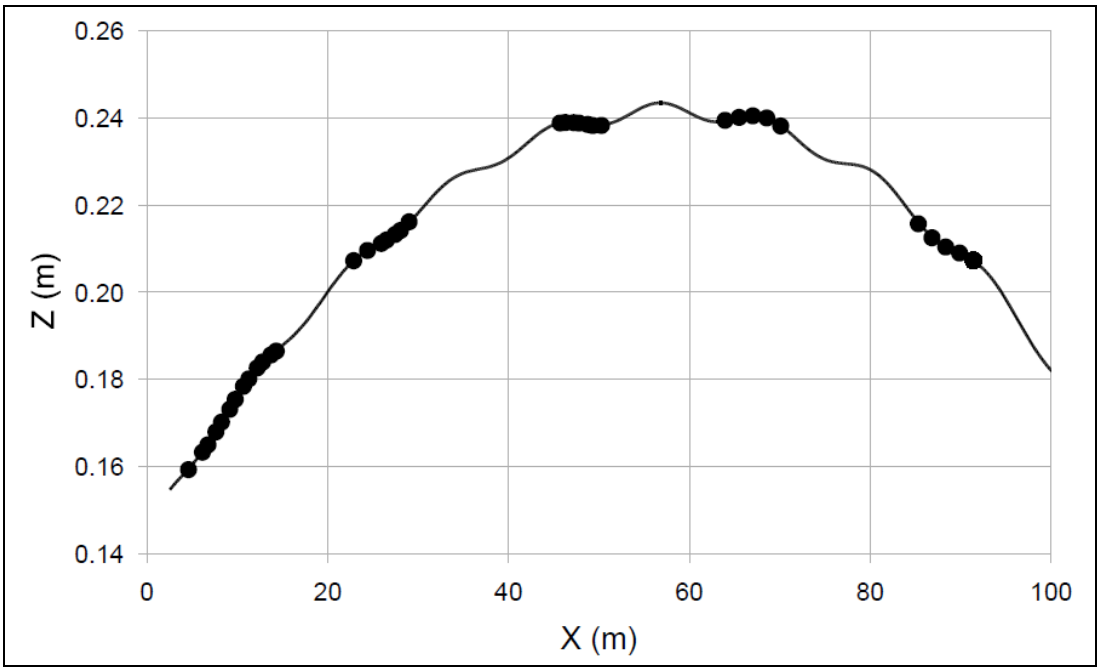

Figure A-7. Vertical position vs. range for round 29271 (M855 at Mach 1.18).

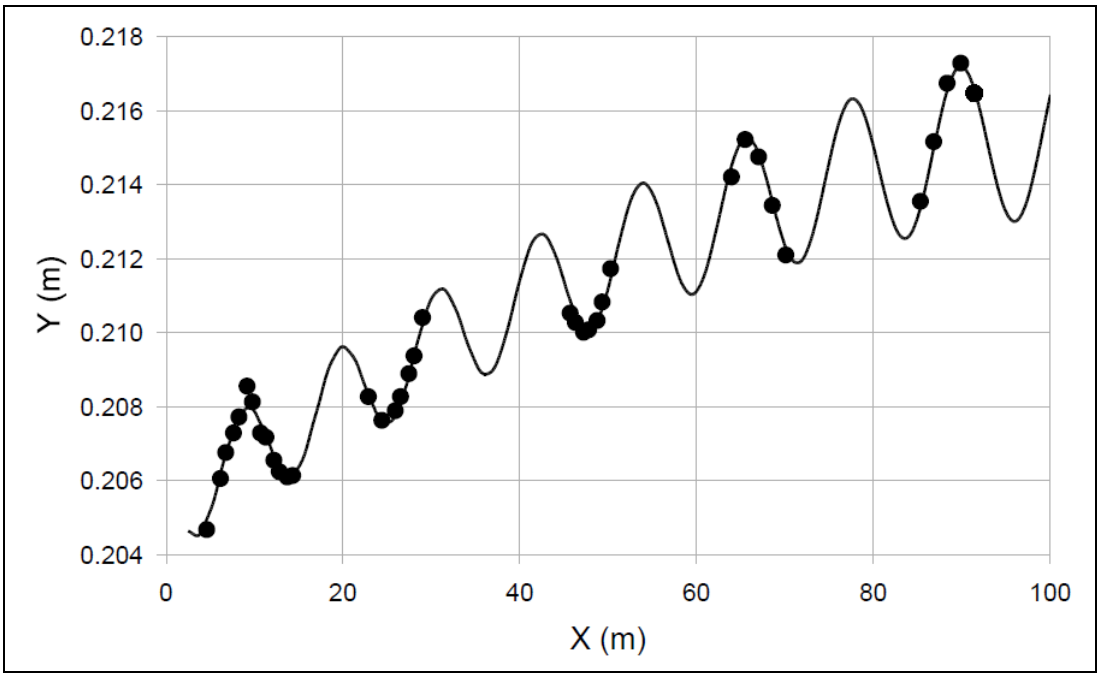

Figure A-8. Lateral position vs. range for round 29271 (M855 at Mach 1.18).

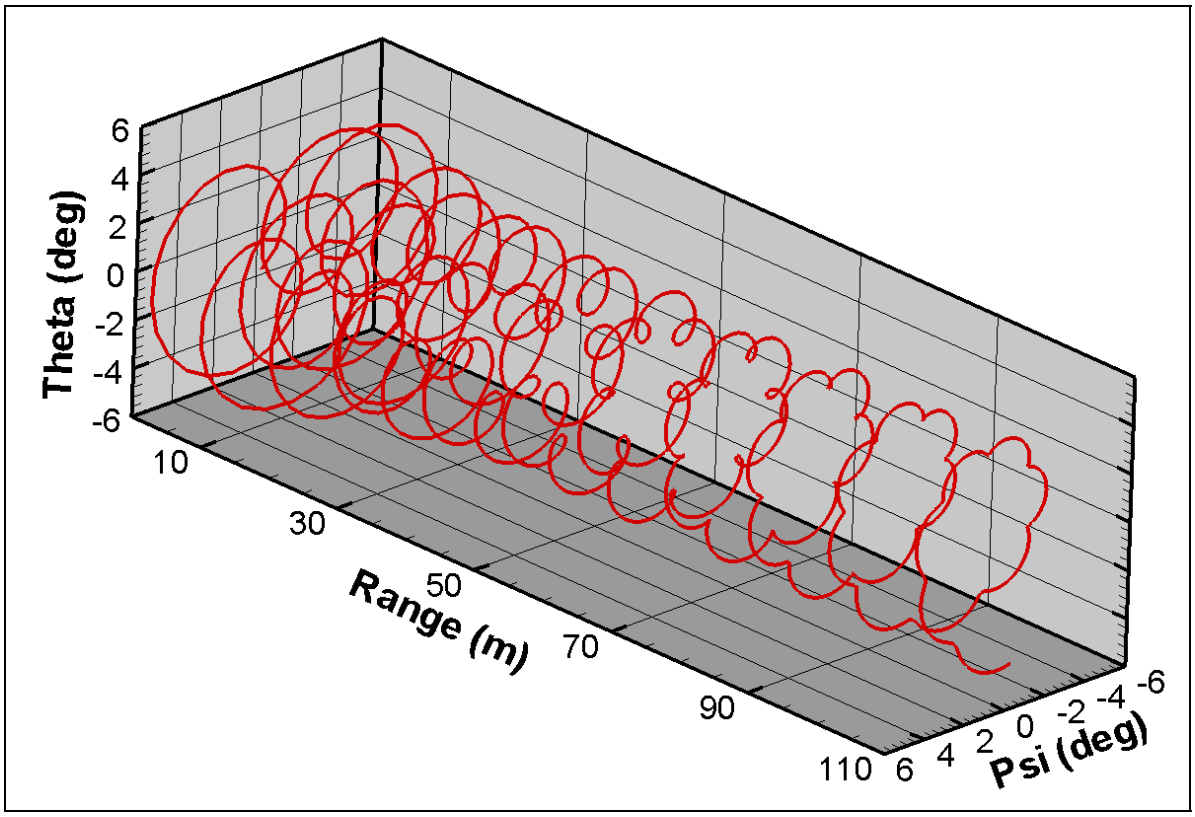

Figure A-9. Three-dimensional projectile motion through the range for round 29271 (M855 at Mach 1.18).

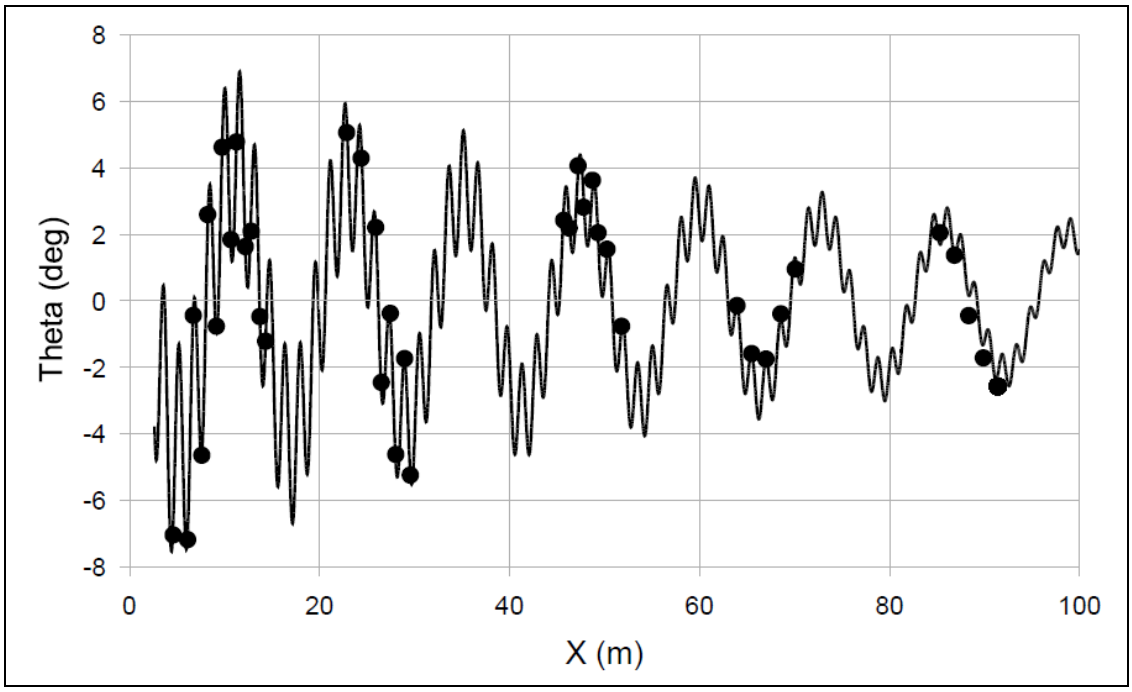

Figure A-10. Pitch angle vs. range for round 27353 (M855 at Mach 1.69).

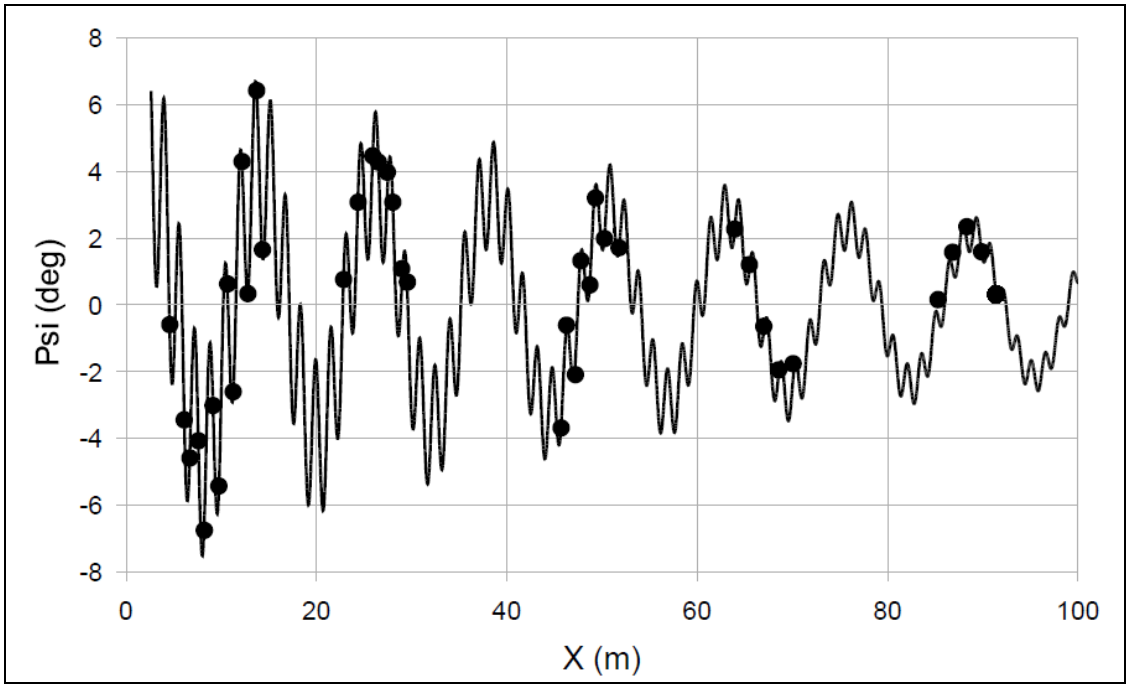

Figure A-11. Yaw angle vs. range for round 27353 (M855 at Mach 1.69).

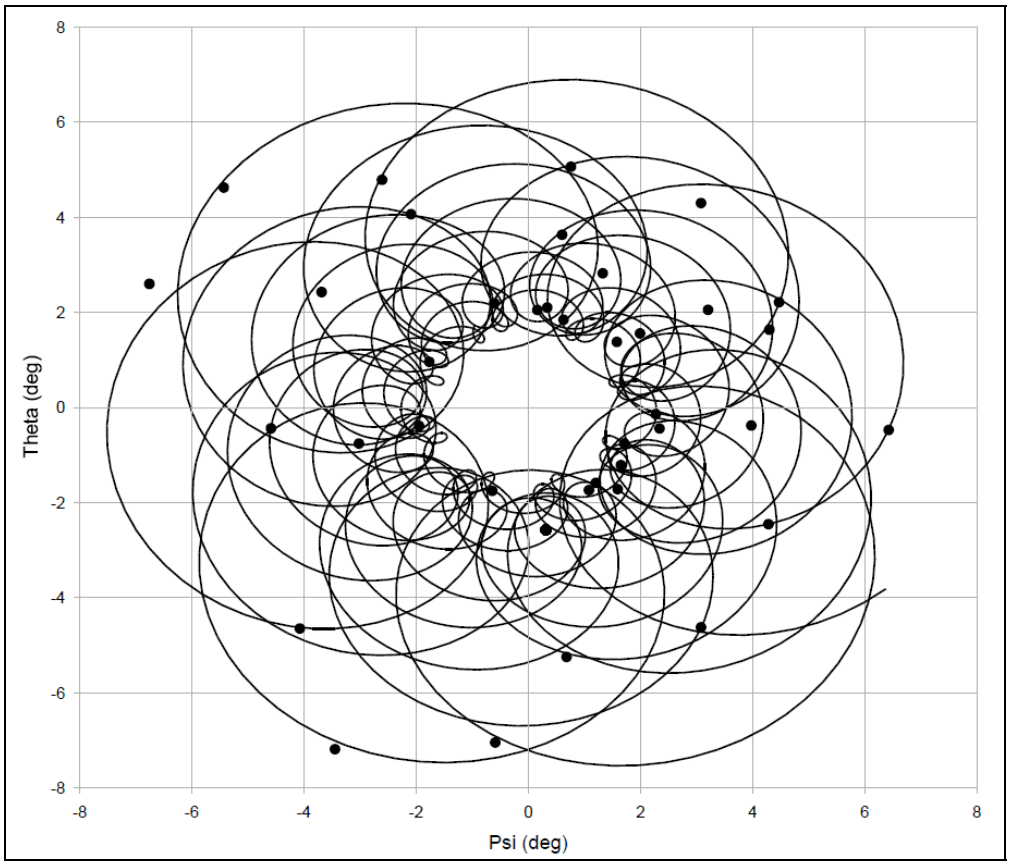

Figure A-12. Pitch angle vs. yaw angle for round 27353 (M855 at Mach 1.69).

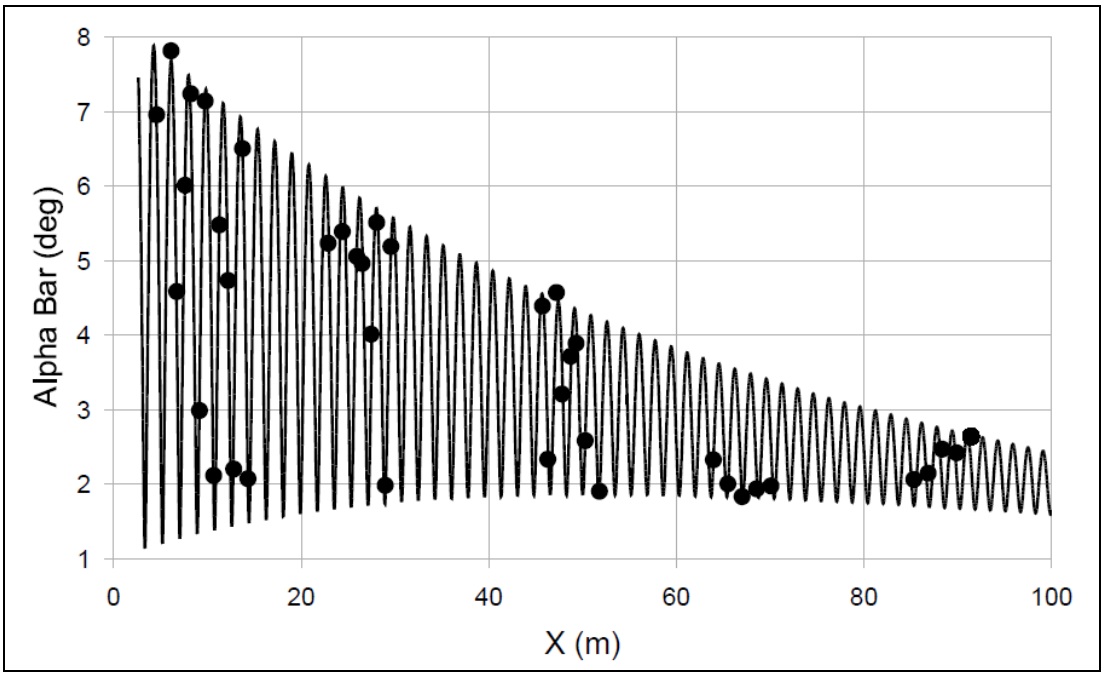

Figure A-13. Total yaw vs. range for round 27353 (M855 at Mach 1.69).

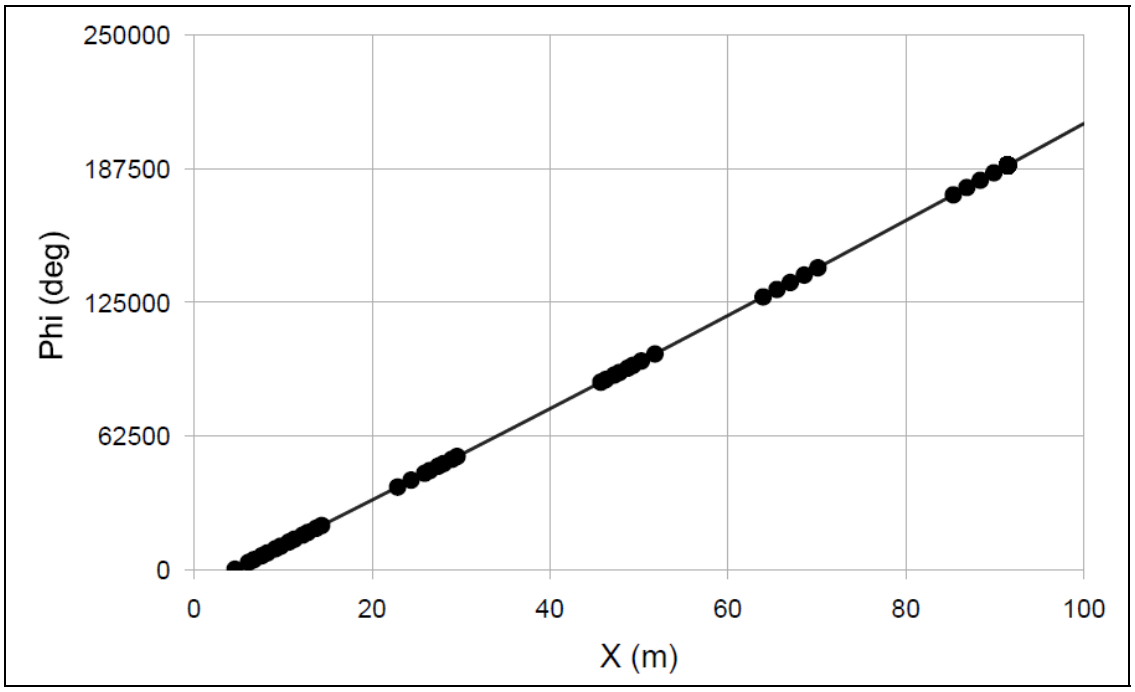

Figure A-14. Roll angle vs. range for round 27353 (M855 at Mach 1.69).

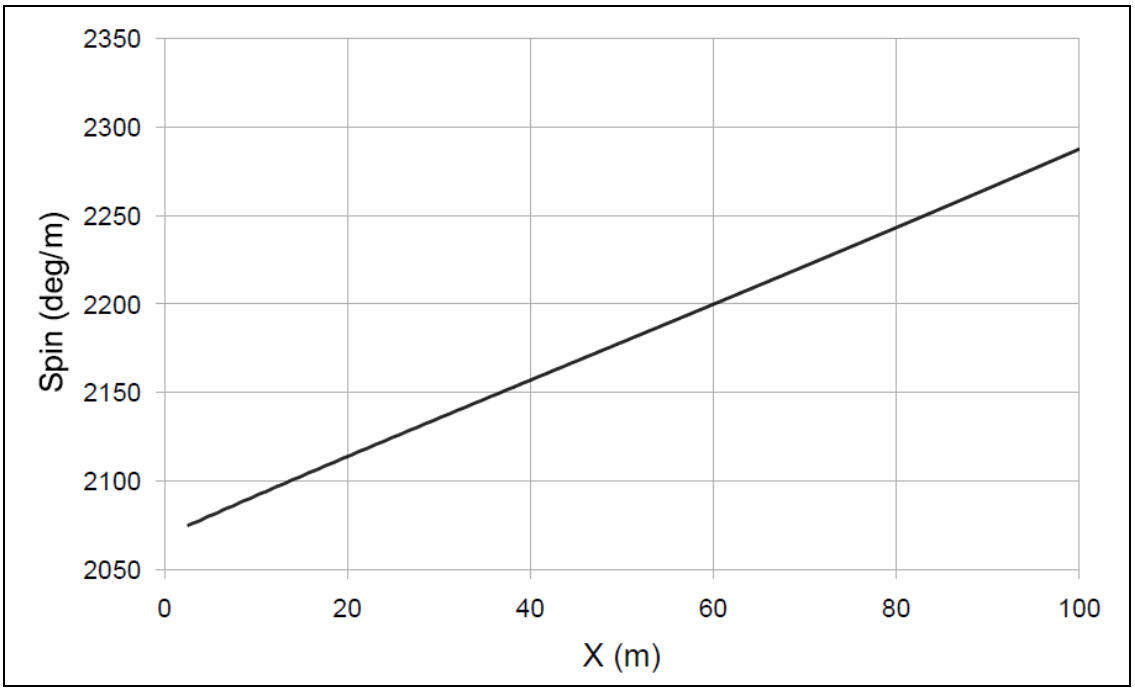

Figure A-15. Spin vs. range for round 27353 (M855 at Mach 1.69).

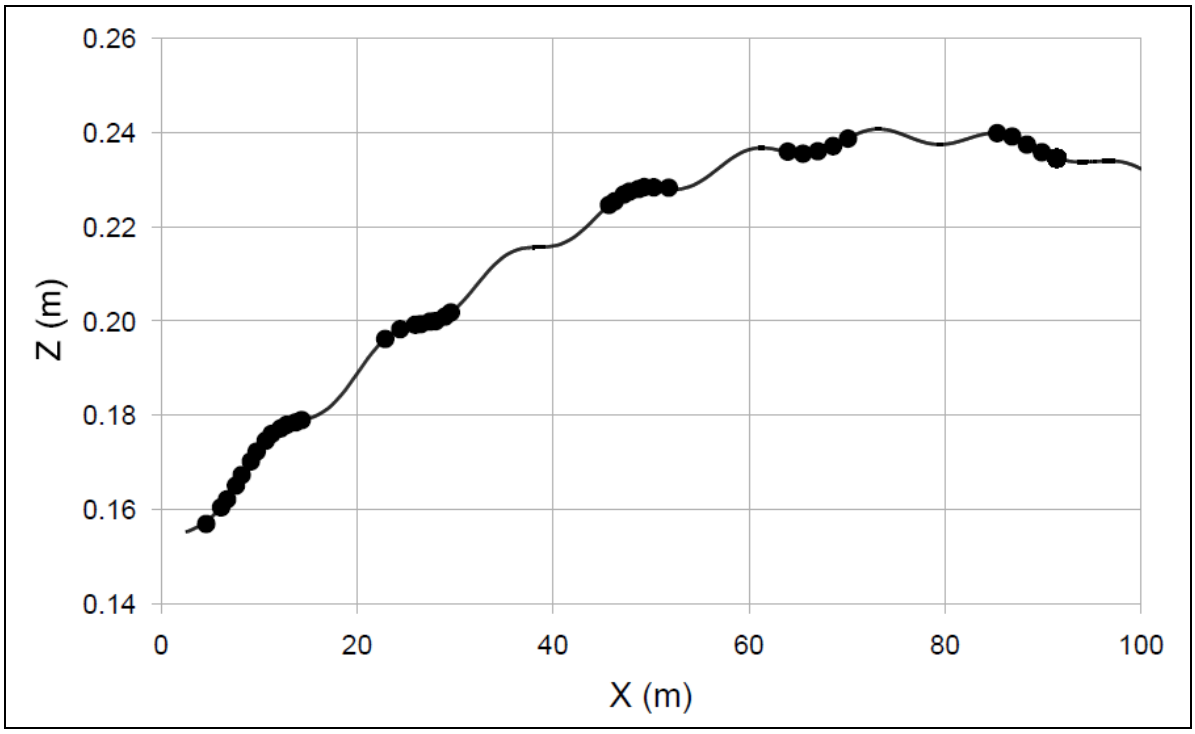

Figure A-16. Vertical position vs. range for round 27353 (M855 at Mach 1.69).

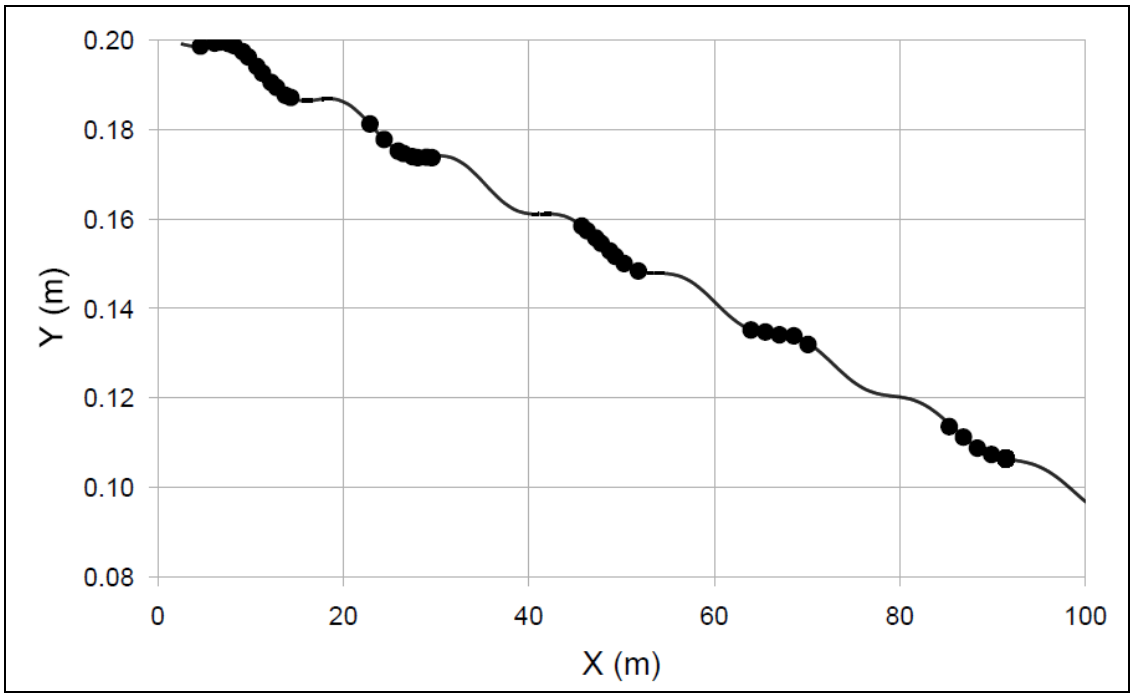

Figure A-17. Lateral position vs. range for round 27353 (M855 at Mach 1.69).

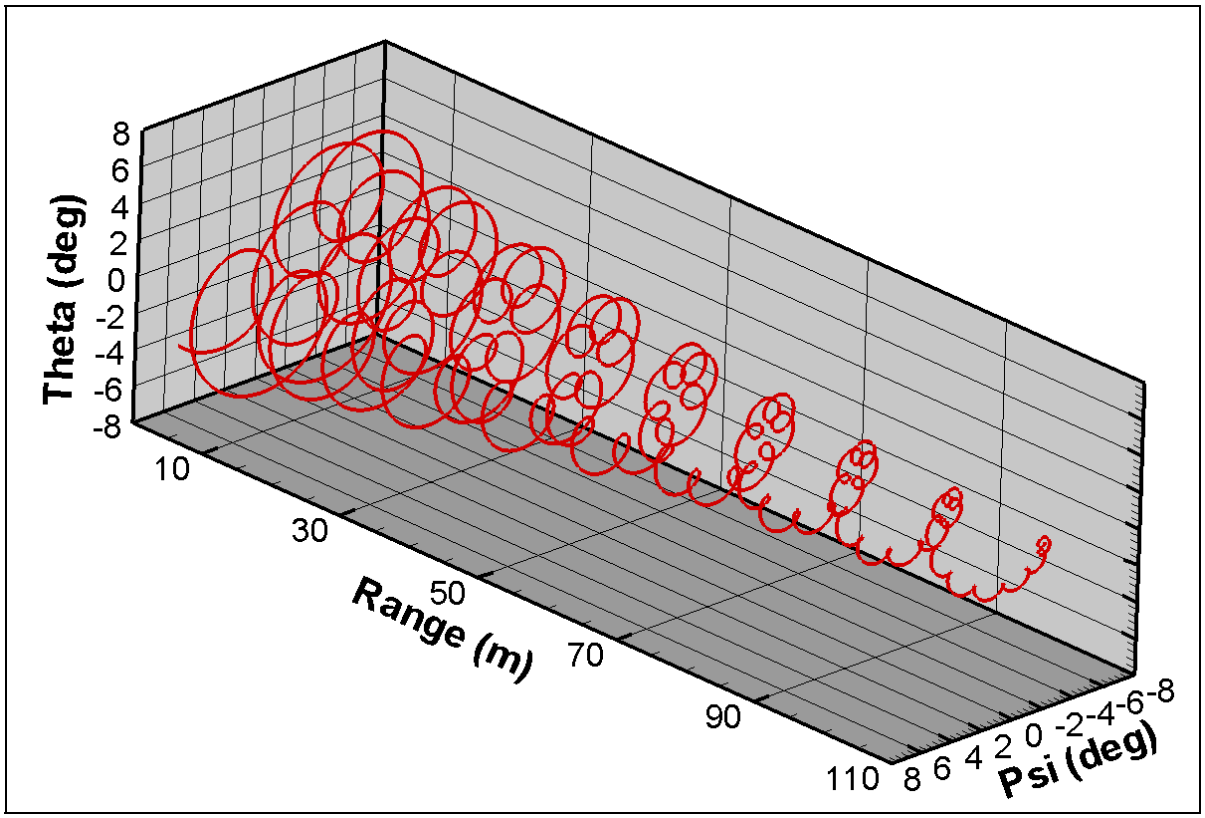

Figure A-18. Three-dimensional projectile motion through the range for round 27353 (M855 at Mach 1.69).

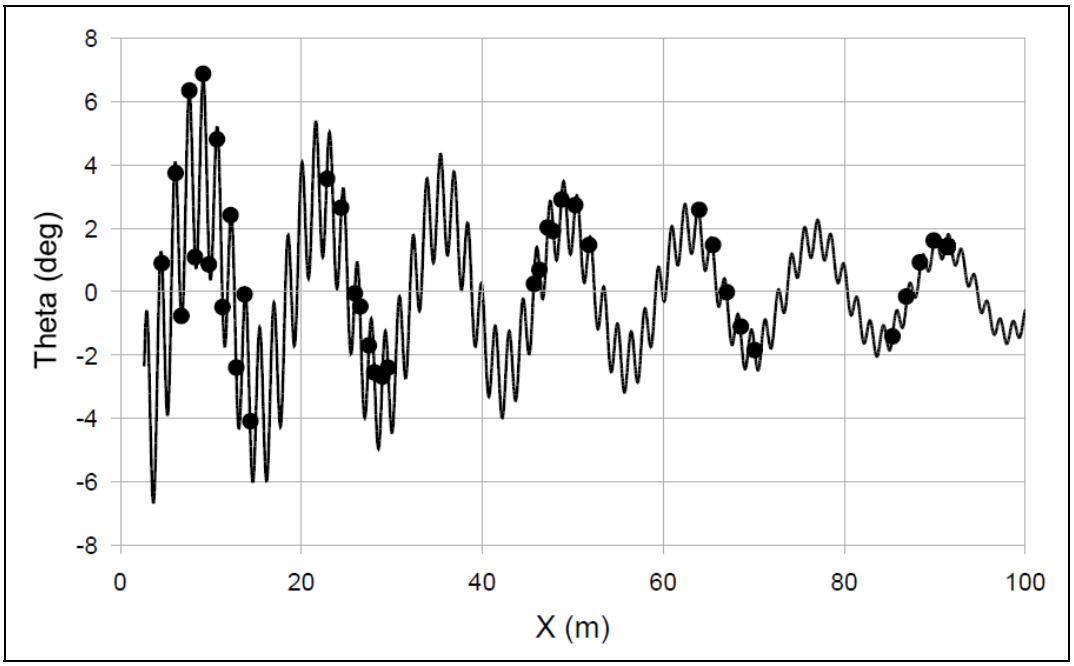

Figure A-19. Pitch angle vs. range for round 26833 (M855 at Mach 2.21).

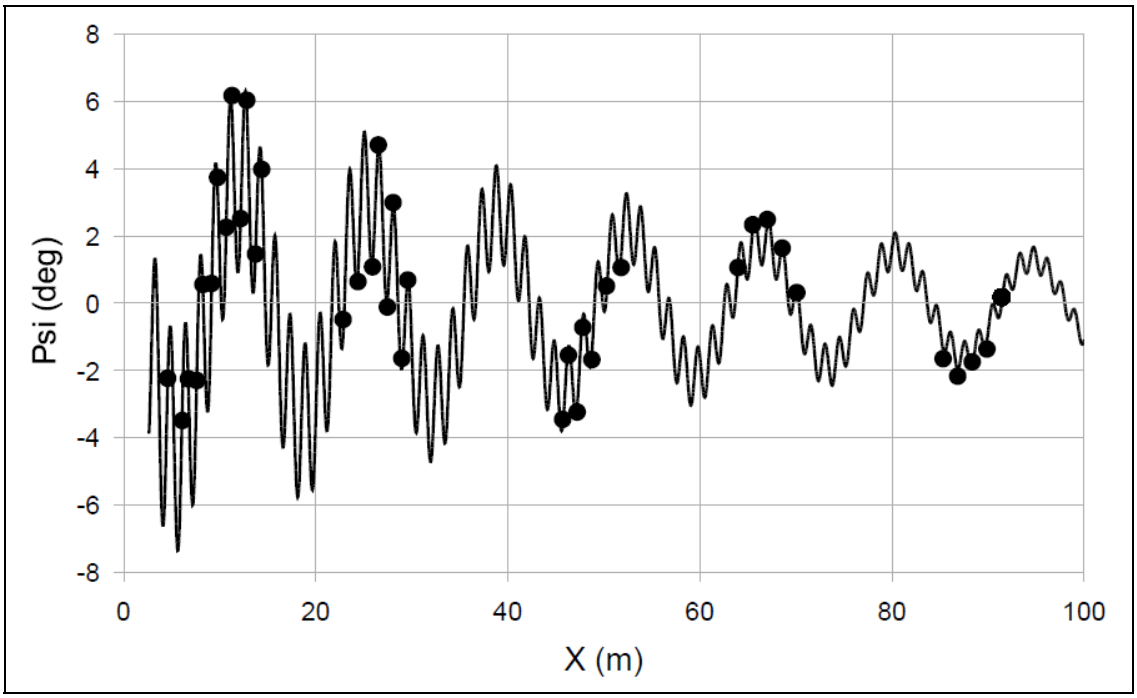

Figure A-20. Yaw angle vs. range for round 26833 (M855 at Mach 2.21).

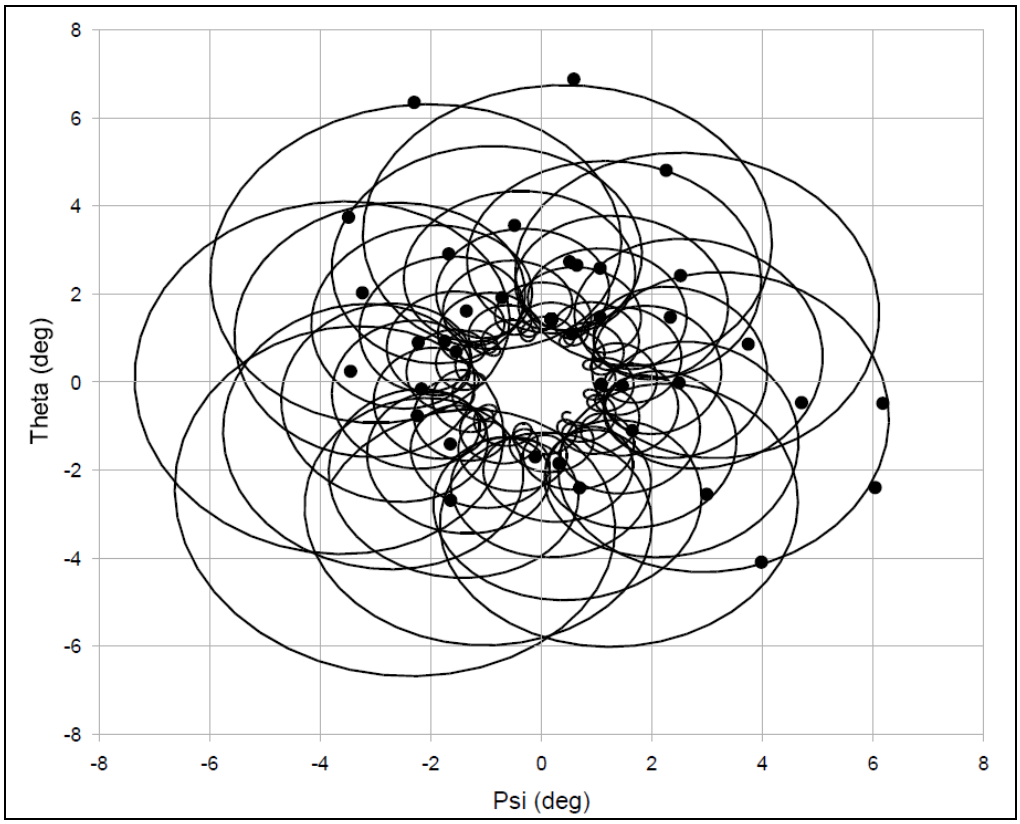

Figure A-21. Pitch angle vs. yaw angle for round 26833 (M855 at Mach 2.21).

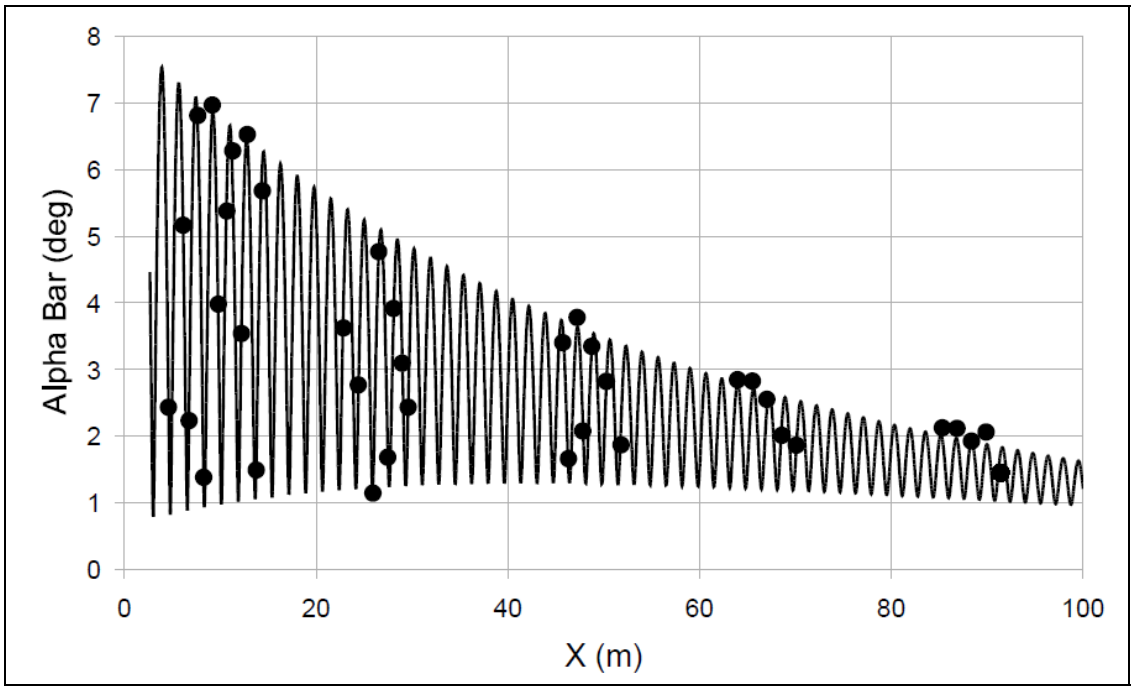

Figure A-22. Total yaw vs. range for round 26833 (M855 at Mach 2.21).

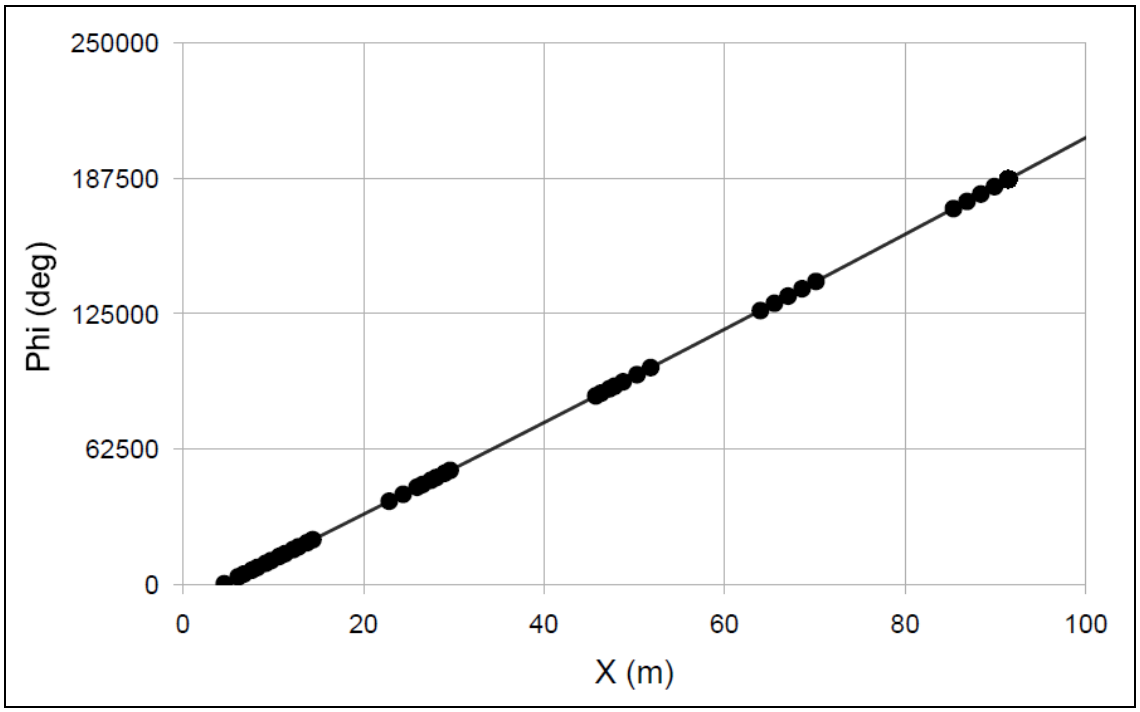

Figure A-23. Roll angle vs. range for round 26833 (M855 at Mach 2.21).

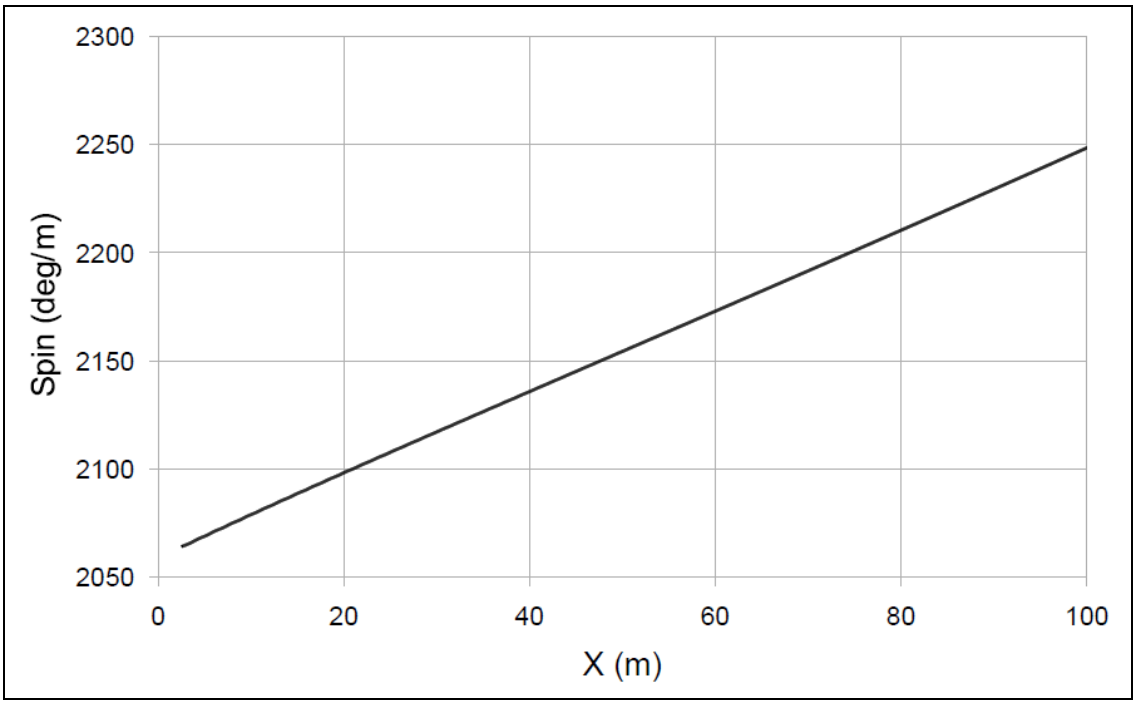

Figure A-24. Spin vs. range for round 26833 (M855 at Mach 2.21).

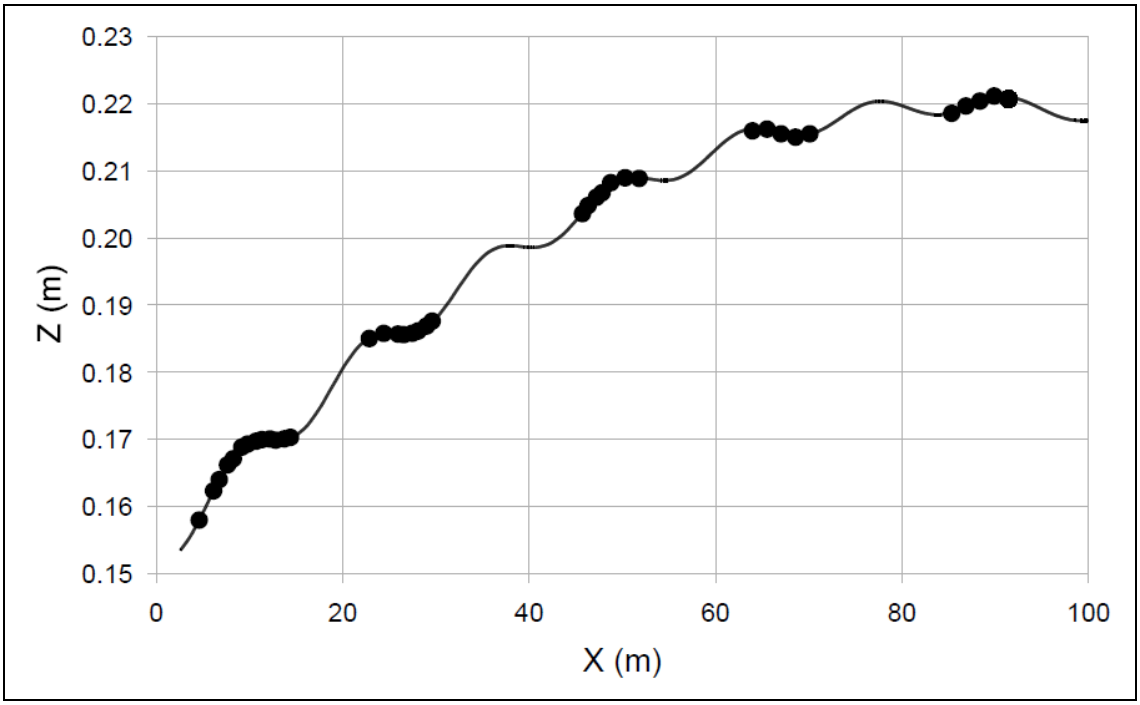

Figure A-25. Vertical position vs. range for round 26833 (M855 at Mach 2.21).

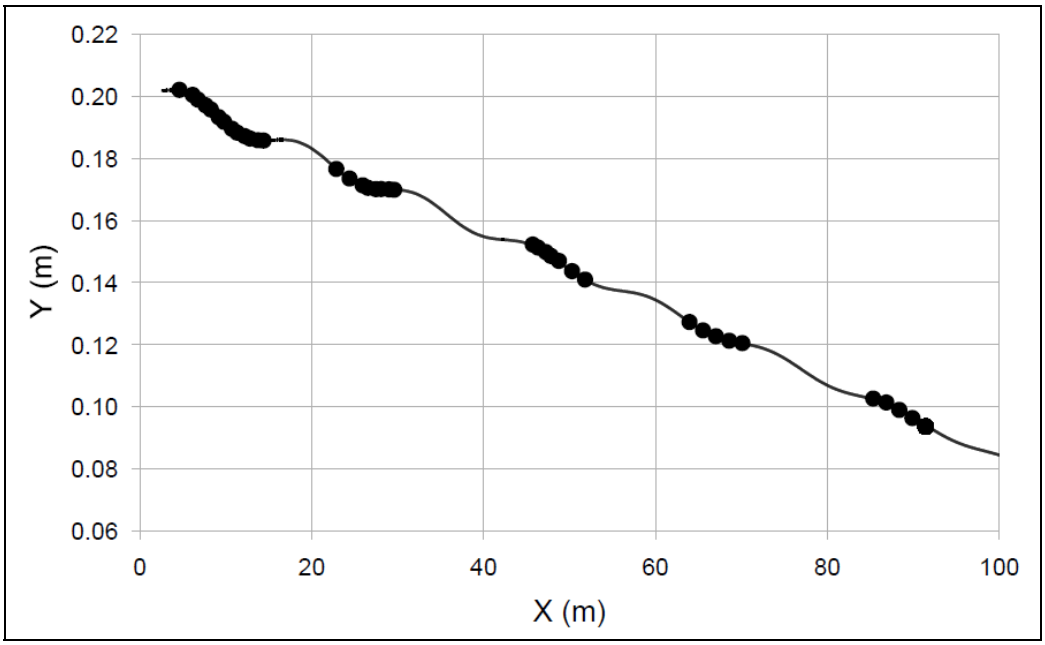

Figure A-26. Lateral position vs. range for round 26833 (M855 at Mach 2.21).

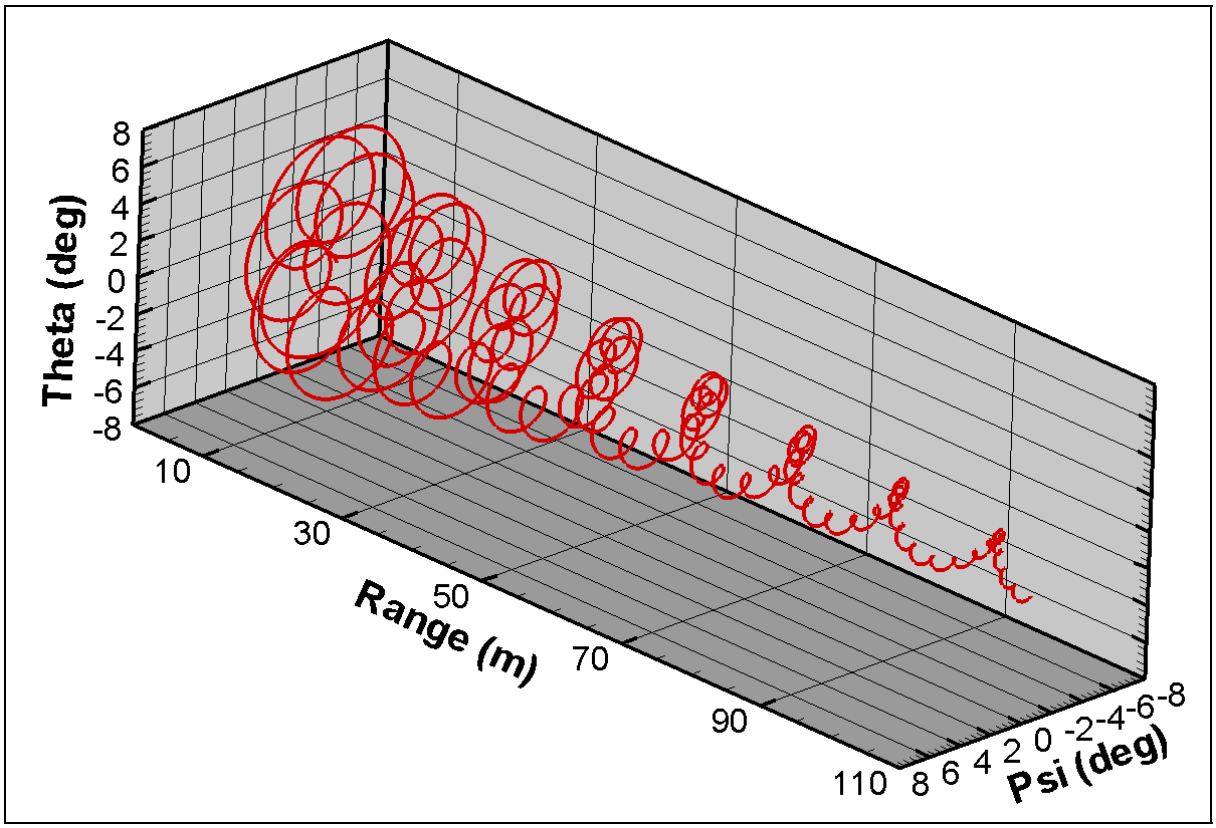

Figure A-27. Three-dimensional projectile motion through the range for round 26833 (M855 at Mach 2.21).

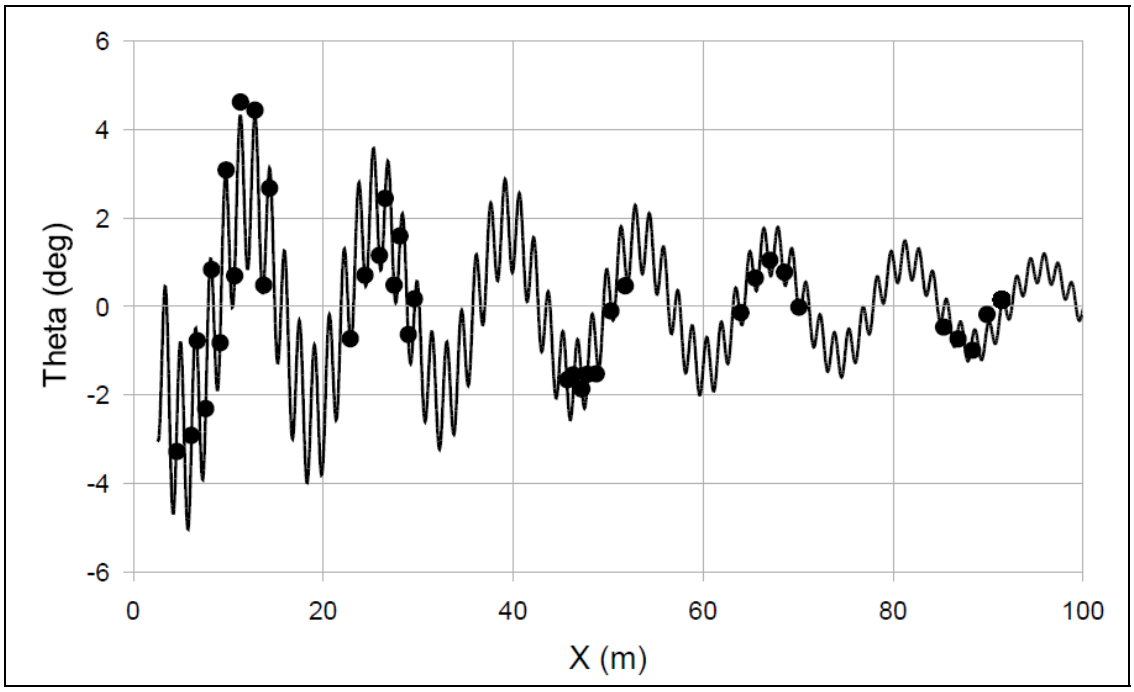

Figure A-28. Pitch angle vs. range for round 26597 (M855 at Mach 2.63).

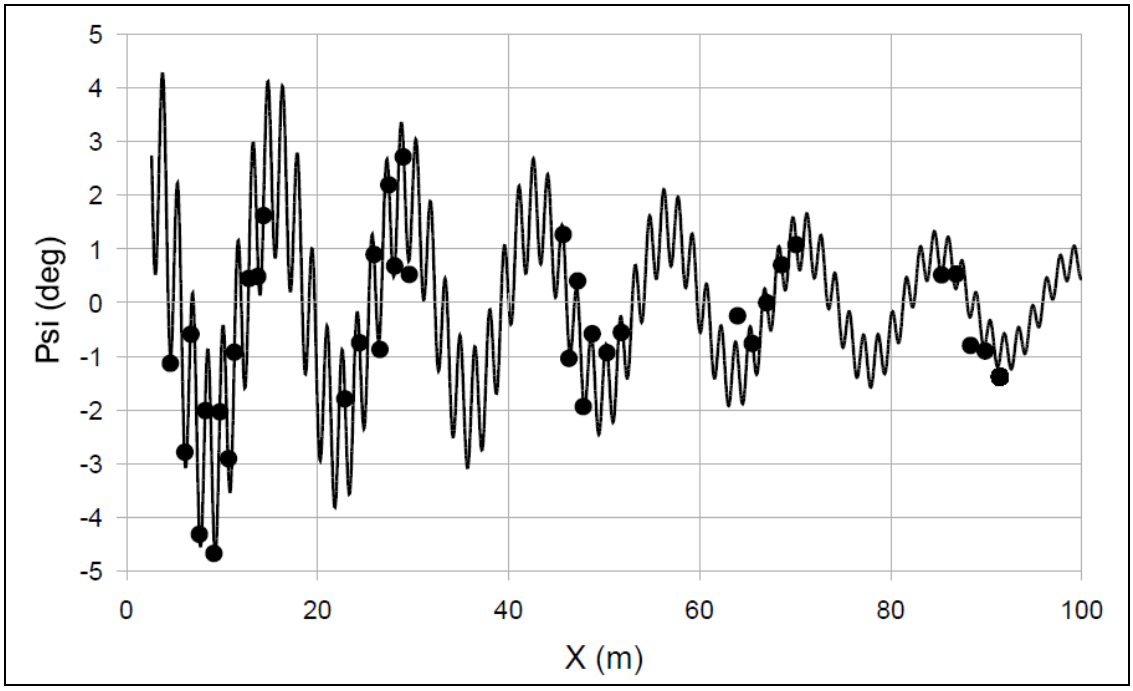

Figure A-29. Yaw angle vs. range for round 26597 (M855 at Mach 2.63).

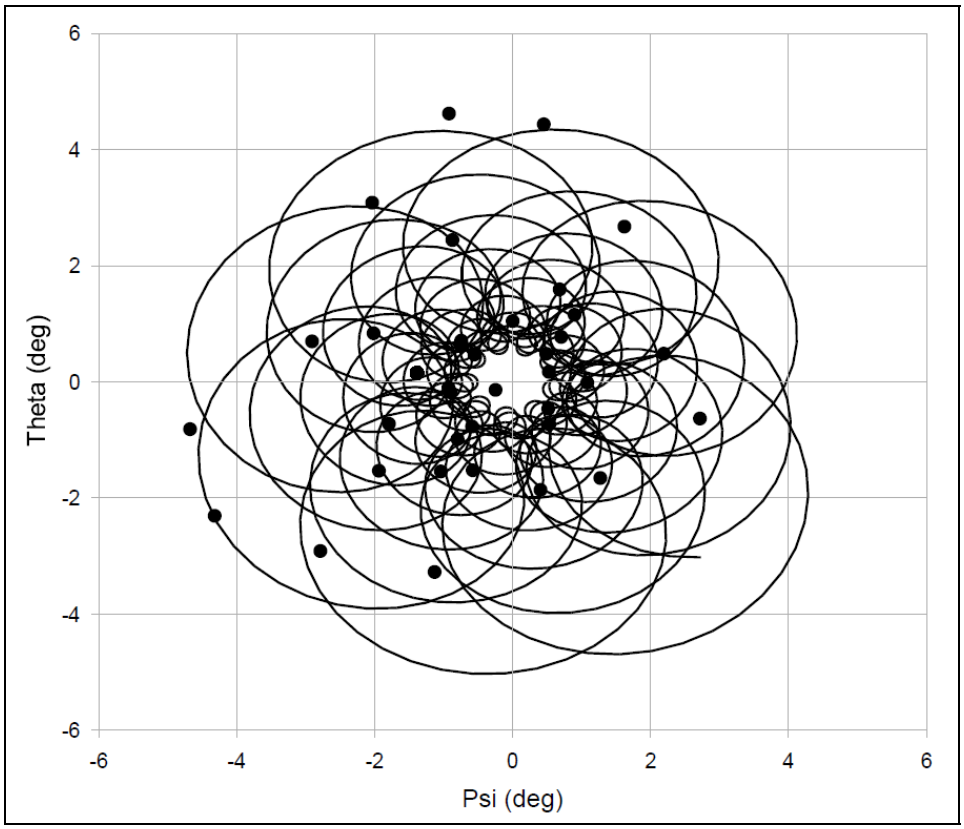

Figure A-30. Pitch angle vs. yaw angle for round 26597 (M855 at Mach 2.63).

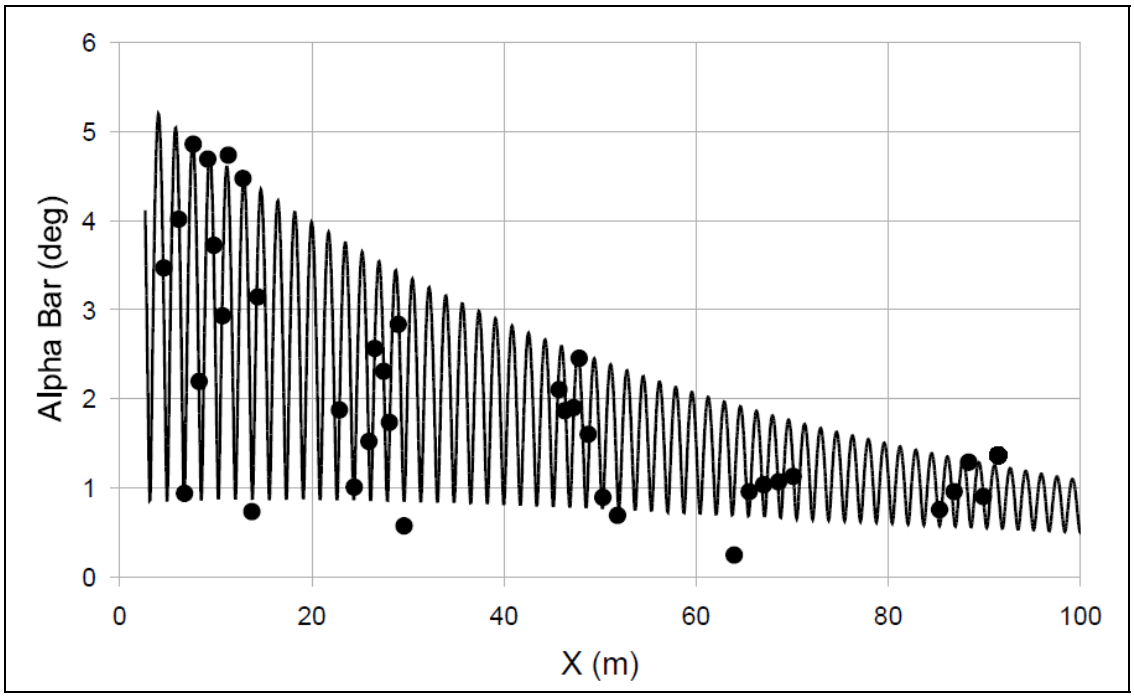

Figure A-31. Total yaw vs. range for round 26597 (M855 at Mach 2.63).

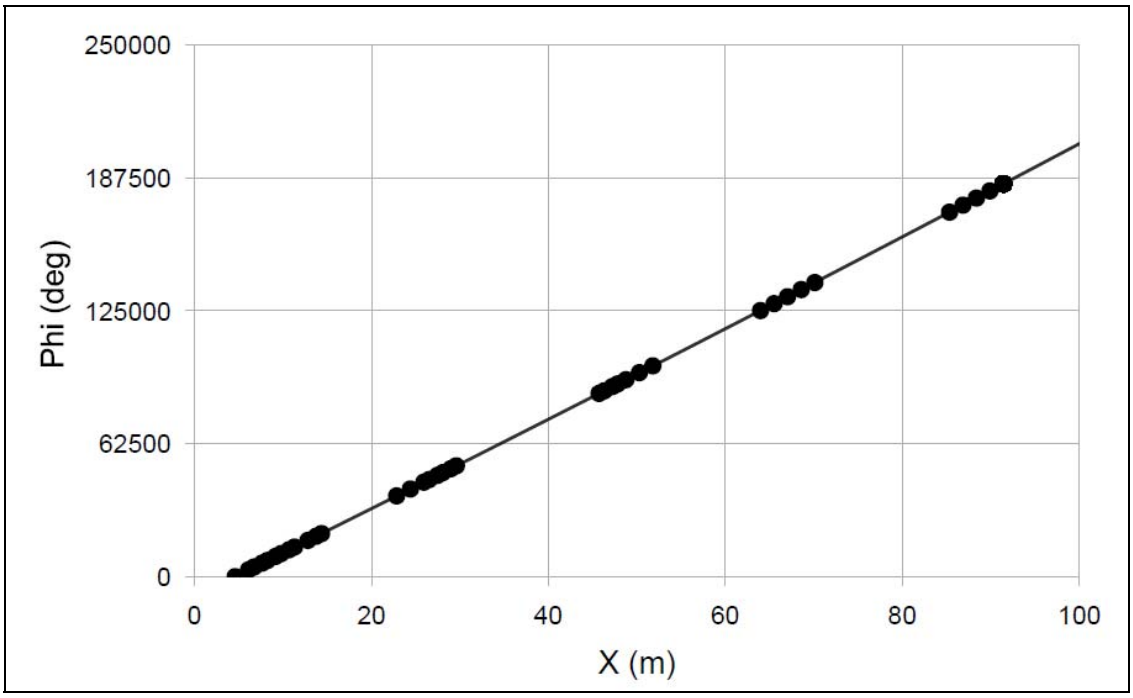

Figure A-32. Roll angle vs. range for round 26597 (M855 at Mach 2.63).

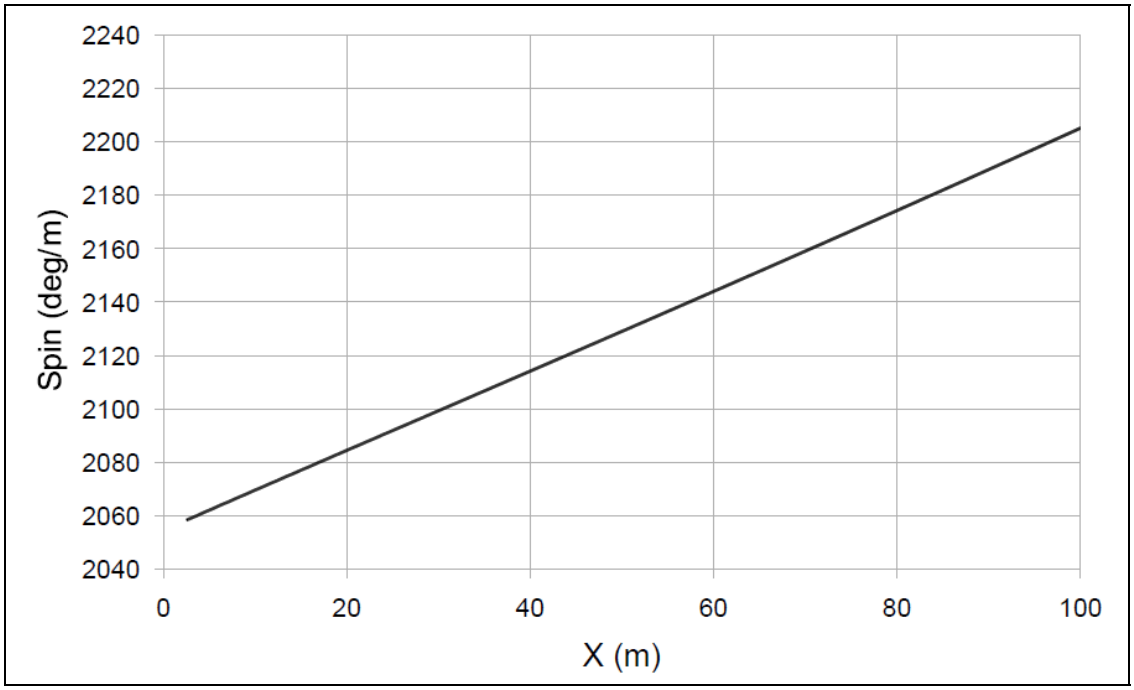

Figure A-33. Spin vs. range for round 26597 (M855 at Mach 2.63).

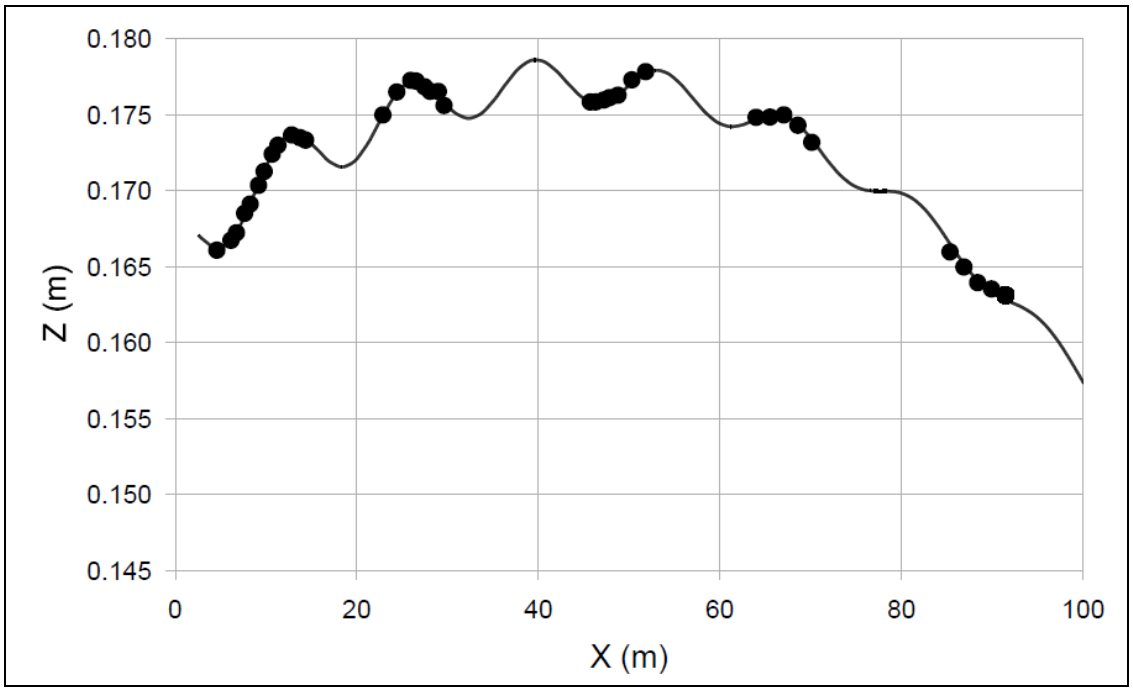

Figure A-34. Vertical position vs. range for round 26597 (M855 at Mach 2.63).

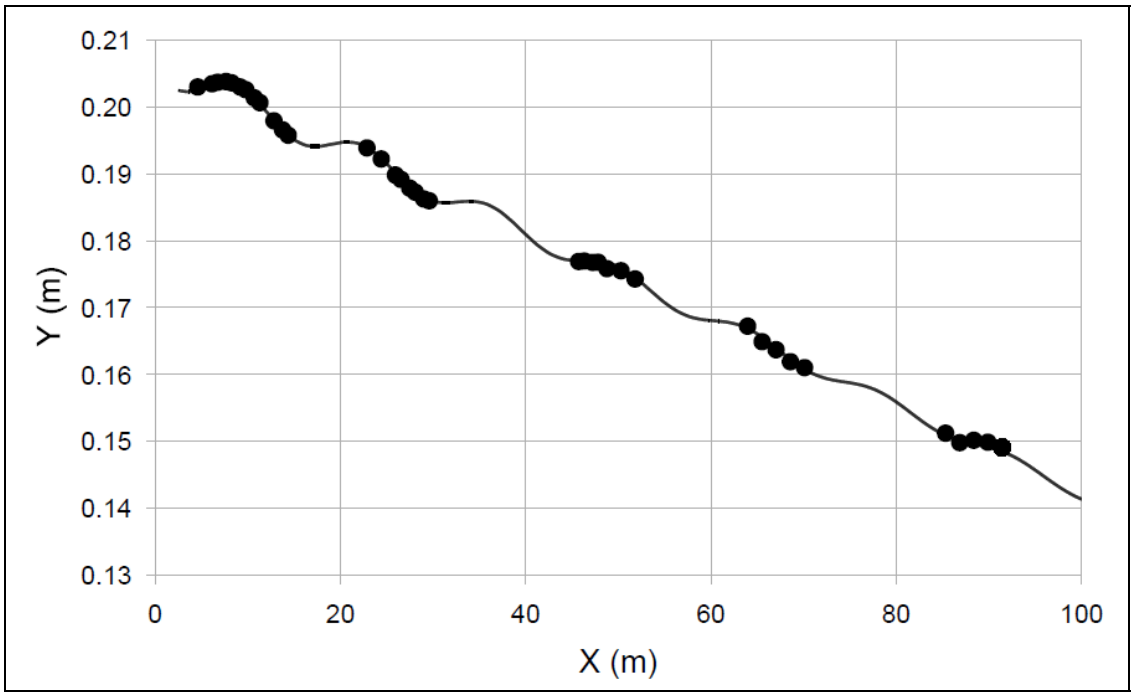

Figure A-35. Lateral position vs. range for round 26597 (M855 at Mach 2.63).

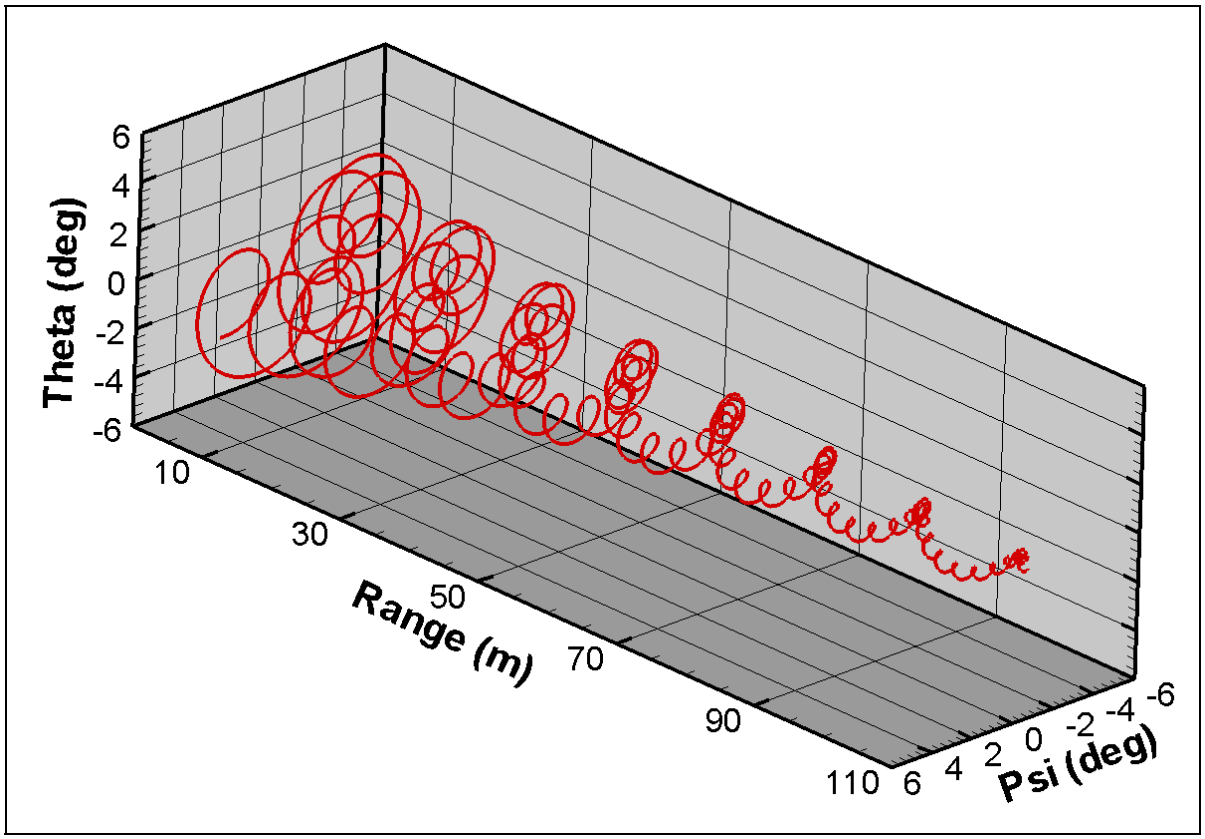

Figure A-36. Three-dimensional projectile motion through the range for round 26597 (M855 at Mach 2.63).

INTENTIONALLY LEFT BLANK.

Appendix B. Complete Set of 6-Degrees-of-Freedom (6-DOF) Fits

This appendix appears in its original form, without editorial change.

M16A2 M855 LR M1.7++ roll pins
6 DOF Summary Output (08-AUG-08 09:42:10)

Shot Number	Date	Time	Ref. CG (mm)	Ref. Length (mm)	Ref.Mach Number	Mach Number	DBSQ (deg2)	Max Angle of Attack (deg)	Standard Error X (m)	Y-Z (m)	Angle (deg)	Roll (deg)
27350	28-FEB-08	16:31:50	14.27	23.06	1.65	1.664	32.000	14.5	0.0005	0.0002	0.188	6.21
27351	28-FEB-08	16:32:24	14.27	23.06	1.65	1.678	29.530	12.1	0.0002	0.0002	0.203	11.65
27344	25-FEB-08	10:58:42	14.27	23.06	1.70	1.686	3.210	2.2	0.0001	0.0001	0.157	5.85
27346	25-FEB-08	11:17:01	14.27	23.06	1.70	1.687	3.142	2.4	0.0001	0.0001	0.197	5.98
27353	25-FEB-08	12:42:18	14.27	23.06	1.70	1.689	13.180	7.7	0.0003	0.0002	0.271	6.84
27352	28-FEB-08	16:32:48	14.27	23.06	1.70	1.702	37.140	15.0	0.0005	0.0003	0.159	8.70
27347	06-AUG-08	14:13:50	14.30	23.06	1.70	1.723	2.121	1.8	0.0006	0.0001	0.185	6.93
27345	25-FEB-08	11:04:18	14.27	23.06	1.70	1.725	4.512	3.1	0.0002	0.0001	0.201	6.57
26827	25-FEB-08	09:10:47	14.27	23.06	2.15	2.172	3.236	3.5	0.0002	0.0002	0.200	7.64
26833	28-FEB-08	16:34:01	14.27	23.06	2.20	2.212	9.357	6.8	0.0002	0.0002	0.231	4.98
26834	25-FEB-08	10:46:04	14.27	23.06	2.20	2.215	14.450	8.7	0.0003	0.0002	0.254	6.70
26826	25-FEB-08	10:09:05	14.27	23.06	2.20	2.224	0.734	1.9	0.0001	0.0002	0.236	7.03
26831	25-FEB-08	09:53:08	14.27	23.06	2.25	2.230	6.353	5.0	0.0002	0.0002	0.179	5.20
26828	28-FEB-08	16:34:18	14.27	23.06	2.25	2.248	2.174	2.8	0.0002	0.0001	0.155	4.55
26829	28-FEB-08	16:34:30	14.27	23.06	2.25	2.250	1.739	2.9	0.0002	0.0001	0.150	4.67
26832	25-FEB-08	09:54:42	14.27	23.06	2.25	2.252	7.421	6.1	0.0002	0.0001	0.208	3.88
26591	28-FEB-08	16:34:41	14.27	23.06	2.60	2.612	1.235	2.5	0.0002	0.0001	0.203	5.26
26598	28-FEB-08	16:34:54	14.27	23.06	2.60	2.613	6.653	6.2	0.0003	0.0006	0.306	4.32
26590	25-FEB-08	08:19:35	14.27	23.06	2.60	2.617	2.046	3.3	0.0003	0.0002	0.275	4.47
26597	28-FEB-08	16:35:07	14.27	23.06	2.65	2.631	4.481	4.9	0.0002	0.0003	0.248	5.16
26592	28-FEB-08	16:35:16	14.27	23.06	2.65	2.632	0.630	1.7	0.0002	0.0002	0.252	6.57

M16A2 M855 LR M1.7++ roll pins
6 DOF Summary Output (08-AUG-08 09:42:10)

Shot Number	Mach Number	DBSQ ABARM	CX CX2	CNa CNa3	CYpa CYpa3	Cma Cma3	Cmq Cmq2	Cnpa Cnpa3	Cnpa5	Clp IX/IY	CXM CmaM	Standard Error X(m) Y-Z(m)	 Angle(deg) Roll(deg)
27350	1.664	32.0	0.387	3.110	-1.00	2.739	-12.7	0.14		-0.0273	-0.12	0.0005	0.188
		14.5	2.300	0.000	0.00	-2.4	0.0	5.1	0.	0.1201	0.00	0.0002	6.210
27351	1.678	29.5	0.384	3.095	-1.00	2.738	-9.9	0.13		-0.0286	-0.07	0.0002	0.203
		12.1	2.300	0.000	0.00	-3.6	0.0	0.0	0.	0.1218	0.00	0.0002	11.650
27344	1.686	3.2	0.374	2.941	-1.00	2.677	-6.4	-0.82		-0.0320	-0.10	0.0001	0.157
		2.2	4.930	0.000	0.00	-2.5	0.0	109.0	0.	0.1204	-0.43	0.0001	5.846
27346	1.687	3.1	0.372	2.884	-1.00	2.656	-4.7	-0.50		-0.0327	-0.10	0.0001	0.197
		2.4	2.300	0.000	0.00	-2.5	0.0	0.0	0.	0.1200	-0.33	0.0001	5.982
27353	1.689	13.2	0.371	2.973	-1.00	2.708	-9.4	-0.01		-0.0303	-0.13	0.0003	0.271
		7.7	4.930	0.000	0.00	0.0	0.0	0.0	0.	0.1220	0.00	0.0002	6.836
27352	1.702	37.1	0.385	3.190	-1.00	2.709	-12.1	0.24		-0.0278	-0.15	0.0005	0.159
		15.0	2.300	0.000	0.00	-2.9	0.0	0.0	0.	0.1216	0.00	0.0003	8.702
27347	1.723	2.1	0.379	2.704	-1.00	2.745	-2.0	-0.62		-0.0469	-0.13	0.0006	0.185
		1.8	3.803	0.000	0.00	0.0	0.0	0.0	0.	0.1235	-0.46	0.0001	6.932
27345	1.725	4.5	0.368	2.722	-1.00	2.662	-7.6	-0.64		-0.0323	-0.10	0.0002	0.201
		3.1	4.930	0.000	0.00	-2.5	0.0	109.0	0.	0.1200	-0.48	0.0001	6.571
26827	2.172	3.2	0.328	2.893	-1.00	2.493	-8.0	-0.22		-0.0247	-0.07	0.0002	0.200
		3.5	3.414	0.000	0.00	-4.0	0.0	0.0	0.	0.1191	0.00	0.0002	7.637
26833	2.212	9.4	0.332	2.958	-1.00	2.521	-12.2	0.19		-0.0255	-0.05	0.0002	0.231
		6.8	3.000	0.000	0.00	-4.0	0.0	0.0	0.	0.1237	0.00	0.0002	4.982
26834	2.215	14.4	0.325	2.960	-1.00	2.514	-13.8	-0.14		-0.0241	-0.01	0.0003	0.254
		8.7	2.310	0.000	0.00	-2.8	0.0	46.9	0.	0.1241	0.00	0.0002	6.704

M16A2 M855 LR M1.7++ roll pins
6 DOF Summary Output (08-AUG-08 09:42:10)

Shot Number	Mach Number	DBSQ ABARM	CX CX2	CNa CNa3	CYpa CYpa3	Cma Cma3	Cmq Cmq2	Cnpa Cnpa3	Cnpa5	Clp IX/IY	CXM CmaM	Standard Error X(m) Y-Z(m)	 Angle(deg) Roll(deg)
26826	2.224	0.7	0.321	3.000	-1.00	2.548	-11.0	0.20		-0.0238	-0.04	0.0001	0.236
		1.9	3.000	0.000	0.00	-4.0	0.0	0.0	0.	0.1214	0.00	0.0002	7.028
26831	2.230	6.4	0.318	2.962	-1.00	2.554	-8.9	0.06		-0.0269	-0.05	0.0002	0.179
		5.0	2.880	0.000	0.00	-4.0	0.0	0.0	0.	0.1238	0.00	0.0002	5.196
26828	2.248	2.2	0.325	3.000	-1.00	2.510	-8.2	-0.29		-0.0251	-0.07	0.0002	0.155
		2.8	3.000	0.000	0.00	-4.0	0.0	0.0	0.	0.1225	0.00	0.0001	4.550
26829	2.250	1.7	0.328	3.160	-1.00	2.534	-11.9	-0.05		-0.0353	-0.06	0.0002	0.150
		2.9	3.000	0.000	0.00	-4.0	0.0	0.0	0.	0.1230	0.00	0.0001	4.673
26832	2.252	7.4	0.317	2.951	-1.00	2.581	-10.2	0.11		-0.0247	-0.05	0.0002	0.208
		6.1	3.414	0.000	0.00	-10.0	0.0	0.0	0.	0.1235	0.00	0.0001	3.883
26591	2.612	1.2	0.298	2.627	-1.00	2.413	-13.1	0.17		-0.0297	-0.06	0.0002	0.203
		2.5	3.000	0.000	0.00	-4.0	0.0	0.0	0.	0.1233	0.00	0.0001	5.261
26598	2.613	6.7	0.294	3.006	-1.00	2.507	-22.8	0.47		-0.0205	-0.06	0.0003	0.306
		6.2	3.000	0.000	0.00	-7.2	0.0	0.0	0.	0.1261	0.00	0.0006	4.319
26590	2.617	2.0	0.304	2.801	-1.00	2.404	-12.6	0.15		-0.0295	-0.06	0.0003	0.275
		3.3	3.000	0.000	0.00	-4.0	0.0	0.0	0.	0.1227	0.00	0.0002	4.474
26597	2.631	4.5	0.293	2.886	-1.00	2.429	-11.4	0.26		-0.0246	-0.03	0.0002	0.248
		4.9	1.000	0.000	0.00	-4.0	0.0	0.0	0.	0.1236	0.00	0.0003	5.161
26592	2.632	0.6	0.292	3.000	-1.00	2.457	-11.0	0.20		-0.0258	-0.06	0.0002	0.252
		1.7	3.000	0.000	0.00	-4.0	0.0	0.0	0.	0.1227	0.00	0.0002	6.565

M16A2 M855 LR M1.7++ roll pins
6 DOF Summary Output (08-AUG-08 09:42:10)

Shot Numbers		Date	Time	Ref. Mach Number	Mach Number	DBSQ (deg2)	Max Angle of Attack (deg)	Standard Error X (m)	Y-Z (m)	Angle (deg)	Roll (deg)
27350	27351	11-JUN-07	10:38:29	1.700	1.683	28.08	14.87	0.0005	0.0003	0.250	11.280
27353	27352										
27350	27351	22-FEB-08	13:58:59	1.700	1.683	28.35	14.96	0.0009	0.0004	0.455	16.530
27352	27353										
27346	27344	06-AUG-08	12:38:32	1.700	1.697	6.00	7.58	0.0005	0.0002	0.230	6.265
27353	27345										
27345	27347	02-APR-08	09:59:34	1.700	1.705	3.18	3.03	0.0003	0.0001	0.219	6.311
27346	27344										
26827	26833	11-JUN-07	10:38:50	2.250	2.211	6.68	8.45	0.0004	0.0002	0.275	6.333
26826	26834										
26831											
26827	26829	22-FEB-08	12:40:56	2.200	2.223	5.38	6.88	0.0009	0.0007	0.213	5.344
26831	26832										
26833											
26826	26828	22-FEB-08	13:05:14	2.200	2.234	6.13	8.46	0.0006	0.0002	0.227	5.573
26831	26832										
26834											
26831	26829	11-JUL-08	11:23:48	2.200	2.239	6.24	8.50	0.0004	0.0002	0.244	5.064
26828	26832										
26834											
26597	26592	11-JUN-07	10:39:11	2.200	2.461	6.10	8.47	0.0003	0.0002	0.266	7.182
26590	26834										
26833											
26590	26591	22-FEB-08	15:04:47	2.650	2.621	2.96	6.02	0.0003	0.0003	0.276	5.159
26592	26598										
26597											
26591	26598	11-JUN-07	10:39:21	2.650	2.621	2.97	5.98	0.0003	0.0004	0.317	5.164
26590	26592										
26597											

M16A2 M855 LR M1.7++ roll pins
6 DOF Summary Output (08-AUG-08 09:42:10)

Shot Numbers		Mach Number	DBSQ ABARM	CX CX2 CX4	CNa CNa3 CNa5	CYpa CYpa3	Cma Cma3 Cma5	Cmq Cmq2 Cmq4	Cnpa Cnpa3 Cnpa5	Clp CXm CmaM	Standard Error X(m) Y-Z(m)	Standard Error Angle(deg) Roll(deg)
27350	27351	1.683	28.1	0.383	2.970	-1.00	2.720	-12.0	0.07	-0.0303	0.0005	0.2496
27353	27352		14.9	2.297	0.000	0.00	-1.978	0.0	8.10	-0.0766	0.0003	11.2800
				0.00	0.00		0.0	0.	0.	-0.294		
27350	27351	1.683	28.4	0.384	3.198	-1.00	2.684	-11.4	0.15	-0.0286	0.0009	0.4548
27352	27353		15.0	2.208	0.000	0.00	0.000	0.0	0.00	-0.1040	0.0004	16.5300
				0.00	0.00		0.0	0.	0.	0.000		
27346	27344	1.697	6.0	0.372	3.136	-1.00	2.658	-9.9	-0.62	-0.0317	0.0005	0.2304
27353	27345		7.6	3.788	0.000	0.00	9.861	0.0	95.00	-0.0861	0.0002	6.2650
				0.00	0.00		0.0	0.	0.	-0.642		
27345	27347	1.705	3.2	0.375	3.000	-1.00	2.665	-6.1	-0.59	-0.0367	0.0003	0.2193
27346	27344		3.0	2.300	0.000	0.00	-2.500	0.0	0.00	-0.1023	0.0001	6.3110
				0.00	0.00		0.0	0.	0.	-0.371		
26827	26833	2.211	6.7	0.320	2.886	-1.00	2.530	-11.5	0.15	-0.0249	0.0004	0.2752
26826	26834		8.5	4.270	0.000	0.00	-5.263	0.0	0.00	-0.0768	0.0002	6.3330
26831				0.00	0.00		0.0	0.	0.	0.000		
26827	26829	2.223	5.4	0.325	0.335	-1.00	0.000	-14.6	0.48	-0.0274	0.0009	0.2134
26831	26832		6.9	3.414303	3.928	0.00	-4.000	0.0	0.00	-0.0603	0.0007	5.3440
26833				0.00	0.00		0.0	0.	0.	0.000		
26826	26828	2.234	6.1	0.322	2.918	-1.00	0.000	-11.4	0.02	-0.0249	0.0006	0.2274
26831	26832		8.5	2.310	0.000	0.00	-4.979	0.0	25.52	-0.0221	0.0002	5.5730
26834				0.00	0.00		0.0	0.	0.	0.000		
26831	26829	2.239	6.2	0.323	3.079	-1.00	2.545	-11.2	0.02	-0.0272	0.0004	0.2441
26828	26832		8.5	3.000	0.000	0.00	-6.835	0.0	21.64	-0.0572	0.0002	5.0640
26834				0.00	0.00		0.0	0.	0.	0.000		
26597	26592	2.461	6.1	0.307	2.891	-1.00	2.469	-11.8	0.19	-0.0268	0.0003	0.2661
26590	26834		8.5	3.824	0.000	0.00	-4.000	0.0	0.00	-0.0687	0.0002	7.1820
26833				0.00	0.00		0.0	0.	0.	-0.224		
26590	26591	2.621	3.0	0.299	3.010	-1.00	0.000	-15.4	0.29	-0.0260	0.0003	0.2762
26592	26598		6.0	3.000	0.000	0.00	-4.000	0.0	1.10	-0.0632	0.0003	5.1590
26597				0.00	0.00		0.0	0.	0.	0.000		
26591	26598	2.621	3.0	0.296	2.928	-1.00	2.449	-15.7	0.32	-0.0260	0.0003	0.3166
26590	26592		6.0	3.000	0.000	0.00	-3.000	0.0	0.00	-0.0617	0.0004	5.1640
26597				0.00	0.00		0.0	0.	0.	0.000		

6 DOF Summary Output

Shot Number	Mach Number	DBSQ ABARM	CX CX2	CNa CNa3	CYpa CYpa3	Cma Cma3	Cmq Cmq2	Cnpa Cnpa3	Cnpa5	Clp IX/IY	CXM CmaM	Standard Error X(m) Y-Z(m)	 Angle(deg) Roll(deg)
27350	1.664	32.0	0.387	3.110	-1.00	2.739	-12.7	0.14		-0.0273	-0.12	0.0005	0.188
			(0.1%)	(1.4%)	(*)	(0.1%)	(3.6%)	(38.4%)		(0.3%)	(4.8%)		
		14.5	2.300	0.000	0.00	-2.4	0.0	5.1	0.	0.1201	0.00	0.0002	6.210
			(*)	(*)	(*)	(8.3%)	(*)	(33.4%)	(*)	(0.0%)	(*)		
27351	1.678	29.5	0.384	3.095	-1.00	2.738	-9.9	0.13		-0.0286	-0.07	0.0002	0.203
			(0.0%)	(0.8%)	(*)	(0.2%)	(4.6%)	(34.8%)		(0.5%)	(3.6%)		
		12.1	2.300	0.000	0.00	-3.6	0.0	0.0	0.	0.1218	0.00	0.0002	11.650
			(*)	(*)	(*)	(10.2%)	(*)	(*)	(*)	(0.0%)	(*)		
27344	1.686	3.2	0.374	2.941	-1.00	2.677	-6.4	-0.82		-0.0320	-0.10	0.0001	0.157
			(0.0%)	(1.9%)	(*)	(0.2%)	(37.8%)	(16.2%)		(0.4%)	(1.6%)		
		2.2	4.930	0.000	0.00	-2.5	0.0	109.0	0.	0.1204	-0.43	0.0001	5.846
			(*)	(*)	(*)	(*)	(*)	(*)	(*)	(0.1%)	(28.8%)		
27346	1.687	3.1	0.372	2.884	-1.00	2.656	-4.7	-0.50		-0.0327	-0.10	0.0001	0.197
			(0.0%)	(1.6%)	(*)	(0.2%)	(43.9%)	(28.9%)		(0.2%)	(1.1%)		
		2.4	2.300	0.000	0.00	-2.5	0.0	0.0	0.	0.1200	-0.33	0.0001	5.982
			(*)	(*)	(*)	(*)	(*)	(*)	(*)	(0.1%)	(36.0%)		
27353	1.689	13.2	0.371	2.973	-1.00	2.708	-9.4	-0.01		-0.0303	-0.13	0.0003	0.271
			(0.0%)	(1.3%)	(*)	(0.1%)	(10.9%)	(-)		(0.3%)	(*)		
		7.7	4.930	0.000	0.00	0.0	0.0	0.0	0.	0.1220	0.00	0.0002	6.836
			(*)	(*)	(*)	(*)	(*)	(*)	(*)	(0.0%)	(*)		
27352	1.702	37.1	0.385	3.190	-1.00	2.709	-12.1	0.24		-0.0278	-0.15	0.0005	0.159
			(0.1%)	(1.4%)	(*)	(0.1%)	(2.8%)	(14.2%)		(0.4%)	(4.2%)		
		15.0	2.300	0.000	0.00	-2.9	0.0	0.0	0.	0.1216	0.00	0.0003	8.702
			(*)	(*)	(*)	(4.7%)	(*)	(*)	(*)	(0.0%)	(*)		
27347	1.723	2.1	0.379	2.704	-1.00	2.745	-2.0	-0.62		-0.0469	-0.13	0.0006	0.185
			(0.0%)	(6.1%)	(*)	(0.2%)	(-)	(27.1%)		(0.2%)	(*)		
		1.8	3.803	0.000	0.00	0.0	0.0	0.0	0.	0.1235	-0.46	0.0001	6.932
			(*)	(*)	(*)	(*)	(*)	(*)	(*)	(0.1%)	(28.4%)		

27345	1.725	4.5	0.368	2.722	-1.00	2.662	-7.6	-0.64		-0.0323	-0.10	0.0002	0.201
			(0.0%)(2.1%)		(*)	(0.2%)(21.4%)(19.9%)				(0.3%)(1.5%)			
		3.1	4.930	0.000	0.00	-2.5	0.0	109.0	0.	0.1200	-0.48	0.0001	6.571
			(*)	(*)	(*)	(*)	(*)	(*)	(*)	(0.1%)(20.6%)			
26827	2.172	3.2	0.328	2.893	-1.00	2.493	-8.0	-0.22		-0.0247	-0.07	0.0002	0.200
			(0.0%)(2.4%)		(*)	(0.2%)(18.5%)(61.4%)				(0.4%)	(*)		
		3.5	3.414	0.000	0.00	-4.0	0.0	0.0	0.	0.1191	0.00	0.0002	7.637
			(*)	(*)	(*)	(*)	(*)	(*)	(*)	(0.0%)	(*)		
26833	2.212	9.4	0.332	2.958	-1.00	2.521	-12.2	0.19		-0.0255	-0.05	0.0002	0.231
			(0.0%)(1.1%)		(*)	(0.1%)(7.3%)(44.7%)				(0.3%)(3.0%)			
		6.8	3.000	0.000	0.00	-4.0	0.0	0.0	0.	0.1237	0.00	0.0002	4.982
			(*)	(*)	(*)	(*)	(*)	(*)	(*)	(0.0%)	(*)		
26834	2.215	14.4	0.325	2.960	-1.00	2.514	-13.8	-0.14		-0.0241	-0.01	0.0003	0.254
			(0.0%)(1.3%)		(*)	(0.3%)(6.9%)(67.1%)				(0.4%)(20.9%)			
		8.7	2.310	0.000	0.00	-2.8	0.0	46.9	0.	0.1241	0.00	0.0002	6.704
			(*)	(*)	(*)	(37.4%)	(*)	(20.9%)	(*)	(0.0%)	(*)		
26826	2.224	0.7	0.321	3.000	-1.00	2.548	-11.0	0.20		-0.0238	-0.04	0.0001	0.236
			(0.0%)	(*)	(*)	(0.5%)	(*)	(*)		(0.4%)(2.8%)			
		1.9	3.000	0.000	0.00	-4.0	0.0	0.0	0.	0.1214	0.00	0.0002	7.028
			(*)	(*)	(*)	(*)	(*)	(*)	(*)	(0.1%)	(*)		
26831	2.230	6.4	0.318	2.962	-1.00	2.554	-8.9	0.06		-0.0269	-0.05	0.0002	0.179
			(0.0%)(1.2%)		(*)	(0.1%)(12.0%)		(-)		(0.3%)(2.9%)			
		5.0	2.880	0.000	0.00	-4.0	0.0	0.0	0.	0.1238	0.00	0.0002	5.196
			(*)	(*)	(*)	(*)	(*)	(*)	(*)	(0.0%)	(*)		
26828	2.248	2.2	0.325	3.000	-1.00	2.510	-8.2	-0.29		-0.0251	-0.07	0.0002	0.155
			(0.0%)	(*)	(*)	(0.2%)(10.9%)(12.7%)				(0.2%)(2.2%)			
		2.8	3.000	0.000	0.00	-4.0	0.0	0.0	0.	0.1225	0.00	0.0001	4.550
			(*)	(*)	(*)	(*)	(*)	(*)	(*)	(0.0%)	(*)		
26829	2.250	1.7	0.328	3.160	-1.00	2.534	-11.9	-0.05		-0.0353	-0.06	0.0002	0.150
			(0.0%)(2.1%)		(*)	(0.2%)(12.8%)		(-)		(0.2%)(1.7%)			
		2.9	3.000	0.000	0.00	-4.0	0.0	0.0	0.	0.1230	0.00	0.0001	4.673
			(*)	(*)	(*)	(*)	(*)	(*)	(*)	(0.1%)	(*)		

6 DOF Summary Output

Shot Number	Mach Number	DBSQ / ABARM	CX / CX2	CNa / CNa3	CYpa / CYpa3	Cma / Cma3	Cmq / Cmq2	Cnpa / Cnpa3	Cnpa5	Clp / IX/IY	CXM / CmaM	Standard Error X(m) / Y-Z(m)	Standard Error Angle(deg) / Roll(deg)
26832	2.252	7.4	0.317	2.951	-1.00	2.581	-10.2	0.11		-0.0247	-0.05	0.0002	0.208
			(0.0%)	(0.9%)	(*)	(0.3%)	(*)	(39.5%)		(0.2%)	(3.0%)		
		6.1	3.414	0.000	0.00	-10.0	0.0	0.0	0.	0.1235	0.00	0.0001	3.883
			(*)	(*)	(*)	(18.1%)	(*)	(*)	(*)	(0.0%)	(*)		
26591	2.612	1.2	0.298	2.627	-1.00	2.413	-13.1	0.17		-0.0297	-0.06	0.0002	0.203
			(0.0%)	(3.9%)	(*)	(0.3%)	(16.5%)	(-)		(0.2%)	(2.3%)		
		2.5	3.000	0.000	0.00	-4.0	0.0	0.0	0.	0.1233	0.00	0.0001	5.261
			(*)	(*)	(*)	(*)	(*)	(*)	(*)	(0.1%)	(*)		
26598	2.613	6.7	0.294	3.006	-1.00	2.507	-22.8	0.47		-0.0205	-0.06	0.0003	0.306
			(0.1%)	(2.7%)	(*)	(0.5%)	(9.6%)	(26.6%)		(0.3%)	(5.7%)		
		6.2	3.000	0.000	0.00	-7.2	0.0	0.0	0.	0.1261	0.00	0.0006	4.319
			(*)	(*)	(*)	(54.3%)	(*)	(*)	(*)	(0.1%)	(*)		
26590	2.617	2.0	0.304	2.801	-1.00	2.404	-12.6	0.15		-0.0295	-0.06	0.0003	0.275
			(0.0%)	(3.5%)	(*)	(0.3%)	(18.3%)	(-)		(0.2%)	(2.9%)		
		3.3	3.000	0.000	0.00	-4.0	0.0	0.0	0.	0.1227	0.00	0.0002	4.474
			(*)	(*)	(*)	(*)	(*)	(*)	(*)	(0.1%)	(*)		
26597	2.631	4.5	0.293	2.886	-1.00	2.429	-11.4	0.26		-0.0246	-0.03	0.0002	0.248
			(0.0%)	(2.1%)	(*)	(0.3%)	(13.5%)	(51.4%)		(0.3%)	(6.0%)		
		4.9	1.000	0.000	0.00	-4.0	0.0	0.0	0.	0.1236	0.00	0.0003	5.161
			(*)	(*)	(*)	(*)	(*)	(*)	(*)	(0.1%)	(*)		
26592	2.632	0.6	0.292	3.000	-1.00	2.457	-11.0	0.20		-0.0258	-0.06	0.0002	0.252
			(0.0%)	(*)	(*)	(0.6%)	(*)	(*)		(0.3%)	(2.5%)		
		1.7	3.000	0.000	0.00	-4.0	0.0	0.0	0.	0.1227	0.00	0.0002	6.565
			(*)	(*)	(*)	(*)	(*)	(*)	(*)	(0.1%)	(*)		

6 DOF Summary Output

Shot Numbers		Mach Number	DBSQ ABARM	CX CX2 CX4	CNa CNa3 CNa5	CYpa CYpa3	Cma Cma3 Cma5	Cmq Cmq2 Cmq4	Cnpa Cnpa3 Cnpa5	Clp CXm CmaM	Standard Error X(m) Y-Z(m)	Standard Error Angle(deg) Roll(deg)
27350	27351	1.683	28.1	0.383	2.970	-1.00	2.720	-12.0	0.07	-0.0303	0.0005	0.2496
				(*) (0.8%)	(*) (0.1%)		(2.4%)	(42.0%)	(*)			
27353	27352		14.9	2.297	0.000	0.00	-1.978	0.0	8.10	-0.0766	0.0003	11.2800
				(*)	(*)	(*) (9.8%)		(*) (12.3%)	(3.6%)			
				0.00	0.00		0.0	0.	0.	-0.294		
				(*)	(*)		(*)	(*)	(*)	(12.8%)		
27350	27351	1.683	28.4	0.384	3.198	-1.00	2.684	-11.4	0.15	-0.0286	0.0009	0.4548
				(0.1%)	(1.3%)	(*) (0.1%)		(4.8%)	(37.2%)	(0.4%)		
27352	27353		15.0	2.208	0.000	0.00	0.000	0.0	0.00	-0.1040	0.0004	16.5300
				(2.3%)	(*)	(*)	(*)	(*)	(*)	(3.0%)		
				0.00	0.00		0.0	0.	0.	0.000		
				(*)	(*)		(*)	(*)	(*)	(*)		
27346	27344	1.697	6.0	0.372	3.136	-1.00	2.658	-9.9	-0.62	-0.0317	0.0005	0.2304
				(*) (1.4%)		(*) (0.1%)		(7.6%)	(9.7%)	(*)		
27353	27345		7.6	3.788	0.000	0.00	9.861	0.0	95.00	-0.0861	0.0002	6.2650
				(*)	(*)	(*) (9.4%)		(*)	(6.6%)	(*)		
				0.00	0.00		0.0	0.	0.	-0.642		
				(*)	(*)		(*)	(*)	(*)	(8.1%)		
27345	27347	1.705	3.2	0.375	3.000	-1.00	2.665	-6.1	-0.59	-0.0367	0.0003	0.2193
				(*)	(*)	(*) (0.1%)		(17.9%)	(4.2%)	(*)		
27346	27344		3.0	2.300	0.000	0.00	-2.500	0.0	0.00	-0.1023	0.0001	6.3110
				(*)	(*)	(*)	(*)	(*)	(*)	(1.0%)		
				0.00	0.00		0.0	0.	0.	-0.371		
				(*)	(*)		(*)	(*)	(*)	(16.5%)		
26827	26833	2.211	6.7	0.320	2.886	-1.00	2.530	-11.5	0.15	-0.0249	0.0004	0.2752
				(*) (1.0%)		(*) (0.2%)		(4.9%)	(33.2%)	(*)		
26826	26834		8.5	4.270	0.000	0.00	-5.263	0.0	0.00	-0.0768	0.0002	6.3330
				(*)	(*)	(*) (14.5%)		(*)	(*)	(1.6%)		
26831				0.00	0.00		0.0	0.	0.	0.000		
				(*)	(*)		(*)	(*)	(*)	(*)		
26827	26829	2.223	5.4	0.325	0.335	-1.00	0.000	-14.6	0.48	-0.0274	0.0009	0.2134
				(*) (26.3%)		(*)	(*) (2.7%)		(7.1%)	(*)		

26831	26832		6.9	3.414	303.928	0.00	-4.000	0.0	0.00	-0.0603		0.0007	5.3440
				(*)	(5.0%)	(*)	(*)	(*)	(*)	(*)			
26833				0.00	0.00		0.0	0.	0.	0.000			
				(*)	(*)		(*)	(*)	(*)	(*)			
26826	26828	2.234	6.1	0.322	2.918	-1.00	0.000	-11.4	0.02	-0.0249		0.0006	0.2274
				(*)	(1.1%)	(*)	(*)	(4.2%)	(-)	(*)			
26831	26832		8.5	2.310	0.000	0.00	-4.979	0.0	25.52	-0.0221		0.0002	5.5730
				(*)	(*)	(*)	(*)	(*)	(17.6%)	(*)			
26834				0.00	0.00		0.0	0.	0.	0.000			
				(*)	(*)		(*)	(*)	(*)	(*)			
26831	26829	2.239	6.2	0.323	3.079	-1.00	2.545	-11.2	0.02	-0.0272		0.0004	0.2441
				(*)	(1.0%)	(*)	(0.1%)	(4.6%)	(-)	(*)			
26828	26832		8.5	3.000	0.000	0.00	-6.835	0.0	21.64	-0.0572		0.0002	5.0640
				(*)	(*)	(*)	(10.0%)	(*)	(21.6%)	(2.1%)			
26834				0.00	0.00		0.0	0.	0.	0.000			
				(*)	(*)		(*)	(*)	(*)	(*)			
26597	26592	2.461	6.1	0.307	2.891	-1.00	2.469	-11.8	0.19	-0.0268		0.0003	0.2661
				(*)	(0.8%)	(*)	(0.1%)	(4.7%)	(26.2%)	(*)			
26590	26834		8.5	3.824	0.000	0.00	-4.000	0.0	0.00	-0.0687		0.0002	7.1820
				(*)	(*)	(*)	(*)	(*)	(*)	(1.3%)			
26833				0.00	0.00		0.0	0.	0.	-0.224			
				(*)	(*)		(*)	(*)	(*)	(5.6%)			
26590	26591	2.621	3.0	0.299	3.010	-1.00	0.000	-15.4	0.29	-0.0260		0.0003	0.2762
				(*)	(1.2%)	(*)	(*)	(6.4%)	(28.1%)	(*)			
26592	26598		6.0	3.000	0.000	0.00	-4.000	0.0	1.10	-0.0632		0.0003	5.1590
				(*)	(*)	(*)	(*)	(*)	(-)	(*)			
26597				0.00	0.00		0.0	0.	0.	0.000			
				(*)	(*)		(*)	(*)	(*)	(*)			
26591	26598	2.621	3.0	0.296	2.928	-1.00	2.449	-15.7	0.32	-0.0260		0.0003	0.3166
				(*)	(1.4%)	(*)	(0.2%)	(7.1%)	(27.1%)	(*)			
26590	26592		6.0	3.000	0.000	0.00	-3.000	0.0	0.00	-0.0617		0.0004	5.1640
				(*)	(*)	(*)	(*)	(*)	(*)	(1.7%)			
26597				0.00	0.00		0.0	0.	0.	0.000			
				(*)	(*)		(*)	(*)	(*)	(*)			

M16A2 M855 LR M1.7++ roll pins
6 DOF Summary (ARL Format) (08-AUG-08 09:42:10)

Shot Number	Mach Number	DBSQ / YAW	CD0 / CD2	CLA0 / CLA3	CYPA / CYPA3	CMA / CMA3	CMQ / CMQ2	CMPA / CMPA3	CMPA5	CLP / IX/IY	CXM / CMAM	Standard Error X(m) / Y-Z(m)	Standard Error Angle(deg) / Roll(deg)
27350	1.664	32.0	0.387	2.72	-0.50	2.74	-6.3	0.07		-0.0137	-0.12	0.0005	0.188
		5.7	5.4	-2.3	0.0	-2.4	0.0	2.6	0.	0.1201	0.00	0.0002	6.210
27351	1.678	29.5	0.384	2.71	-0.50	2.74	-4.9	0.07		-0.0143	-0.07	0.0002	0.203
		5.4	5.4	-2.3	0.0	-3.6	0.0	0.0	0.	0.1218	0.00	0.0002	11.650
27344	1.686	3.2	0.374	2.57	-0.50	2.68	-3.2	-0.41		-0.0160	-0.10	0.0001	0.157
		1.8	7.9	-4.9	0.0	-2.5	0.0	54.5	0.	0.1204	-0.43	0.0001	5.846
27346	1.687	3.1	0.372	2.51	-0.50	2.66	-2.3	-0.25		-0.0163	-0.10	0.0001	0.197
		1.8	5.2	-2.3	0.0	-2.5	0.0	0.0	0.	0.1200	-0.33	0.0001	5.982
27353	1.689	13.2	0.371	2.60	-0.50	2.71	-4.7	0.00		-0.0151	-0.13	0.0003	0.271
		3.6	7.9	-4.9	0.0	0.0	0.0	0.0	0.	0.1220	0.00	0.0002	6.836
27352	1.702	37.1	0.385	2.80	-0.50	2.71	-6.0	0.12		-0.0139	-0.15	0.0005	0.159
		6.1	5.5	-2.3	0.0	-2.9	0.0	0.0	0.	0.1216	0.00	0.0003	8.702
27347	1.723	2.1	0.379	2.33	-0.50	2.74	-1.0	-0.31		-0.0235	-0.13	0.0006	0.185
		1.5	6.5	-3.8	0.0	0.0	0.0	0.0	0.	0.1235	-0.46	0.0001	6.932
27345	1.725	4.5	0.368	2.35	-0.50	2.66	-3.8	-0.32		-0.0161	-0.10	0.0002	0.201
		2.1	7.6	-4.9	0.0	-2.5	0.0	54.5	0.	0.1200	-0.48	0.0001	6.571
26827	2.172	3.2	0.328	2.56	-0.50	2.49	-4.0	-0.11		-0.0124	-0.07	0.0002	0.200
		1.8	6.3	-3.4	0.0	-4.0	0.0	0.0	0.	0.1191	0.00	0.0002	7.637
26833	2.212	9.4	0.332	2.63	-0.50	2.52	-6.1	0.09		-0.0127	-0.05	0.0002	0.231
		3.1	6.0	-3.0	0.0	-4.0	0.0	0.0	0.	0.1237	0.00	0.0002	4.982
26834	2.215	14.4	0.325	2.64	-0.50	2.51	-6.9	-0.07		-0.0121	-0.01	0.0003	0.254
		3.8	5.3	-2.3	0.0	-2.8	0.0	23.5	0.	0.1241	0.00	0.0002	6.704

M16A2 M855 LR M1.7++ roll pins
6 DOF Summary (ARL Format) (08-AUG-08 09:42:10)

Shot Number	Mach Number	DBSQ / YAW	CD0 / CD2	CLA0 / CLA3	CYPA / CYPA3	CMA / CMA3	CMQ / CMQ2	CMPA / CMPA3	CMPA5	CLP / IX/IY	CXM / CMAM	Standard Error X(m) / Y-Z(m)	Standard Error Angle(deg) / Roll(deg)
26826	2.224	0.7	0.321	2.68	-0.50	2.55	-5.5	0.10		-0.0119	-0.04	0.0001	0.236
		0.9	6.0	-3.0	0.0	-4.0	0.0	0.0	0.	0.1214	0.00	0.0002	7.028
26831	2.230	6.4	0.318	2.64	-0.50	2.55	-4.4	0.03		-0.0134	-0.05	0.0002	0.179
		2.5	5.8	-2.9	0.0	-4.0	0.0	0.0	0.	0.1238	0.00	0.0002	5.196
26828	2.248	2.2	0.325	2.67	-0.50	2.51	-4.1	-0.15		-0.0125	-0.07	0.0002	0.155
		1.5	6.0	-3.0	0.0	-4.0	0.0	0.0	0.	0.1225	0.00	0.0001	4.550
26829	2.250	1.7	0.328	2.83	-0.50	2.53	-5.9	-0.02		-0.0176	-0.06	0.0002	0.150
		1.3	6.2	-3.0	0.0	-4.0	0.0	0.0	0.	0.1230	0.00	0.0001	4.673
26832	2.252	7.4	0.317	2.63	-0.50	2.58	-5.1	0.06		-0.0123	-0.05	0.0002	0.208
		2.7	6.4	-3.4	0.0	-10.0	0.0	0.0	0.	0.1235	0.00	0.0001	3.883
26591	2.612	1.2	0.298	2.33	-0.50	2.41	-6.6	0.09		-0.0148	-0.06	0.0002	0.203
		1.1	5.6	-3.0	0.0	-4.0	0.0	0.0	0.	0.1233	0.00	0.0001	5.261
26598	2.613	6.7	0.294	2.71	-0.50	2.51	-11.4	0.23		-0.0102	-0.06	0.0003	0.306
		2.6	6.0	-3.0	0.0	-7.2	0.0	0.0	0.	0.1261	0.00	0.0006	4.319
26590	2.617	2.0	0.304	2.50	-0.50	2.40	-6.3	0.08		-0.0148	-0.06	0.0003	0.275
		1.4	5.8	-3.0	0.0	-4.0	0.0	0.0	0.	0.1227	0.00	0.0002	4.474
26597	2.631	4.5	0.293	2.59	-0.50	2.43	-5.7	0.13		-0.0123	-0.03	0.0002	0.248
		2.1	3.9	-1.0	0.0	-4.0	0.0	0.0	0.	0.1236	0.00	0.0003	5.161
26592	2.632	0.6	0.292	2.71	-0.50	2.46	-5.5	0.10		-0.0129	-0.06	0.0002	0.252
		0.8	6.0	-3.0	0.0	-4.0	0.0	0.0	0.	0.1227	0.00	0.0002	6.565

M16A2 M855 LR M1.7++ roll pins
6 DOF Summary (ARL Format) (08-AUG-08 09:42:10)

Shot Numbers		Mach Number	DBSQ Yaw	CD0 CD2 CDR	CLA0 CLA3 CLR	CYPA CYPA3	CMA CMA3 CMA5	CMQ CMQ2 CMQ4	CMPA CMPA3 CMPA5	CLP CXm CmaM	Standard Error X(m) Y-Z(m)	Standard Error Angle(deg) Roll(deg)
27350	27351	1.683	28.1	0.383	2.59	-0.50	2.72	-6.0	0.04	-0.0151	0.0005	0.2496
27353	27352		5.3	5.3	-2.3	0.0	-2.0	0.0	4.05	-0.0766	0.0003	11.2800
				0.426	2.554		0.0	0.	0.	-0.294		
27350	27351	1.683	28.4	0.384	2.81	-0.50	2.68	-5.7	0.08	-0.0143	0.0009	0.4548
27352	27353		5.3	5.4	-2.2	0.0	0.0	0.0	0.00	-0.1040	0.0004	16.5300
				0.429	2.781		0.0	0.	0.	0.000		
27346	27344	1.697	6.0	0.372	2.76	-0.50	2.66	-5.0	-0.31	-0.0159	0.0005	0.2304
27353	27345		2.4	6.9	-3.8	0.0	9.9	0.0	47.50	-0.0861	0.0002	6.2650
				0.385	2.754		0.0	0.	0.	-0.642		
27345	27347	1.705	3.2	0.375	2.63	-0.50	2.67	-3.0	-0.29	-0.0183	0.0003	0.2193
27346	27344		1.8	5.3	-2.3	0.0	-2.5	0.0	0.00	-0.1023	0.0001	6.3110
				0.380	2.622		0.0	0.	0.	-0.371		
26827	26833	2.211	6.7	0.320	2.57	-0.50	2.53	-5.7	0.08	-0.0125	0.0004	0.2752
26826	26834		2.6	7.2	-4.3	0.0	-5.3	0.0	0.00	-0.0768	0.0002	6.3330
26831				0.334	2.554		0.0	0.	0.	0.000		
26827	26829	2.223	5.4	0.325	0.01	-0.50	0.00	-7.3	0.24	-0.0137	0.0009	0.2134
26831	26832		2.3	3.7	300.3	0.0	-4.0	0.0	0.00	-0.0603	0.0007	5.3440
26833				0.332	0.501		0.0	0.	0.	0.000		
26826	26828	2.234	6.1	0.322	2.60	-0.50	0.00	-5.7	0.01	-0.0124	0.0006	0.2274
26831	26832		2.5	5.2	-2.3	0.0	-5.0	0.0	12.76	-0.0221	0.0002	5.5730
26834				0.332	2.588		0.0	0.	0.	0.000		
26831	26829	2.239	6.2	0.323	2.76	-0.50	2.54	-5.6	0.01	-0.0136	0.0004	0.2441
26828	26832		2.5	6.1	-3.0	0.0	-6.8	0.0	10.82	-0.0572	0.0002	5.0640
26834				0.334	2.748		0.0	0.	0.	0.000		
26597	26592	2.461	6.1	0.307	2.58	-0.50	2.47	-5.9	0.10	-0.0134	0.0003	0.2661
26590	26834		2.5	6.7	-3.8	0.0	-4.0	0.0	0.00	-0.0687	0.0002	7.1820
26833				0.320	2.574		0.0	0.	0.	-0.224		
26590	26591	2.621	3.0	0.299	2.71	-0.50	0.00	-7.7	0.14	-0.0130	0.0003	0.2762
26592	26598		1.7	6.0	-3.0	0.0	-4.0	0.0	0.55	-0.0632	0.0003	5.1590
26597				0.304	2.707		0.0	0.	0.	0.000		
26591	26598	2.621	3.0	0.296	2.63	-0.50	2.45	-7.9	0.16	-0.0130	0.0003	0.3166
26590	26592		1.7	5.9	-3.0	0.0	-3.0	0.0	0.00	-0.0617	0.0004	5.1640
26597				0.301	2.628		0.0	0.	0.	0.000		

M16A2 M855 LR M1.7++ roll pins
6 DOF Summary (ARL Format) (08-AUG-08 09:42:10)

Shot Numbers	Mach Number	DBSQ Yaw	CD0 CD2 CDR	CLA0 CLA3 CLR	CYPA CYPA3	CMA CMA3 CMA5	CMQ CMQ2 CMQ4	CMPA CMPA3 CMPA5	CLP CXm CmaM	Standard Error X(m) Y-Z(m)	Angle(deg) Roll(deg)

M16A2 M855 LR M1.5 roll pins
6 DOF Summary Output (11-JUL-08 10:23:41)

Shot	Number	Date	Time	Ref. CG (mm)	Ref. Length (mm)	Ref.Mach Number	Mach Number	DBSQ (deg2)	Max Angle of Attack (deg)	Standard Error X (m)	Y-Z (m)	Angle (deg)	Roll (deg)
	29270	08-JUL-08	16:03:04	14.30	23.06	1.15	1.151	13.090	4.2	0.0004	0.0002	0.173	8.18
	29266	09-JUL-08	08:31:25	14.30	23.06	1.15	1.157	6.372	3.7	0.0012	0.0003	0.194	0.00
	29271	08-JUL-08	10:28:05	14.30	23.06	1.20	1.180	13.900	5.8	0.0005	0.0002	0.172	8.54
	29268	08-JUL-08	11:25:56	14.30	23.06	1.20	1.186	10.110	4.1	0.0007	0.0002	0.195	0.00
	29267	08-JUL-08	11:24:32	14.30	23.06	1.20	1.188	16.020	7.3	0.0005	0.0002	0.194	0.00
	29269	08-JUL-08	11:35:00	14.30	23.06	1.20	1.201	12.390	5.8	0.0004	0.0002	0.204	0.00
	28106	14-FEB-08	14:14:37	14.27	23.06	1.45	1.457	8.963	5.1	0.0001	0.0001	0.162	8.39
	28099	14-FEB-08	14:14:38	14.27	23.06	1.45	1.458	8.675	5.4	0.0001	0.0001	0.138	3.97
	28092	11-MAR-08	10:36:32	14.27	23.06	1.45	1.459	6.820	3.5	0.0001	0.0001	0.196	0.00
	28096	25-FEB-08	14:12:16	14.27	23.06	1.45	1.467	9.598	6.3	0.0001	0.0001	0.144	10.13
	28097	14-FEB-08	14:14:41	14.27	23.06	1.45	1.473	5.459	4.1	0.0001	0.0001	0.162	4.43
	28104	25-FEB-08	14:17:16	14.27	23.06	1.45	1.473	23.300	10.6	0.0003	0.0001	0.224	6.75
	28098	14-FEB-08	14:14:43	14.27	23.06	1.50	1.485	2.705	2.1	0.0001	0.0001	0.166	4.86
	28105	14-FEB-08	14:14:44	14.27	23.06	1.50	1.485	16.330	8.2	0.0001	0.0001	0.178	6.70
	28107	25-FEB-08	13:45:23	14.27	23.06	1.50	1.488	8.774	6.0	0.0002	0.0001	0.148	5.55
	28093	11-MAR-08	10:34:23	14.27	23.06	1.50	1.490	2.801	2.7	0.0001	0.0002	0.157	0.00
	28094	11-MAR-08	10:41:41	14.27	23.06	1.50	1.490	3.546	3.0	0.0001	0.0001	0.158	0.00

M16A2 M855 LR M1.5 roll pins
6 DOF Summary Output (11-JUL-08 10:23:41)

Shot Number	Mach Number	DBSQ ABARM	CX CX2	CNa CNa3	CYpa CYpa3	Cma Cma3	Cmq Cmq2	Cnpa Cnpa3	Cnpa5	Clp IX/IY	CXM CmaM	Standard Error X(m) Y-Z(m)	 Angle(deg) Roll(deg)
29270	1.151	13.1	0.446	2.791	-1.00	2.847	-11.0	-1.21		-0.0231	-0.06	0.0004	0.173
		4.2	5.198	0.000	0.00	0.0	0.0	159.4	0.	0.1224	0.00	0.0002	8.184
29266	1.157	6.4	0.450	2.309	-1.00	2.823	-1.8	-1.31		-0.0270	-0.14	0.0012	0.194
		3.7	5.226	0.000	0.00	0.0	0.0	179.4	0.	0.1199	0.00	0.0003	0.000
29271	1.180	13.9	0.438	2.721	-1.00	2.811	-9.1	-0.90		-0.0286	-0.14	0.0005	0.172
		5.8	5.326	0.000	0.00	9.7	0.0	97.4	0.	0.1217	0.00	0.0002	8.536
29268	1.186	10.1	0.444	2.731	-1.00	2.861	-6.5	-0.62		-0.0270	-0.11	0.0007	0.195
		4.1	5.356	0.000	0.00	0.0	0.0	0.0	0.	0.1212	0.00	0.0002	0.000
29267	1.188	16.0	0.440	2.739	-1.00	2.878	-8.8	-0.67		-0.0270	-0.17	0.0005	0.194
		7.3	5.361	0.000	0.00	2.8	0.0	56.7	0.	0.1219	0.00	0.0002	0.000
29269	1.201	12.4	0.441	2.642	-1.00	2.784	-8.8	-0.97		-0.0270	-0.13	0.0004	0.204
		5.8	5.422	0.000	0.00	17.7	0.0	119.4	0.	0.1223	0.00	0.0002	0.000
28106	1.457	9.0	0.399	2.868	-1.00	2.734	-7.4	-0.24		-0.0283	-0.16	0.0001	0.162
		5.1	4.467	0.000	0.00	0.0	0.0	0.0	0.	0.1192	0.00	0.0001	8.390
28099	1.458	8.7	0.413	2.911	-1.00	2.734	-8.3	-0.24		-0.0258	-0.17	0.0001	0.138
		5.4	4.482	0.000	0.00	0.0	0.0	0.0	0.	0.1202	0.00	0.0001	3.966
28092	1.459	6.8	0.420	2.858	-1.00	2.810	-9.2	-0.51		-0.0300	-0.13	0.0001	0.196
		3.5	4.477	0.000	0.00	0.0	0.0	0.0	0.	0.1205	0.00	0.0001	0.000
28096	1.467	9.6	0.407	2.850	-1.00	2.699	-9.9	-0.20		-0.0324	-0.16	0.0001	0.144
		6.3	4.430	0.000	0.00	0.0	0.0	21.0	0.	0.1188	0.00	0.0001	10.130
28097	1.473	5.5	0.396	2.906	-1.00	2.824	-10.9	-0.20		-0.0276	-0.16	0.0001	0.162
		4.1	4.402	0.000	0.00	0.0	0.0	0.0	0.	0.1228	0.00	0.0001	4.426

M16A2 M855 LR M1.5 roll pins
6 DOF Summary Output (11-JUL-08 10:23:41)

Shot Number	Mach Number	DBSQ / ABARM	CX / CX2	CNa / CNa3	CYpa / CYpa3	Cma / Cma3	Cmq / Cmq2	Cnpa / Cnpa3	Cnpa5	Clp / IX/IY	CXM / CmaM	Standard Error X(m) / Y-Z(m)	Standard Error Angle(deg) / Roll(deg)
28104	1.473	23.3	0.394	2.945	-1.00	2.792	-9.8	0.03		-0.0307	-0.22	0.0003	0.224
		10.6	4.422	0.000	0.00	0.0	0.0	0.0	0.	0.1218	0.00	0.0001	6.753
28098	1.485	2.7	0.403	3.021	-1.00	2.824	-19.1	-0.40		-0.0339	-0.15	0.0001	0.166
		2.1	4.352	0.000	0.00	0.0	0.0	0.0	0.	0.1230	0.00	0.0001	4.864
28105	1.485	16.3	0.392	2.923	-1.00	2.763	-9.0	-0.05		-0.0301	-0.16	0.0001	0.178
		8.2	4.366	0.000	0.00	0.0	0.0	0.0	0.	0.1212	0.00	0.0001	6.699
28107	1.488	8.8	0.398	3.049	-1.00	2.799	-8.8	-0.24		-0.0295	-0.14	0.0002	0.148
		6.0	4.400	0.000	0.00	0.0	0.0	21.0	0.	0.1216	0.00	0.0001	5.547
28093	1.490	2.8	0.396	3.002	-1.00	2.798	-10.1	-0.36		-0.0300	-0.15	0.0001	0.157
		2.7	4.355	0.000	0.00	0.0	0.0	0.0	0.	0.1198	0.00	0.0002	0.000
28094	1.490	3.5	0.406	3.002	-1.00	2.793	-15.7	-0.26		-0.0270	-0.13	0.0001	0.158
		3.0	4.335	0.000	0.00	0.0	0.0	0.0	0.	0.1204	0.00	0.0001	0.000

M16A2 M855 LR M1.5 roll pins
6 DOF Summary Output (11-JUL-08 10:23:41)

Shot Numbers		Date	Time	Ref. Mach Number	Mach Number	DBSQ (deg2)	Max Angle of Attack (deg)	Standard Error X (m)	Y-Z (m)	Angle (deg)	Roll (deg)
29270	29271	08-JUL-08	11:38:22	1.200	1.181	13.04	7.27	0.0005	0.0002	0.215	5.199
29267	29269										
29268											
28099	28092	12-JUL-07	12:20:44	1.450	1.466	10.61	10.61	0.0004	0.0001	0.212	6.062
28096	28097										
28104											
28106	28107	09-JUL-08	13:31:41	1.500	1.474	13.29	10.54	0.0004	0.0001	0.172	7.587
28096	28104										
28105											
28096	28106	20-FEB-08	09:39:57	1.500	1.476	6.03	6.29	0.0007	0.0002	0.166	6.193
28097	28094										
28093											
28098	28093	09-JUL-08	13:44:14	1.450	1.477	6.45	6.29	0.0006	0.0001	0.164	5.899
28107	28096										
28099											
28098	28105	12-JUL-07	12:46:30	1.500	1.488	6.73	8.24	0.0004	0.0002	0.241	4.438
28107	28093										
28094											

M16A2 M855 LR M1.5 roll pins
6 DOF Summary Output (11-JUL-08 10:23:41)

Shot Numbers		Mach Number	DBSQ ABARM	CX CX2 CX4	CNa CNa3 CNa5	CYpa CYpa3	Cma Cma3 Cma5	Cmq Cmq2 Cmq4	Cnpa Cnpa3 Cnpa5	Clp CXm CmaM	Standard Error X(m) Y-Z(m)	Standard Error Angle(deg) Roll(deg)
29270	29271	1.181	13.0	0.449	2.718	-1.00	2.812	-8.6	-0.82	-0.0260	0.0005	0.2146
29267	29269		7.3	3.360	0.000	0.00	11.816	0.0	75.87	-0.1371	0.0002	5.1990
29268				0.00	0.00		0.0	0.	0.	0.000		
28099	28092	1.466	10.6	0.404	2.852	-1.00	0.000	-10.9	-0.29	-0.0295	0.0004	0.2116
28096	28097		10.6	4.422	0.000	0.00	0.000	0.0	31.07	-0.1608	0.0001	6.0620
28104				0.00	0.00		0.0	0.	0.	0.000		
28106	28107	1.474	13.3	0.402	2.869	-1.00	0.000	-10.2	-0.20	-0.0302	0.0004	0.1719
28096	28104		10.5	4.366	0.000	0.00	-1.632	0.0	22.13	-0.1523	0.0001	7.5870
28105				0.00	0.00		0.0	0.	0.	0.000		
28096	28106	1.476	6.0	0.399	2.606	-1.00	0.000	-11.6	-0.32	-0.0373	0.0007	0.1658
28097	28094		6.3	4.355	0.000	0.00	0.000	0.0	66.16	-0.1055	0.0002	6.1930
28093				0.00	0.00		0.0	0.	0.	0.000		
28098	28093	1.477	6.5	0.400	3.133	-1.00	0.000	-10.4	-0.49	-0.0308	0.0006	0.1642
28107	28096		6.3	6.809	0.000	0.00	0.000	0.0	86.59	-0.2014	0.0001	5.8990
28099				0.00	0.00		0.0	0.	0.	0.000		
28098	28105	1.488	6.7	0.404	3.105	-1.00	2.780	-10.2	-0.39	-0.0373	0.0004	0.2405
28107	28093		8.2	4.335	0.000	0.00	0.000	0.0	48.17	-0.1426	0.0002	4.4380
28094				0.00	0.00		0.0	0.	0.	0.000		

6 DOF Summary Output

Shot Number	Mach Number	DBSQ / ABARM	CX / CX2	CNa / CNa3	CYpa / CYpa3	Cma / Cma3	Cmq / Cmq2	Cnpa / Cnpa3	Cnpa5	Clp / IX/IY	CXM / CmaM	Standard Error X(m) / Y-Z(m)	Standard Error Angle(deg) / Roll(deg)
29270	1.151	13.1	0.446	2.791	-1.00	2.847	-11.0	-1.21		-0.0231	-0.06	0.0004	0.173
			(0.1%)	(2.1%)	(*)	(0.1%)	(15.4%)	(11.1%)		(0.5%)	(*)		
		4.2	5.198	0.000	0.00	0.0	0.0	159.4	0.	0.1224	0.00	0.0002	8.184
			(*)	(*)	(*)	(*)	(*)	(18.9%)	(*)	(0.1%)	(*)		
29266	1.157	6.4	0.450	2.309	-1.00	2.823	-1.8	-1.31		-0.0270	-0.14	0.0012	0.194
			(0.1%)	(9.9%)	(*)	(0.2%)	(*)	(9.6%)		(*)	(7.6%)		
		3.7	5.226	0.000	0.00	0.0	0.0	179.4	0.	0.1199	0.00	0.0003	0.000
			(*)	(*)	(*)	(*)	(*)	(22.3%)	(*)	(0.1%)	(*)		
29271	1.180	13.9	0.438	2.721	-1.00	2.811	-9.1	-0.90		-0.0286	-0.14	0.0005	0.172
			(0.1%)	(3.1%)	(*)	(0.5%)	(12.6%)	(16.0%)		(0.4%)	(*)		
		5.8	5.326	0.000	0.00	9.7	0.0	97.4	0.	0.1217	0.00	0.0002	8.536
			(*)	(*)	(*)	(32.7%)	(*)	(29.6%)	(*)	(0.1%)	(*)		
29268	1.186	10.1	0.444	2.731	-1.00	2.861	-6.5	-0.62		-0.0270	-0.11	0.0007	0.195
			(0.1%)	(3.9%)	(*)	(0.1%)	(19.1%)	(15.0%)		(*)	(*)		
		4.1	5.356	0.000	0.00	0.0	0.0	0.0	0.	0.1212	0.00	0.0002	0.000
			(*)	(*)	(*)	(*)	(*)	(*)	(*)	(0.0%)	(*)		
29267	1.188	16.0	0.440	2.739	-1.00	2.878	-8.8	-0.67		-0.0270	-0.17	0.0005	0.194
			(0.1%)	(2.7%)	(*)	(0.2%)	(10.1%)	(15.7%)		(*)	(2.6%)		
		7.3	5.361	0.000	0.00	2.8	0.0	56.7	0.	0.1219	0.00	0.0002	0.000
			(*)	(*)	(*)	(45.4%)	(*)	(21.8%)	(*)	(0.0%)	(*)		
29269	1.201	12.4	0.441	2.642	-1.00	2.784	-8.8	-0.97		-0.0270	-0.13	0.0004	0.204
			(0.1%)	(2.9%)	(*)	(0.6%)	(14.4%)	(18.9%)		(*)	(3.1%)		
		5.8	5.422	0.000	0.00	17.7	0.0	119.4	0.	0.1223	0.00	0.0002	0.000
			(*)	(*)	(*)	(23.5%)	(*)	(33.0%)	(*)	(0.1%)	(*)		
28106	1.457	9.0	0.399	2.868	-1.00	2.734	-7.4	-0.24		-0.0283	-0.16	0.0001	0.162
			(0.0%)	(1.2%)	(*)	(0.1%)	(12.1%)	(33.1%)		(0.4%)	(0.8%)		
		5.1	4.467	0.000	0.00	0.0	0.0	0.0	0.	0.1192	0.00	0.0001	8.390
			(*)	(*)	(*)	(*)	(*)	(*)	(*)	(0.0%)	(*)		

28099	1.458	8.7	0.413	2.911	-1.00	2.734	-8.3	-0.24		-0.0258	-0.17	0.0001	0.138
			(0.0%)	(1.0%)	(*)	(0.1%)	(9.6%)	(30.7%)			(0.3%)	(0.7%)	
		5.4	4.482	0.000	0.00	0.0	0.0	0.0	0.	0.1202	0.00	0.0001	3.966
			(*)	(*)	(*)	(*)	(*)	(*)	(*)	(0.0%)	(*)		
28092	1.459	6.8	0.420	2.858	-1.00	2.810	-9.2	-0.51		-0.0300	-0.13	0.0001	0.196
			(0.0%)	(1.5%)	(*)	(0.2%)	(19.2%)	(24.5%)			(*)	(1.1%)	
		3.5	4.477	0.000	0.00	0.0	0.0	0.0	0.	0.1205	0.00	0.0001	0.000
			(*)	(*)	(*)	(*)	(*)	(*)	(*)	(0.1%)	(*)		
28096	1.467	9.6	0.407	2.850	-1.00	2.699	-9.9	-0.20		-0.0324	-0.16	0.0001	0.144
			(0.0%)	(1.1%)	(*)	(0.1%)	(7.4%)	(35.5%)			(0.4%)	(0.8%)	
		6.3	4.430	0.000	0.00	0.0	0.0	21.0	0.	0.1188	0.00	0.0001	10.130
			(*)	(*)	(*)	(*)	(*)	(*)	(*)	(0.0%)	(*)		
28097	1.473	5.5	0.396	2.906	-1.00	2.824	-10.9	-0.20		-0.0276	-0.16	0.0001	0.162
			(0.0%)	(1.3%)	(*)	(0.1%)	(11.1%)	(54.0%)			(0.2%)	(0.7%)	
		4.1	4.402	0.000	0.00	0.0	0.0	0.0	0.	0.1228	0.00	0.0001	4.426
			(*)	(*)	(*)	(*)	(*)	(*)	(*)	(0.0%)	(*)		
28104	1.473	23.3	0.394	2.945	-1.00	2.792	-9.8	0.03		-0.0307	-0.22	0.0003	0.224
			(0.1%)	(1.3%)	(*)	(0.1%)	(7.1%)	(-)			(0.3%)	(1.4%)	
		10.6	4.422	0.000	0.00	0.0	0.0	0.0	0.	0.1218	0.00	0.0001	6.753
			(*)	(*)	(*)	(*)	(*)	(*)	(*)	(0.0%)	(*)		
28098	1.485	2.7	0.403	3.021	-1.00	2.824	-19.1	-0.40		-0.0339	-0.15	0.0001	0.166
			(0.0%)	(1.9%)	(*)	(0.3%)	(21.4%)	(41.2%)			(0.2%)	(0.8%)	
		2.1	4.352	0.000	0.00	0.0	0.0	0.0	0.	0.1230	0.00	0.0001	4.864
			(*)	(*)	(*)	(*)	(*)	(*)	(*)	(0.2%)	(*)		
28105	1.485	16.3	0.392	2.923	-1.00	2.763	-9.0	-0.05		-0.0301	-0.16	0.0001	0.178
			(0.0%)	(0.6%)	(*)	(0.1%)	(7.5%)	(-)			(0.3%)	(0.7%)	
		8.2	4.366	0.000	0.00	0.0	0.0	0.0	0.	0.1212	0.00	0.0001	6.699
			(*)	(*)	(*)	(*)	(*)	(*)	(*)	(0.0%)	(*)		
28107	1.488	8.8	0.398	3.049	-1.00	2.799	-8.8	-0.24		-0.0295	-0.14	0.0002	0.148
			(0.0%)	(1.2%)	(*)	(0.1%)	(8.9%)	(32.9%)			(0.3%)	(1.0%)	
		6.0	4.400	0.000	0.00	0.0	0.0	21.0	0.	0.1216	0.00	0.0001	5.547
			(*)	(*)	(*)	(*)	(*)	(*)	(*)	(0.0%)	(*)		

6 DOF Summary Output

Shot Number	Mach Number	DBSQ ABARM	CX CX2	CNa CNa3	CYpa CYpa3	Cma Cma3	Cmq Cmq2	Cnpa Cnpa3	Cnpa5	Clp IX/IY	CXM CmaM	Standard Error X(m) Y-Z(m)	 Angle(deg) Roll(deg)
28093	1.490	2.8	0.396	3.002	-1.00	2.798	-10.1	-0.36		-0.0300	-0.15	0.0001	0.157
			(0.0%)	(2.3%)	(*)	(0.2%)	(20.3%)	(42.8%)		(*)	(1.1%)		
		2.7	4.355	0.000	0.00	0.0	0.0	0.0	0.	0.1198	0.00	0.0002	0.000
			(*)	(*)	(*)	(*)	(*)	(*)	(*)	(0.1%)	(*)		
28094	1.490	3.5	0.406	3.002	-1.00	2.793	-15.7	-0.26		-0.0270	-0.13	0.0001	0.158
			(0.0%)	(1.6%)	(*)	(0.2%)	(13.3%)	(47.7%)		(*)	(0.8%)		
		3.0	4.335	0.000	0.00	0.0	0.0	0.0	0.	0.1204	0.00	0.0001	0.000
			(*)	(*)	(*)	(*)	(*)	(*)	(*)	(0.1%)	(*)		

6 DOF Summary Output

Shot Numbers		Mach Number	DBSQ ABARM	CX CX2 CX4	CNa CNa3 CNa5	CYpa CYpa3	Cma Cma3 Cma5	Cmq Cmq2 Cmq4	Cnpa Cnpa3 Cnpa5	Clp CXm CmaM	Standard Error X(m) Y-Z(m)	Standard Error Angle(deg) Roll(deg)
29270	29271	1.181	13.0	0.449 (*)	2.718 (1.3%)	-1.00 (*)	2.812 (0.2%)	-8.6 (6.1%)	-0.82 (5.8%)	-0.0260 (*)	0.0005	0.2146
29267	29269		7.3	3.360 (*)	0.000 (*)	0.00 (*)	11.816 (7.9%)	0.0 (*)	75.87 (8.2%)	-0.1371 (*)	0.0002	5.1990
29268				0.00 (*)	0.00 (*)		0.0 (*)	0. (*)	0. (*)	0.000 (*)		
28099	28092	1.466	10.6	0.404 (*)	2.852 (1.0%)	-1.00 (*)	0.000 (*)	-10.9 (4.2%)	-0.29 (14.5%)	-0.0295 (*)	0.0004	0.2116
28096	28097		10.6	4.422 (*)	0.000 (*)	0.00 (*)	0.000 (*)	0.0 (*)	31.07 (6.2%)	-0.1608 (0.8%)	0.0001	6.0620
28104				0.00 (*)	0.00 (*)		0.0 (*)	0. (*)	0. (*)	0.000 (*)		
28106	28107	1.474	13.3	0.402 (*)	2.869 (0.7%)	-1.00 (*)	0.000 (*)	-10.2 (3.0%)	-0.20 (14.6%)	-0.0302 (*)	0.0004	0.1719
28096	28104		10.5	4.366 (*)	0.000 (*)	0.00 (*)	-1.632 (19.5%)	0.0 (*)	22.13 (7.0%)	-0.1523 (*)	0.0001	7.5870
28105				0.00 (*)	0.00 (*)		0.0 (*)	0. (*)	0. (*)	0.000 (*)		
28096	28106	1.476	6.0	0.399 (*)	2.606 (2.2%)	-1.00 (*)	0.000 (*)	-11.6 (4.8%)	-0.32 (14.6%)	-0.0373 (*)	0.0007	0.1658
28097	28094		6.3	4.355 (*)	0.000 (*)	0.00 (*)	0.000 (*)	0.0 (*)	66.16 (10.4%)	-0.1055 (*)	0.0002	6.1930
28093				0.00 (*)	0.00 (*)		0.0 (*)	0. (*)	0. (*)	0.000 (*)		

28098	28093	1.477	6.5	0.400	3.133	-1.00	0.000	-10.4	-0.49	-0.0308	0.0006	0.1642
				(*)	(1.7%)	(*)	(*)	(4.7%)	(9.4%)	(*)		
28107	28096		6.3	6.809	0.000	0.00	0.000	0.0	86.59	-0.2014	0.0001	5.8990
				(*)	(*)	(*)	(*)	(*)	(6.8%)	(*)		
28099				0.00	0.00		0.0	0.	0.	0.000		
				(*)	(*)		(*)	(*)	(*)	(*)		
28098	28105	1.488	6.7	0.404	3.105	-1.00	2.780	-10.2	-0.39	-0.0373	0.0004	0.2405
				(*)	(1.1%)	(*)	(0.1%)	(6.7%)	(15.6%)	(*)		
28107	28093		8.2	4.335	0.000	0.00	0.000	0.0	48.17	-0.1426	0.0002	4.4380
				(*)	(*)	(*)	(*)	(*)	(8.9%)	(0.9%)		
28094				0.00	0.00		0.0	0.	0.	0.000		
				(*)	(*)		(*)	(*)	(*)	(*)		
28098	28105	1.488	6.7	0.404	3.105	-1.00	2.780	-10.2	-0.39	-0.0373	0.0004	0.2405
				(*)	(1.1%)	(*)	(0.1%)	(6.7%)	(15.6%)	(*)		
28107	28093		8.2	4.335	0.000	0.00	0.000	0.0	48.17	-0.1426	0.0002	4.4380
				(*)	(*)	(*)	(*)	(*)	(8.9%)	(0.9%)		
28094				0.00	0.00		0.0	0.	0.	0.000		
				(*)	(*)		(*)	(*)	(*)	(*)		

M16A2 M855 LR M1.5 roll pins
6 DOF Summary (ARL Format) (11-JUL-08 10:23:41)

Shot Number	Mach Number	DBSQ YAW	CD0 CD2	CLA0 CLA3	CYPA CYPA3	CMA CMA3	CMQ CMQ2	CMPA CMPA3	CMPA5	CLP IX/IY	CXM CMAM	Standard Error X(m) Y-Z(m)	 Angle(deg) Roll(deg)
29270	1.151	13.1	0.446	2.34	-0.50	2.85	-5.5	-0.60		-0.0116	-0.06	0.0004	0.173
		3.6	8.0	-5.2	0.0	0.0	0.0	79.7	0.	0.1224	0.00	0.0002	8.184
29266	1.157	6.4	0.450	1.86	-0.50	2.82	-0.9	-0.65		-0.0135	-0.14	0.0012	0.194
		2.5	7.5	-5.2	0.0	0.0	0.0	89.7	0.	0.1199	0.00	0.0003	0.000
29271	1.180	13.9	0.438	2.28	-0.50	2.81	-4.6	-0.45		-0.0143	-0.14	0.0005	0.172
		3.7	8.0	-5.3	0.0	9.7	0.0	48.7	0.	0.1217	0.00	0.0002	8.536
29268	1.186	10.1	0.444	2.29	-0.50	2.86	-3.2	-0.31		-0.0135	-0.11	0.0007	0.195
		3.2	8.1	-5.4	0.0	0.0	0.0	0.0	0.	0.1212	0.00	0.0002	0.000
29267	1.188	16.0	0.440	2.30	-0.50	2.88	-4.4	-0.34		-0.0135	-0.17	0.0005	0.194
		4.0	8.1	-5.4	0.0	2.8	0.0	28.4	0.	0.1219	0.00	0.0002	0.000
29269	1.201	12.4	0.441	2.20	-0.50	2.78	-4.4	-0.48		-0.0135	-0.13	0.0004	0.204
		3.5	8.1	-5.4	0.0	17.7	0.0	59.7	0.	0.1223	0.00	0.0002	0.000
28106	1.457	9.0	0.399	2.47	-0.50	2.73	-3.7	-0.12		-0.0142	-0.16	0.0001	0.162
		3.0	7.3	-4.5	0.0	0.0	0.0	0.0	0.	0.1192	0.00	0.0001	8.390
28099	1.458	8.7	0.413	2.50	-0.50	2.73	-4.1	-0.12		-0.0129	-0.17	0.0001	0.138
		2.9	7.4	-4.5	0.0	0.0	0.0	0.0	0.	0.1202	0.00	0.0001	3.966
28092	1.459	6.8	0.420	2.44	-0.50	2.81	-4.6	-0.25		-0.0150	-0.13	0.0001	0.196
		2.6	7.3	-4.5	0.0	0.0	0.0	0.0	0.	0.1205	0.00	0.0001	0.000
28096	1.467	9.6	0.407	2.44	-0.50	2.70	-4.9	-0.10		-0.0162	-0.16	0.0001	0.144
		3.1	7.3	-4.4	0.0	0.0	0.0	10.5	0.	0.1188	0.00	0.0001	10.130
28097	1.473	5.5	0.396	2.51	-0.50	2.82	-5.4	-0.10		-0.0138	-0.16	0.0001	0.162
		2.3	7.3	-4.4	0.0	0.0	0.0	0.0	0.	0.1228	0.00	0.0001	4.426

M16A2 M855 LR M1.5 roll pins
6 DOF Summary (ARL Format) (11-JUL-08 10:23:41)

Shot Number	Mach Number	DBSQ YAW	CD0 CD2	CLA0 CLA3	CYPA CYPA3	CMA CMA3	CMQ CMQ2	CMPA CMPA3	CMPA5	CLP IX/IY	CXM CMAM	Standard Error X(m) Y-Z(m)	Angle(deg) Roll(deg)
28104	1.473	23.3	0.394	2.55	-0.50	2.79	-4.9	0.02		-0.0153	-0.22	0.0003	0.224
		4.8	7.4	-4.4	0.0	0.0	0.0	0.0	0.	0.1218	0.00	0.0001	6.753
28098	1.485	2.7	0.403	2.62	-0.50	2.82	-9.6	-0.20		-0.0169	-0.15	0.0001	0.166
		1.6	7.4	-4.4	0.0	0.0	0.0	0.0	0.	0.1230	0.00	0.0001	4.864
28105	1.485	16.3	0.392	2.53	-0.50	2.76	-4.5	-0.02		-0.0151	-0.16	0.0001	0.178
		4.0	7.3	-4.4	0.0	0.0	0.0	0.0	0.	0.1212	0.00	0.0001	6.699
28107	1.488	8.8	0.398	2.65	-0.50	2.80	-4.4	-0.12		-0.0147	-0.14	0.0002	0.148
		3.0	7.4	-4.4	0.0	0.0	0.0	10.5	0.	0.1216	0.00	0.0001	5.547
28093	1.490	2.8	0.396	2.61	-0.50	2.80	-5.1	-0.18		-0.0150	-0.15	0.0001	0.157
		1.7	7.4	-4.4	0.0	0.0	0.0	0.0	0.	0.1198	0.00	0.0002	0.000
28094	1.490	3.5	0.406	2.60	-0.50	2.79	-7.9	-0.13		-0.0135	-0.13	0.0001	0.158
		1.9	7.3	-4.3	0.0	0.0	0.0	0.0	0.	0.1204	0.00	0.0001	0.000

M16A2 M855 LR M1.5 roll pins
6 DOF Summary (ARL Format) (11-JUL-08 10:23:41)

Shot Numbers		Mach Number	DBSQ Yaw	CD0 CD2 CDR	CLA0 CLA3 CLR	CYPA CYPA3	CMA CMA3 CMA5	CMQ CMQ2 CMQ4	CMPA CMPA3 CMPA5	CLP CXm CmaM	Standard Error X(m) Y-Z(m)	Standard Error Angle(deg) Roll(deg)
29270	29271	1.181	13.0	0.449	2.27	-0.50	2.81	-4.3	-0.41	-0.0130	0.0005	0.2146
29267	29269		3.6	6.1	-3.4	0.0	11.8	0.0	37.94	-0.1371	0.0002	5.1990
29268				0.473	2.250		0.0	0.	0.	0.000		
28099	28092	1.466	10.6	0.404	2.45	-0.50	0.00	-5.5	-0.14	-0.0147	0.0004	0.2116
28096	28097		3.3	7.3	-4.4	0.0	0.0	0.0	15.53	-0.1608	0.0001	6.0620
28104				0.427	2.429		0.0	0.	0.	0.000		
28106	28107	1.474	13.3	0.402	2.47	-0.50	0.00	-5.1	-0.10	-0.0151	0.0004	0.1719
28096	28104		3.6	7.2	-4.4	0.0	-1.6	0.0	11.07	-0.1523	0.0001	7.5870
28105				0.430	2.443		0.0	0.	0.	0.000		
28096	28106	1.476	6.0	0.399	2.21	-0.50	0.00	-5.8	-0.16	-0.0186	0.0007	0.1658
28097	28094		2.5	7.0	-4.4	0.0	0.0	0.0	33.08	-0.1055	0.0002	6.1930
28093				0.411	2.196		0.0	0.	0.	0.000		
28098	28093	1.477	6.5	0.400	2.73	-0.50	0.00	-5.2	-0.25	-0.0154	0.0006	0.1642
28107	28096		2.5	9.9	-6.8	0.0	0.0	0.0	43.29	-0.2014	0.0001	5.8990
28099				0.419	2.717		0.0	0.	0.	0.000		
28098	28105	1.488	6.7	0.404	2.70	-0.50	2.78	-5.1	-0.19	-0.0186	0.0004	0.2405
28107	28093		2.6	7.4	-4.3	0.0	0.0	0.0	24.09	-0.1426	0.0002	4.4380
28094				0.419	2.689		0.0	0.	0.	0.000		

INTENTIONALLY LEFT BLANK.

Appendix C. Complete Set of Magnus Moment Plots

Figures C-1–C-5 illustrate the Magnus moment and stability bounds of several groups with Mach numbers ranging from 1.68 to 2.62. At each of these Mach numbers, C_{n_p} remains within the stability bounds over the range of angles of attack tested, indicating that a Magnus moment instability is not likely present at these Mach numbers. Plots displaying the Magnus moment and stability bounds at Machs 1.18, 1.47, 1.48, and 1.7, showing a possible Magnus moment instability, can be found in the main body of the report. As Mach 1.7 shows an instability and Mach 1.68 does not, it is likely that the round is neutrally stable near Mach 1.7 in the underspun condition.

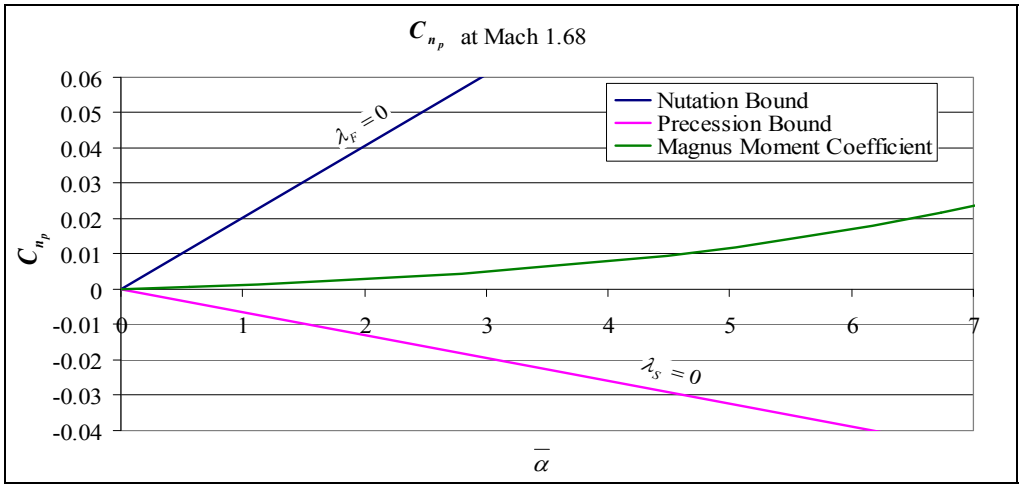

Figure C-1. Magnus moment coefficient with stability bounds at Mach 1.68.

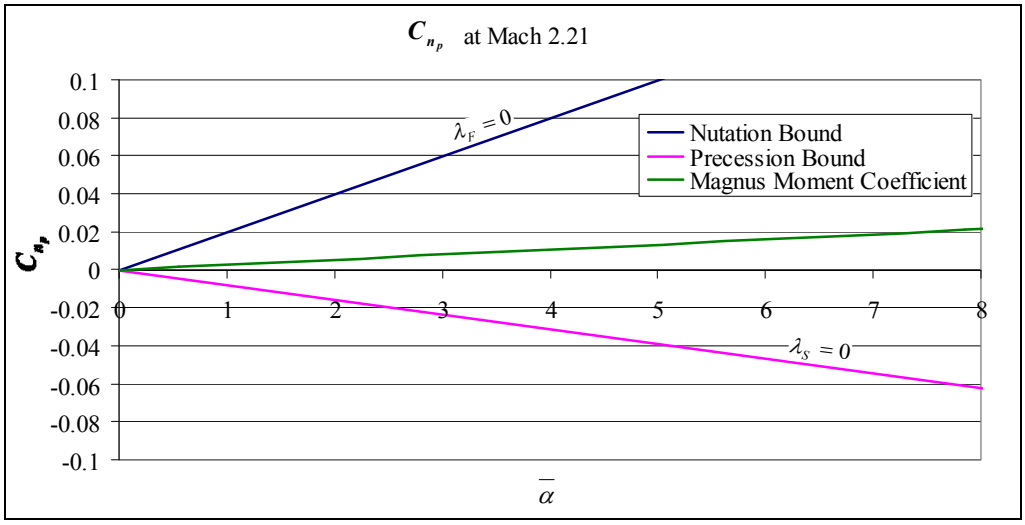

Figure C-2. Magnus moment coefficient with stability bounds at Mach 2.21.

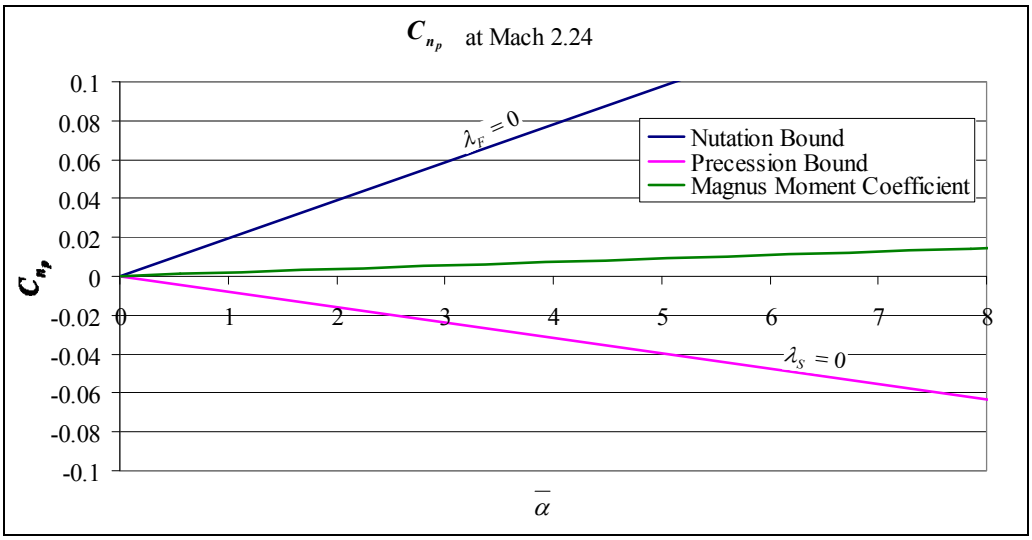

Figure C-3. Magnus moment coefficient with stability bounds at Mach 2.24.

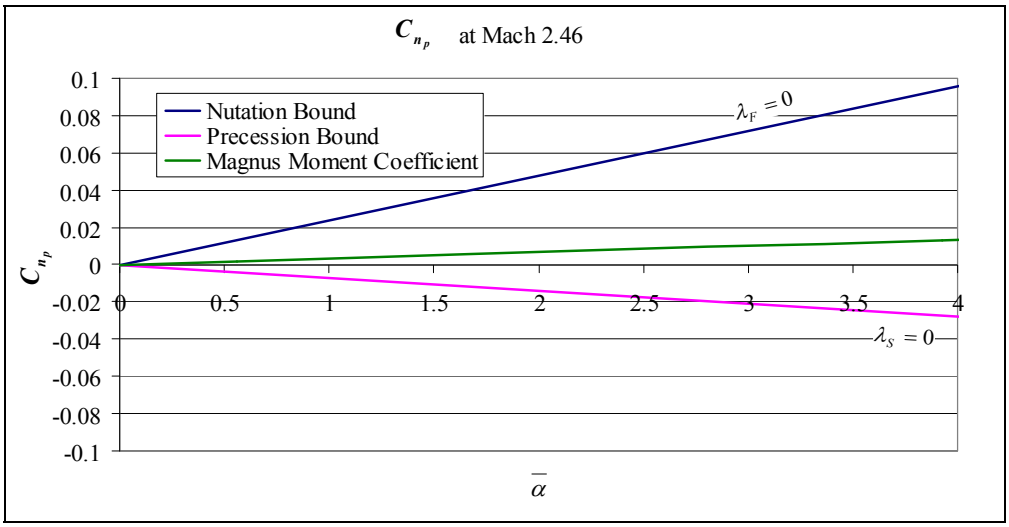

Figure C-4. Magnus moment coefficient with stability bounds at Mach 2.46.

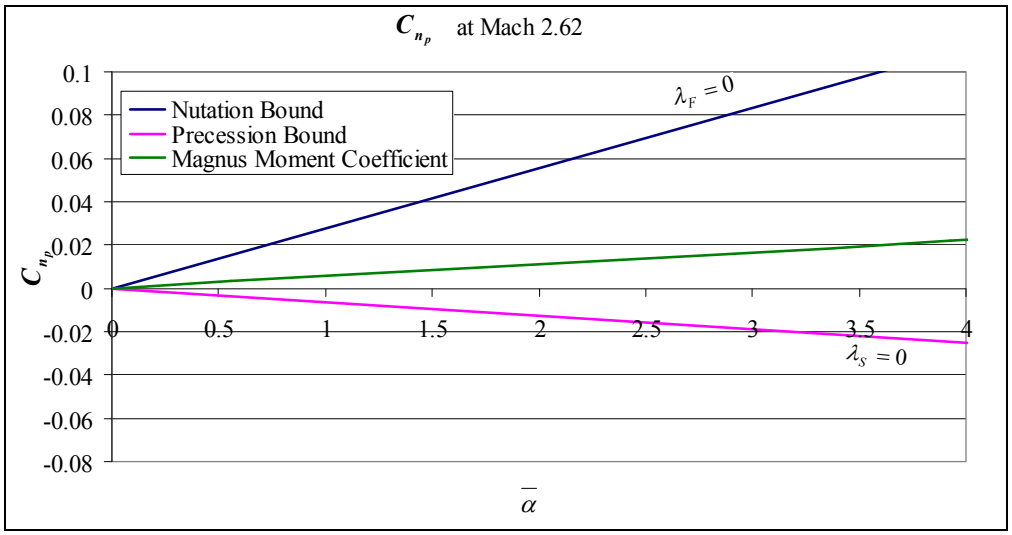

Figure C-5. Magnus moment coefficient with stability bounds at Mach 2.62.

NO. OF
COPIES ORGANIZATION

1 (PDF only) DEFENSE TECHNICAL INFORMATION CTR
DTIC OCA
8725 JOHN J KINGMAN RD
STE 0944
FORT BELVOIR VA 22060-6218

1 DIRECTOR
US ARMY RESEARCH LAB
IMNE ALC HRR
2800 POWDER MILL RD
ADELPHI MD 20783-1197

1 DIRECTOR
US ARMY RESEARCH LAB
RDRL CIM L
2800 POWDER MILL RD
ADELPHI MD 20783-1197

1 DIRECTOR
US ARMY RESEARCH LAB
RDRL CIM P
2800 POWDER MILL RD
ADELPHI MD 20783-1197

1 DIRECTOR
US ARMY RESEARCH LAB
RDRL D
2800 POWDER MILL RD
ADELPHI MD 20783-1197

ABERDEEN PROVING GROUND

1 DIR USARL
RDRL CIM G (BLDG 4600)

NO. OF COPIES	ORGANIZATION
1	COMMANDER US ARMY MATL CMD AMXMI INT 9301 CHAPEK RD FORT BELVOIR VA 22060-5527
1	PRODUCT MGR SML AND ME CAL AMMO SFAE AMO MAS SMC LTC WOODS BLDG 354 PICATINNY ARSENAL NJ 07806-5000
4	APM SML AND ME CAL AMMO SFAE AMO MAS SMC R KOWALSKI F HANZL P RIGGS G DEROSA BLDG 354 PICATINNY ARSENAL NJ 07806-5000
1	US ARMY ARDEC AMSRD AAR AEM T M NICOLICH BLDG 65S PICATINNY ARSENAL NJ 07806-5000
1	US ARMY ARDEC AMSRD AAR AEM L D VO BLDG 65 S PICATINNY ARSENAL NJ 07806-5000
1	US ARMY ARDEC AMSRD AAR AEM S S MUSALLI BLDG 65S PICATINNY ARSENAL NJ 07806-5000
1	US ARMY ARDEC AMSRD AAR EMB R CARR BLDG 1 PICATINNY ARSENAL NJ 07806-5000

NO. OF COPIES	ORGANIZATION
1	US ARMY ARDEC AMSRD AAR AEM L R SAYER BLDG 65 PICATINNY ARSENAL NJ 07806-5000
1	US ARMY ARDEC AMSRD AAR AEW D M MINISI BLDG 65N PICATINNY ARSENAL NJ 07806-5000
2	US ARMY ARDEC AMSRD AAR AIJ V SCHISSLER K SPIEGEL BLDG 65 PICATINNY ARSENAL NJ 07806-5000
3	US ARMY ARDEC AMSRD AAR AEM I J MIDDLETON BLDG 65N PICATINNY ARSENAL NJ 07806-5000
1	COMMANDER US ARMY ARDEC AMSRD AAR ATD B MACHAK BLDG 1 PICATINNY ARSENAL NJ 07806-5000
1	US ARMY ARDEC AMSTA AAR AEW A (D) M CHIEFA BLDG 1 PICATINNY ARSENAL NJ 07806-5000
1	US ARMY ARDEC AMSTA AR FSP G M SCHIKSNIS BLDG 1 PICATINNY ARSENAL NJ 07806-5000

NO. OF COPIES ORGANIZATION

1 US ARMY ARDEC
AMSTA AR FSP G
D CARLUCCI
BLDG 1
PICATINNY ARSENAL NJ
07806-5000

14 COMMANDER
US ARMY TACOM ARDEC
AMSRD AAR AEM A
C LIVECCHIA
J GRAU
B WONG
A FARINA
G MALEJKO
E VAZQUEZ
W TOLEDO
L YEE
R TROHANOWSKY
S HAN
W KOENIG
S CHUNG
C WILSON
T RECCHIA
BLDG 95
PICATINNY ARSENAL NJ 07806-5000

ABERDEEN PROVING GROUND

4 COMMANDER
US ARMY ATC
G NIEWENHOUSE
G POWERS
T HUMISTON
J AYERS
BLDG 400
APG MD 21005

4 COMMANDER
US ARMY TACOM ARDEC
AMSRD AR AEF D
R LIESKE
J MATTS
A SOWA
J FONNER
BLDG 305
APG MD 21005

NO. OF COPIES ORGANIZATION

29 DIR USARL
RDRL HRS B
T FRY
RDRL SLB D
R KINSLER
RDRL WM
P PLOSTINS
RDRL WMB D
B FORCH
RDRL WML
J NEWILL
M ZOLTOSKI
RDRL WML A
C MERMAGEN
W OBERLE
J SOUTH
S WANSACK
D WEBB
RDRL WML E
I CELMINS
G COOPER
J DESPIRITO
F FRESCONI
J GARNER
B GUIDOS
K HEAVEY
B HOWELL
J SAHU
S SILTON
P WEINACHT
RDRL WML F
D LYON
RDRL WML H
C CANDLAND
T EHLERS
L MAGNESS
RDRL WMM F
R CARTER
RDRL WMP
P BAKER
RDRL WMS
T ROSENBERGER